5-1966

Streaming Current and Streaming Potential Induced by Water Flow Through Porous Media

Mohamed M. I. Abaza

ABSTRACT

Abaza, Mohamed M. I.; 1936; Streaming Current and Streaming Potential Induced by Water Flow Through Porous Media; Department of Civil Engineering; Dr. Calvin G. Clyde, major professor.

This study was conducted to investigate analytically and experimentally the relationship between the rate of flow of water through porous material and the streaming current and streaming potential induced by this flow. The effect of dissolved salts in the permeating solution and the size of the soil particles was also investigated.

Results and conclusions of this study are summarized as follows:

1. A modified procedure using the appropriate delay to insure stead state conditions was used for the measurements of both streaming current and streaming potential.

2. The flow-pressure relationship was the same irrespective of the counter electro-osmosis (resulting from the streaming potential) and the change in salt concentration. Flows through the samples tested thus followed Darcy's Law.

3. The rate of flow (at a constant salt concentration and soil particle diameter) is directly proportional to the induced streaming current and streaming potential. Emperical equations in the form of $I = C_1 q$ and $E = C_2 q$ are suggested.

4. A decrease in both streaming current and streaming potential was observed with increase of salt concentrate in the permeating solution. Comparable results were obtained for simulated natural

waters and NaCl and KCl solutions, provided that the conductance of the solution was taken as a parameter.

5. A decrease in current and potential was observed with increase of soil particle diameter.

6. Relationships of the form $\alpha = bN^a$ and $\beta = C \log N + d$ are suggested to express the effects of particle size and salt concentration on the streaming current and the streaming potential induced by the flow.

7. Induced streaming potential was found to increase with the decrease in temperature.

8. The analytical relationships developed together with the experimental work could probably be used as the basis of a method for measuring the rate of flow through porous material.

ACKNOWLEDGMENTS

I am indebted to Dr. Calvin G. Clyde, major professor and thesis director, for his continuous encouragement, deep interest, valuable advice, guidance throughout this work, and finally for his active interest in providing an environment conducive to research by acquiring necessary equipment in short time.

Special thanks are due to Dr. S. A. Taylor, member of the doctoral committee, who introduced me to irreversible thermodynamics, for his painstaking review of that part of the dissertation.

I am also grateful to Dr. V. E. Hansen, Dr. G. Z. Watters, and Dr. D. V. Sisson for serving as members of my doctoral committee.

The writer acknowledges the United Arab Republic Government for financial support, and the Engineering Experiment Station and the Utah Water Research Laboratory for making available necessary funds for equipment.

Finally, I express my deep appreciation for my wife, Raga, for her encouragement during the course of our graduate study.

Mohamed Abaza

TABLE OF CONTENTS

LIST OF TABLES

LIST OF FIGURES

Figure Page

Symbol	Notations
A_o	Cross sectional area perpendicular to the direction of the flow
a	Average radius of pore
Amp	Ampers
C	Cell constant
C_s	Specific conductance
C_1, C_2	Proportionality constants
D	Dielectric constant
d	Effective sample diameter; d_{10}
E_{str}; E	Streaming potential; electrical potential difference across the system
i_{str}	Charge carried per second per liquid per unit surface length
I_{str}, I	Streaming current; electric current through the system
I_c	Conduction current
J_e	Current flow rate
J_w	Volume rate of fluid flow
K	Coefficient of permeability
k	Total conductance
K_B	Specific bulk conductivity
K_o	Coefficient $= \frac{(1-\sigma)^2}{\beta d^2 \sigma^2}$
K_s	Specific surface conductivity
L	Length of the sample

Symbol	Notations
L_{11}, L_p	Represent hydrodynamic conductance
L_{12}	Represent electro osmosis
L_{21}	Represent streaming potential
L_{22}, L_e	Represent electrical conductance
m	Effective area of pores; superficial porosity
m.a.	Milliampers
m.V.	Millivolts
N	Normality of salt solution
p	Pressure difference across the system
P_s	Total perimeter of liquid-solid interface in a cross-section area of the sample
q	Discharge; volume rate of flow
q_p	Rate of flow that would exist in absence of coupling
R	Resistance
S_1	Sample one
S_2	Sample two
t	Temperature
V	Velocity at any distance from the center of the pore
v	Local velocity
$\bar{v}$	Seepage velocity
V.	Volts
W	Simulated natural water
α	Slope of E vs q curve $= \frac{E}{q}$
β	Slope of I vs q curve $= \frac{I}{q}$

Symbol	Notations
$\mathfrak{K}$	Kozeny coefficient
∇^2	Laplacian operator
ψ	Electrostatic potential
ψ_o	Potential at the surface of the wall
ψ_d	Potential at the two layer interface
η	Dynamic viscosity
σ'	Electronic charge
σ	Porosity
ρ	Electrical charge density
ζ	Zeta potential; potential at the hydrodynamic plane of shear

CHAPTER I

INTRODUCTION

The problem of developing sufficient water supplies for industry, agriculture and domestic use is rapidly growing more serious and may well become of basic worldwide concern if the present rate of population growth and economic development is maintained.

In developing ground water supplies there is often a need for detailed information concerning the rate and direction of ground water movement in order to evaluate the ultimate safe yield of ground water reservoirs. Measurements of the velocity of fluid flow through porous media have been of concern to the hydrologist, soil mechanician, petroleum engineer and sanitary engineer for more than half a century. Seepage through earth dams, leakage from irrigation canals and the intrusion of sea water into fresh water aquifer are some examples of situations where a more thorough understanding of rate variation of fluid movement through permeable media would be desirable.

The rate of fluid movement varies with many factors, such as length of the path, grain size, effective grain size, driving force, grain shape, orientation of particles, packing of the grains, temperature of the permeant fluid and its composition and concentrations. Major velocity (and rate of flow) variations occurring during the movement of fluids through a complex system of voids in naturally formed porous strata are particularly dependent on the anistropic

and heterogeneous characteristics of the medium.

Most equations relating head to discharge, time, space and hydrologic properties have been derived through application of Darcy's law to the continuity equation. Thus, determination of the hydraulic constants of an aquifer requires not only measurement of the head distribution in space and time but also measurements of discharge from or recharge to the aquifer at the same location where the shape of the flow-field boundary is known. Thus, at most locations in an aquifer, it is not practical to obtain by direct measurements the data needed for application of the available analytic equations.

If some method for measuring ground water velocity can be found, the utility of the tests to determine the hydraulic constants of the aquifer can be greatly extended. The obvious approach is to include, in the testing and the analysis, the observation of variables that are directly dependent on the velocity of the flow. Therefore, new approaches to the measurement problems appear desirable to supplement knowledge of these variables, especially if thereby certain quantities become measurable which are beyond the reach of present methods.

Some idea of the rate of flow of water from one place to another may be gained by the use of dyes and other flow detectors. However, the use of tracers, whether they be dyes, salts, or radioactive materials, is unsatisfactory in some respects because the general direction of flow must be known before such methods are used. Also, the chemical and physical effects to which the tracer material will be subjected underground are not completely known.

The simultaneous transfer of heat and the flow of water underground result in head and temperature distributions which can be expressed by differential equations. Some of these qualitative relations have been published. Some quantitative experiments relating temperature and velocity changes have yet to be conducted before valid conclusions can be derived. Therefore, a new approach is suggested in this work. That is to utilize electrokinetic phenomena, known and extensively used in colloidal and biological science, for the evaluation of discharge and velocity for flow of fluids through porous materials.

When a solid comes in contact with liquid, an electric potential difference between the two comes into existance at the interface. Consequently, the liquid will be charged opposite to the solid (wall). Ions of the liquid accumulate near the solid surface and cause an electrical double layer at the solid-liquid interface to arise. Thus when the liquid is forced to flow through a capillary tube, the liquid stream carries with it part of the mobile part of that electrical double layer near the walls of the capillary. The convection of electrical charges having density ρ with local velocity v results in a "streaming current" having density $v\rho$. As a consequence of the streaming current a potential difference will be set up between the ends of the capillary which in turn generates a conductive current opposite in sense with the streaming current. At steady state, when the two currents equal each other, the potential difference induced will be the "streaming potential." This streaming current and potential have been shown to be related to the pressure forcing the liquid

to flow. This phenomena is now well understood for uniform capillaries and has been shown also to exist when flow occurs through porous plugs and diaphragms (see Abramson, 1934; Kraemer, 1942; Glasstone, 1946; Overbeek and Wigga, 1946; Partington, 1949; Butler, 1951; Overbeek, 1953a and b; Rutgers, 1954; Bikerman, 1958; Bier, 1959; Mysels, 1959; Adamson, 1960; Schulman and Parriera, 1963; and Davies and Rideal, 1963). Many measurements of streaming potential have been utilized in studying the structural and electrochemical properties of solid surfaces in contact with liquids (Neale and Peters, 1945; Buchanan and Heyman, 1948 and 1949a and b; Goring and Mason, 1950; Dulin and Elton, 1952 and 1953; Fuerstenau, 1953; Gaudin and Fuerstenau, 1955; Biefer and Mason, 1959; Martinez, 1960; Parriera and Schulman, 1961).

It is well known that, when liquid flows through porous materials, the velocity of the flow (if no other flows are operating) is related to the applied pressure that forced the flow (e.g. Darcy's law). If this relationship is tied together with the previous relationships, relating streaming current, I, and streaming potential, E, to the pressure, a new relationship will be established between the velocity (and the rate of flow) and the streaming potential and current. So, measurements of E and I induced through porous media where water is flowing could be used to evaluate the rate of that flow. Experimental procedures, instruments and apparatus with reliable precision must be available before such phenomena can be fully utilized.

In order to establish these relationships and to produce the

needed experimental procedures, this study has been undertaken. Experimental procedures developed and equipment used in this work have proved to be reliable enough to investigate the approach suggested. Analytical relationships developed together with the experimental work could probably be used as the basis of a reliable method for measuring the rate of flow through porous materials.

Objectives

The objectives of this study are:

1. To develop the analytical relationship between the rate of flow of fluid through porous material and streaming current, I, and streaming potential, E, induced by this flow.

2. To establish a reliable experimental procedure for the measurement of E and I developed by flow of water through porous material.

3. To investigate experimentally the relationships between E, I, and the flow in connection with the analytical approach.

4. To investigate the effects of dissolved salts in the permeating solution and the size of the soil particles upon developed potentials and the rate of the flow through porous material.

CHAPTER II

ELECTROKINETIC PHENOMENA

Historical

Electrokinetic phenomena were observed as far back as the beginning of the 19th century. In 1808 Reuss discovered that flow through a capillary element can be induced by the application of an electric field. About half a century later, in 1852, Wiedmann performed a number of quantitative experiments and promulgated one of the fundamental theories of electrokinetics. His theory, which has been verified many times, states that the volumetric flow transported through porous material by galvanic current is directly proportional to the intensity of the applied current. In 1859 Quinke discovered the phenomena of streaming potential which is the converse of electro-osmosis. His experiments showed that when fluid was forced through a diaphragm, the voltage developed across the diaphragm was proportional to the pressure differential causing the flow. In every case of this experiment an electric current flowed in the same direction as that in which the liquid moved.

In 1873 Zollner (cited by Abramson, 1934) attempted to explain the origin of the earth's current by a similar mechanism and was the first investigator to demonstrate streaming potential in capillaries. Those previous findings together with development of the hydrodynamic and electric theories, led to the basic theoretical treatment by Helmoholtz and what is known in Colloidal Science as Helmoholtz theory.

In 1879 Helmoholtz developed the double layer theory which related analytically the electrical and fluid flow parameters of electrokinetic transport. Although subsequently modified, his development stood the test of time and still represents an acceptable formulation of the electroosmosis phenomena in most capillary material. Actuated by an interest in the nature of stability of suspensions, Smoluchowski (1921) reinvestigated the theory of Helmoholtz. Freundlich (1909) published and discussed the results of some prior comprehensive experiments performed by other investigators. His demonstration—based on Saxen's experimental results (1892)—showed that if both electroosmosis and streaming potential are measured in the same system, then the proportionality constant in electroosmosis relating volumetric flow to electric current was identical with that relating streaming potential and applied pressure. From that time on the field of electrokinetics received contributions from many scientists and research workers, especially those in the field of Colloidal Science who gave valuable information on the electrochemical double layer (Abramson, 1934; Biekerman, 1940; Butler, 1951; Kruyt, 1952; Adamson, 1960; and Davis and Ridel, 1963).

A comprehensive review and treatment of the classical theories of the phenomena is available in two monographs on electrokinetics by the University of Michigan (1953) and in a recently published report by Burgreen and Nakachi (1963 and 1964).

Recent Theories and Modifications to Helmoholtz

Helmoholtz theory

The basic premise of Helmoholtz development is that when a liquid and solid come into contact, there is usually an accumulation of ions of the liquid near the surface of the solid to produce a double layer. Helmoholtz envisaged the double layer as two parallel planes of oppositely charged ions. The fixed layer adheres to the surface and a neutralizing counter ion layer that exists in a single plane parallel to the surface at a distance x into the liquid. He considered the mutual action between the ions to be negligible.

Gouy theory

In 1910 Gouy introduced a more realistic concept of the potential and charge distribution in the fluid adjacent to the solid wall. He assumed a mutual action on the charged ions between the electric forces which are responsible for the existance of the double layer and the osmotic forces which tend to maintain homogenity. He postulated nothing in regards to the inner adsorbed layer which was described by Helmoholtz as fixed to the surface. On this account there will be no sudden change in the concentration of any kind of ions in the vicinity of the double layer, but merely a gradual increase of concentration of ions of one sign and refraction of ions of the other. Gouy showed that the electrical density of the ionic atmosphere fell off according to an exponential law (rather than to the linear law of Helmoholtz), and that the electrical center of gravity exists at a distance, d, where d is a function of the salt valence, Z, and salt concentration, c.

Stern theory

In 1924 Stern suggested a type of double layer which is a combination of the simple Helmoholtz fixed layer with the Gouy diffuse layer. Roughly the potential is assumed to vary with distance as shown in Figure 1. In Stern's picture of the double layer, he considered the possibility of specific adsorption of ions and assumed that these ions were also located in the plane x. This layer of adsorbed ions is called the Stern layer. The total potential drop is accordingly divided into a potential drop over the diffuse part of the double layer and that over the molecular condenser.

Present theory

With all these modifications the theory now reaches acceptable status that could be summarized as follows: The charge on the solid wall (of the particle) attracts counter ions and repels similar ions. Some of the counter ions may be immobilized in Stern layer, while the rest of the ions form a diffuse Gouy layer. The decay of the potential within this double layer is measured by its thickness, which is very sensitive to the concentration and valence of the counter ions. The surface charge density is also very sensitive to those factors. Potential at two points in the double layer are of special importance: Ψ_o at the surface of the wall and $\zeta = \Psi_d$ at the hydrodynamic plane of shear (Figure 1).

Streaming potential and streaming current

If the double layer discussed before at a solid-liquid interface is disturbed by the application of external forces, the static

equilibrium conditions are destroyed and a series of electrokinetic effects may be observed. Each may be distinguished primarily by the nature of the disturbing force, which may be mechanical or electrical. One of these effects is the streaming potential. In this case the disturbing force is mechanical movement which creates an electric current. When the liquid is forced to flow through the charged capillary, current flows with the liquid and is known as the streaming current (see Chapter IV). This current can build up a potential difference between two electrodes situated at the ends of the capillary known as streaming potential.

Factors Affecting Streaming Potential in Porous Media

As may be seen, the streaming potential is dependent upon three major factors: the composition of the liquid phase (permeant solution), the material of the solid phase or plug, and the size and shape of the solid particles. Each may affect the potential separately or in interaction with the other factors. One major variable on which streaming potential is dependent and which reflects the effects of both solid and liquid phases is the ζ potential.

Effect of the solid phase

The solid phase effects are due to the nature of its charge and its density. The vast majority of solids tested in contact with dilute aqueous solution of inert electrolytes are charged negatively. Positively charged solid surfaces are much less numerous (Biekerman, 1958). With Ottowa sand the surface charge is negative with sand in

contact with pure water or dilute solutions. This charge arises either from the adsorption of hydroxyl ions (or dissociation of H^+ ions) or the adsorption of negative ions from electrolyte solutions. For example, with potassium or sodium chloride solutions tested, the negative potential of sand could be as shown in Figure 1, Appendix.

Effect of the composition of liquid phase

The effect of the composition of the liquid is detected in the electrokinetic behavior of streaming potential for liquids containing dissolved electrolyte. That effect will be recognized through its effect on the double layer thickness and the conductivity of the system. The nature of the electrolyte is as important as its concentration. The results found for the influence of ions on ζ potential (consequently on streaming potential) may be summarized as:

1. The nature of the counter ions is more effective than that adsorbed on the soil surface.

2. Ions of higher valency are more effective than those of lower valency.

Utilization of Streaming Potential for the Determination of Flow Parameters

Although this phenomena was first observed about a century ago, it was not until recently that some thoughts have been given to its utilization in obtaining some flow parameters and other phenomenon involved with the flow.

Bocquet and associates (1956) were the first to report that turbulence in pipe flow will develop an instantaneous fluctuation of

streaming potential. Investigations of the relation between turbulence and streaming potential with an objective being the use of electrokinetics as a tool for turbulence measurements in pipe flow have been conducted (Cermak and Baldwin, 1963). The research accomplished by Binder (1960) showed that streaming potential might be a valuable tool in the study of turbulence and unsteady water flows. Chaung and Duckstein (1962) (cited by Cermak and Baldwin, 1963) succeeded in adapting the electrokinetic electrode to the study of fully developed pipe flow (see also Binder and Cermak, 1963). Some thoughts have been given also by Bocquet (1952) at the University of Michigan regarding the measurement of blood flow in veins by streaming potential techniques.

In the field of soils (porous media), not much work has been done on the usage of streaming potential for fluid flow measurements although many investigators suggested it would be possible. Alexander (1946) reported that such a study, including particularly the effect of electrolyte concentration, would be of great value especially with drilling wells. Also, Scott (1962) and Jumkis (1962) advocated that a measurement of the streaming potential developed in a soil through which flow is taking place could be correlated with the flow quantity.

In connection with flow through saturated soils, one should note here the work done by Michaels and Lin (1955) and by H. W. Olsen (1961) investigating streaming potential in Kaolinite and its effects on the flow. Their work aimed to determine if the electro-osmotic flow induced by the developed streaming potential could

account for the non-Darcy behavior of flow through Kaolinite. Olsen (1966) conducted an experimental investigation to study values of the induced hydraulic and potential difference across Kaolinite sample as affected by the form of the externally imposed inducing force. These forces were in the form of liquid flow, current and NaCl concentration difference across the sample.

The research work reported in here, however, is intended to develop an analytical relationship between streaming potential and streaming current induced through sand beds by flowing solutions and the rate of flow of these solutions. The experimental investigations were conducted to test this analytical relationship; also to determine how this relationship will be affected by electrolyte concentration in the percolating solutions and the size of the particles forming those beds. These relationships are then discussed in order to determine the possibility of their use as a new method to evaluate quantitatively the rate of flow through porous materials.

CHAPTER III

DERIVATION OF THE ANALYTICAL EQUATIONS

Streaming Current

Assume that Poiseull's theory for velocity distribution (parabolic velocity distribution) in a capillary is valid for each infinitesimal length of the flow channels. Then in a length δL of the flow channel of average radius a, the axial velocity of flow of liquid (of viscosity η) at a point any distance from the center under a differential pressure δp (where $\delta p = \alpha h$ as the flow channels are horizontal with $\delta z = o$).

$$V_{(r)} = \frac{\delta p}{4\eta \delta L} (a^2 - r^2) \quad . \quad . \quad . \quad . \quad . \quad . \quad (1)$$

According to Poisson's law of electrostatics, the electrostatic potential ψ (the positive charge in this case) in a solution in the neighborhood of a charged solid wall is held near the wall by the negative charge of the wall. The distribution is given by

$$\nabla^2 \psi = - \frac{4\pi\rho}{D} \quad . \quad . \quad . \quad . \quad . \quad . \quad . \quad . \quad (2)$$

where ρ is the volume electric charge density (electric charge per cm^3), D is the dielectric constant of the fluid, and ∇^2 is laplacian operator.

For an infinitesimal length of the flow channel, the wall can be assumed flat and $\nabla^2 \psi = \frac{d^2\psi}{dx^2} = - \frac{4\pi\rho}{D}$ from which

$$\rho = -\frac{D}{4\pi} \frac{d^2\psi}{dx^2} \quad . \quad . \quad . \quad . \quad . \quad . \quad . \quad . \quad . \quad (3)$$

If, as is usually the case, the ionic atmosphere at the wall (the diffuse double layer) is extremely thin in comparison with the pore diameter, then the gradient of the velocity, $\frac{dv}{dr}$, can be assumed to be constant inside the layer, and the velocity, $v_{(x)}$ at any distance, x(x = a-r), from the wall is given by

$$v_{(x)} = \int_o^{\bar{x}} (\frac{dv}{dx})_{x=o} \, dx \quad . \quad . \quad . \quad . \quad . \quad . \quad . \quad (4)$$

as

$$(\frac{dv}{dx})_{x=o} = -\frac{pa}{2\eta L} \quad . \quad . \quad . \quad . \quad . \quad . \quad . \quad (5)$$

therefore

$$v_{(x)} = \int_o^x (\frac{dv}{dx})_{x=o} \, dx = -\frac{pax}{2\eta L} \quad . \quad . \quad . \quad (6)$$

The motion of the electrically charged liquid near the wall is accompanied by an electric current (convective current), i_{str}. By definition, i_{str} (charges carried per second by the liquid per unit surface length) is

$$i_{str} = \int_{x=xo}^{a} \rho v_{(x)} \, dx \quad . \quad . \quad . \quad . \quad . \quad . \quad . \quad (7a)$$

Substituting from (3) and (6) into (7a)

$$i_{str} = \int_{x=xo}^{a} \frac{D}{4\pi} \frac{d^2\psi}{d^2x^2} \cdot \frac{pax}{2\eta L} \, dx$$

$$= \frac{paD}{8\pi\eta L} \int_{x=xo}^{a} \frac{d^2\psi}{dx^2} \, x \, dx \quad . \quad . \quad . \quad . \quad (7b)$$

Integrating by parts gives

$$i_{str} = \frac{paD}{8\eta\pi L} \left[\left(\frac{x d\Psi}{dx}\right)_{x=x_o}^{x=a} - \int_{x=x_o}^{x=a} \frac{d\Psi}{dx} \, dx \right]$$

$$= \frac{paD}{8\pi\eta L} \left[\left(\frac{x d\Psi}{dx}\right)_{x=x_o}^{x=a} - (\Psi)_{x=x_o}^{x=a} \right]$$

when $x = a$ $\quad \frac{d\Psi}{dx} = o$ $\quad$ and $\Psi = o$

when $x = x_o$ (x_o is relatively very small) $\quad \Psi = \zeta$ $\quad$ (ζ = zeta potential)

So, $\quad i_{str} = \frac{paD\zeta}{8\pi\eta L}$

and then the total streaming current crossing the cross section of the tube in unit time is

$$I_{str} = \frac{paD\zeta}{8\pi\eta L} P_s \quad . \quad . \quad . \quad . \quad . \quad . \quad . \quad . \quad . \quad (8)$$

where P_s is the total perimeter of liquid - solid interface in the cross section of the bed.

The previous formulas have been derived assuming a small portion of the solid boundary to be flat (see also derivations by Rutgers, 1940 and 1954; Neale, 1946; Wood, 1946b; and Gibbings and Hignett, 1966). However, the same equation could have been derived for a circular surface. In this case we use r, φ and Z (cylindrical) coordinates. In this coordinate, the Laplacian will be

$$\nabla^2\Psi = \frac{1}{r} \frac{\partial}{\partial r} \left(r \frac{\partial\Psi}{\partial r}\right) + \frac{1}{r^2} \frac{\partial^2\Psi}{\partial\varphi^2} + \frac{\partial^2\Psi}{\partial z^2} \quad . \quad . \quad . \quad (9)$$

But $\frac{\partial\Psi}{\partial\varphi} = 0$; axial symmetry, and $\frac{\partial^2\Psi}{\partial z^2} = 0$; linear potential gradient along the Z-axis, so

$$\nabla^2\Psi = \frac{1}{r} \frac{d}{dr} \left(r \frac{d\Psi}{dr}\right) \quad . \quad . \quad . \quad . \quad . \quad . \quad . \quad (10)$$

and consequently equation (5) becomes

$$\frac{4\pi\rho}{D} = -\frac{1}{r}\frac{d}{dr}\left(r\frac{d\Psi}{dr}\right) \quad . \quad . \quad . \quad . \quad . \quad . \quad . \quad (11)$$

The other changes will be that, instead of integrating with respect to x from $x = x_o$ to $x = a$, we shall now integrate from $r = o$ to $r = r_o$ where r_o corresponds to the radius of shear (Figure 1). Now we repeat the previous derivation which would lead to the same results provided that $r = r_o$.

Multiplying and dividing the right hand side part of equation (8) by A_o, where A_o is the cross sectional area perpendicular to the direction of the flow, gives

$$I_{str} = \frac{D\zeta}{8\pi\eta}\left(\frac{a P_s}{A_o}\right)\frac{A_o p}{L} \quad . \quad . \quad . \quad . \quad . \quad . \quad . \quad (12)$$

but $\frac{a P_s}{A_o} = \frac{\text{area of pores}}{\text{cross sectional area}}$

$$= \text{effective area of pores} = m = \text{superficial porosity}$$

then

$$I_{str} = \frac{D\zeta}{8\pi\eta}\, m\, \frac{A_o p}{L} \quad . \quad . \quad . \quad . \quad . \quad . \quad . \quad (13)$$

where $\frac{p}{L}$ is the hydraulic slope.

The quantity of flow (also called the quantity of seepage, discharge quantity or discharge) is $q = m A_o \bar{v}$ where $\bar{v}$ is the seepage velocity which is equal to $\frac{v}{m}$ where v is the discharge velocity (also called supervicial velocity).

From Darcy's Law

$$v = K\frac{dp}{dL}$$

where K is the coefficient of permeability

for uniform packing of homogeneous media $\frac{dp}{d} \cong \frac{p}{L}$

then

$$\frac{P}{L} = \frac{v}{K}$$

Kozeny's formula (cited by Leibenzon, 1947) gives

$$K = \beta \frac{d^2}{\eta} \quad \frac{\sigma^3}{(1-\sigma)^2} \qquad . \quad . \quad . \quad . \quad . \quad . \quad . \quad . \quad (14)$$

where σ is the porosity, d is the effective diameter (d_{10}), the viscosity of the fluid and β is Kozeny's coefficient considered to be constant for water. However, Zermin (cited by Polubarinova-Kochina, 1962) proposed for β the expression

$$\beta = 8.40\ (1.275 - 1.5\sigma)^2$$

therefore

$$I_{str} = \frac{D\zeta}{8\pi\eta}\ m\ A_o\ v\ \frac{\eta\ (1-\sigma)^2}{\beta\ d^2\ \sigma^3}$$

as the average value of m; superficial velocity is equal to σ ; volumetric porosity (Harr, 1962)

$$I_{str} = \frac{D\zeta}{8\pi}\ A_o\ v\ \frac{(1-\sigma)^2}{\beta d^2\ \sigma^2}$$

$$= \frac{D\zeta}{8\pi}\ q\ \frac{(1-\sigma)^2}{\beta d^2\ \sigma^2} = \frac{D\zeta}{8\pi}\ \frac{(1-\sigma)^2}{\beta d^2\ \sigma^2}\ .\ q \qquad . \qquad (15a)$$

For a certain porous bed, σ, d, and β are constants, and for a certain solid-liquid interface ζ and D are constant. Therefore

$$I_{str} = \text{constant x } q \text{ ..... } = C_1\ q \qquad . \quad . \quad . \quad . \qquad (15b)$$

Streaming Potential

This streaming current (convective current) is responsible for the streaming potential E_{str}. As a consequence of the streaming current, a potential difference will be set up between the ends of the bed which in turn will cause an electric conduction current I_c opposite in sense with the streaming current. At steady state, I_{str} will be balanced by I_c and the potential difference, "streaming potential," will remain steady as

$$I_c = - I_{str}$$

and the total current will be

$$I_c + I_{str} = o \qquad . \quad . \quad . \quad . \quad . \quad . \quad . \quad (16)$$

The conducting of the charge back will be through the liquid and solid surface so,

$$I_c = E_{str} \cdot \left(\frac{\text{pore area}}{L}\right) \cdot K_B + E_{str} \cdot \left(\frac{\text{Interface surface}}{L}\right) \cdot K_s$$

$$= E_{str} \cdot \left(\frac{P_s \times a}{L}\right) K_B + E_{str} \cdot \frac{P_s}{L} \cdot K_s = E_{str} \frac{P_s \cdot a}{L} \left(K_B + \frac{K_s}{a}\right)$$

where K_B and K_s the specific bulk and surface conductivity

$$I_c = E_{str} \cdot k \qquad . \quad . \quad . \quad . \quad . \quad . \quad . \quad . \quad . \quad (17)$$

where k is the total conductance which equals to

$$\frac{\text{pore area}}{L} \; K_B + (\text{perimeter}) \; K_s$$

The resistance of the electrolyte in the plug could be used for the total conductance (as $\frac{1}{R} = k$) of the plug in the previous equation, considering the surface conductance of the mineral could be neglected. However, experimental results (see for example Rutger,

1940; Jones and Wood, 1945; Gaudin and Feurestenau, 1955) showed that the contribution of surface conductance to the conductance of the electrolyte in the plug could be appreciable. This contribution is usually compensated by the use of a cell constant. In such case $k = \frac{C}{R}$, where R is the no-flow resistance between electrodes and C is the cell constant and

$$I_{str} = I_c = E_{str} \times \frac{C}{R}$$

So,

$$E_{str} = I_{str} \times \frac{R}{C}$$

$$= \frac{D\zeta}{8\pi} \frac{(1-\sigma)^2}{d^2 \sigma} \cdot \frac{R}{C} \cdot q \quad . \quad . \quad . \quad . \quad . \quad (18a)$$

under the previously mentioned conditions and as $\frac{R}{C}$ is constant, then

$$E_{str} = \text{Constant} \cdot q = C_2 q \quad . \quad . \quad . \quad . \quad . \quad (18b)$$

Equations (15) and (18) are valid only if the following conditions are fulfilled:

(a) The width of the pores 2a must considerably exceed the thickness of the electrical double layer δ (i.e. $\delta/a \ll 1$). Otherwise the condition $\psi = o$ at $r = a$ will not be satisfied and the streaming current or potential will be anomalously different.

(b) The length of the flow channel must considerably exceed the "characteristic flow length of the liquid" given by $\bar{v}D/4\pi k$, where $\bar{v}$ is seepage velocity and k is the specific conductance of solution.

(c) The flow must be laminar. If pressure and rates of flow are so high as to lead to turbulent flow, the streaming potential

(or current) increases nonlinearly with p . While this effect is not important for aqueous solutions under practical conditions, it is significant for non-aqueous solutions where the ionic double layer is much more diffuse and may extend into the region of turbulent flow.

(d) Darcy Law is valid and the media is homogeneous and isotropic.

Limitations and Assumptions

The previous conditions are to be satisfied for the validity of equations (15) and (18). The following is a discussion for those limitations in general and degree of approximation in cases where any of these conditions is no longer satisfied.

Laminar flow condition. The condition that the flow of the liquid must be laminar is easily fulfilled in practice. At high flow rates (Reynolds number $\simeq \frac{\rho V d}{\eta} > 1$), the flow becomes turbulent through a core constituting most of the pore space in which the velocity is nearly constant but the flow may remain laminar in a thin sublayer next to the solid boundary. The thickness of that layer is shown to be proportional to Reynolds number and pore diameter (space). The velocity gradient in the laminar sublayer during turbulent flow is much higher than that in equation (5), since most of the velocity gradient occurs in that region. Stewart and Street (1961) found measured indications of change in the $\frac{E}{p}$ slope (where E is the induced streaming potential and p the applied pressure) in pyrex glass capillaries when Reynolds number approached 2000. Those previous findings contrasted with those of Bocquet, Sliepcevich and Bohr (1956) who

concluded no effect in their work. However, Rutger, Desmet and Myer (1957) established such an effect for diffuse double layer (as in the case of benzene in contact with glass) in capillaries and were able to develop a relationship between streaming current and the average velocity $\bar{V}$ ($\bar{V}$ = discharge/cross sectional area) for turbulent flow as follows:

$$I_{str} = \frac{D\zeta\, a}{2\delta}\ \bar{V}$$

where I_{str}, D, ζ, are as defined before, δ is the thickness of diffuse part of double layer and a is the radius of the capillary. Similar equations were obtained by Davis and Ridel (1963). Boumans (cited by Davies and Rideal, 1963) developed the analysis for the case where some of the ions from the ionic sphere near the wall will extend into the turbulent core. His terms should be added to either Rutger or Davis equation to get the total streaming current.

The condition that the capillary radius should be large compared with the thickness of the double layer would appear, from practical point of view, not very restrictive. Only in very dilute solution and in very fine pores might this condition be questionable. White and his associates (1932, 1941) have shown that this assumption is valid in capillaries of diameter greater than 10 microns. However, a complete line of studies has been made to consider cases where the vurvature of the solid wall and capillary size were taken into account. Komogata (1934) (cited by Oldham and associates, 1962) solved for the streaming potential taking capillary size and wall curvature into account. Oldham, Young and Osterie (1962) gave an analytical derivation for cases where the capillary radius is not comparatively

large with respect to the thickness of the double layer. Burgreen and Nakache (1964) developed another analytical solution for the case of the ultrafine slit. Rice and Whitehead (1965) developed a solution for the case of fine cylindrical capillaries. In both it was shown that the electrokinetic potential is dependent upon electrokinetic radius which is directly proportional to the capillary radius. They suggested that their function be used in the case of ultrafine pores instead of the classical Helmoholtz equations in which the potential is considered to be independent of the capillary (pore) size.

Dielectric constant D and dynamic viscosity, η, factors. In the previous derivation, the dielectric constant, D, and the dynamic viscosity, η, of the liquid in the double layer were taken, as usual, the same as for bulk solutions. Some authors have pointed out that this assumption may be in error, especially in connection with dielectric constant. Gurney (1953) indicated that the presence of a concentration, c, of ions affects the viscosity, η, by a factor dependent upon the mobility of the ions and its concentration and absolute temperature. However, for low concentration levels obtained in streaming current flow, Hignett (1963) and Hignett and Gibbins (1965) showed that this effect of concentration upon the viscosity is insignificant. To account for the difference, in cases of higher concentrations and applied potential field where D and η might vary, Overbeek (1953a) and Davies and Rideal (1963) substituted for $\frac{D}{\eta}$ in their equations the term $\int_0^{\psi_o} \frac{D}{\eta} d\psi$. Biekerman (1940) also showed how correction could be made for cases of alternating current. The electrical field around a charged particle is also expected to

influence both η and D. However, comparison of theoretical results with experiment showed that both effects are rather small under most conditions (Hunter, 1966). Chattoraj and Bull (1959) and Hoydon (1960) have previously shown that for liquid surface having adsorbed films giving charge densities less than 30,000 esu/cm^2, a good agreement with the true potential may be obtained by assuming a bulk value for D and η in the double layer.

Surface charge densities are calculated from ζ potential by means of Gouy theory, for uni-univalent electrolyte at 25^{o}C it is (Parriera and Schulman, 1961)

$$\sigma' = \frac{c^{\frac{1}{2}}}{134} \text{ Sinh } \frac{\zeta}{51.5} \qquad . \quad . \quad . \quad . \quad . \quad . \quad (19)$$

where σ' is the electrokinetic charge, in electron charge/angstrom, c is the salt concentration in mole/litre, and ζ is zeta potential in millivolt.

In our case in here, ζ varies between 200 and 20 millivolt with salt concentration from 10^{-4} to 10^{-2} normal. Thus σ' is far below that specific value and no correction is necessary for assuming D and η to have bulk values. However, D, dielectric constant, depression in water caused by the addition of electrolyte could be considered. Investigations on that depression were first made by Haggis, Hasted and Buchman (1952). They investigated the previously published data by Hasted, Robinson and Collie (1948), for dielectric properties of aqueous ionic solutions. A reduction in D proportional to salt concentration c in moles/litre has been concluded by Glueckauf (1964).

Another variation in D with temperature has been conducted

experimentally using resonance method and Linton and Maoss have formulated those results as

$$D = 79.80 \left[1 - 4.28 \times 10^{-3} (t - 25) + 2.12 \times 10^{-5} (t - 25)^2 - 4.1 \times 10^{-7} (t - 25)^3 \right]$$

Partington (1954) has developed the following formula

$$D = 78.54 \left[1 - .0046 (t - 25) + 88 \times 10^{-5} (t - 25)^2 \right]$$

He also reported measured values for water at 25°C to be 80.37 and 79.2. Buchman and Heymann (1949c) reported D = 85.5, 80.8 and 76.5 for 6, 18 and 30°C respectively.

Our experiments were conducted in the constant temperature room where the temperatures were kept at a fairly constant temperature of 80 ± .5°F. At such controlled temperature, the temperature of water and solutions was generally kept at 25°C ± .2°C. So, D values in our calculation will be taken as an average value of 80 for pure water, NaCl, and KCl solutions.

The condition that Darcy's Law is applicable

Darcy's Law is applicable provided that the following conditions are satisfied (Olsen, 1961):

The soil particles are approximately (a) uniform, (b) larger than one micron, (c) small enough so that the liquid flow is laminar, (d) flow channels are uniform in size.

These four previously mentioned assumptions are satisfied with our samples and so Darcy's Law is applicable.

Thermodynamics of Irreversible Processes

Streaming current and streaming potentials

Since all electrokinetic processes are irreversible, the thermodynamics of irreversible (non-equilibrium) processes can be applied to derive general relationships between different electrokinetic processes including streaming potential and streaming current (Staverman, 1952; DeGroot, Mazur and Overbeek, 1952; Overbeek, 1953b; Guggenheim, 1957; Taylor, 1960, 1963 and 1964; Zaslavsky and Ravina, 1965).

When transport of liquid and transport of electric charge take place by simultaneous electrical and hydrodynamic processes, the electrical and viscous flows interfere with each other giving rise to irreversible processes (coupling phenomena) known as electrokinetic phenomena.

For saturated soil in absence of a composition gradient and salt concentration difference, in its linear region, the general relation between the "flows" q and I and forces "p" and "E" will be (Taylor, 1963)

$$\text{Flow rate} = J_w = q = L_{11}\, p + L_{12}\, E \qquad . \quad . \quad . \quad . \quad . \quad (20a)$$

$$\text{Current flow rate} = J_e = I = L_{21}\, p + L_{22}\, E \qquad . \quad . \quad . \quad (20b)$$

where

I = electric current through the system, q = volume rate of fluid flow through the system, E = electrical potential difference across the system, p = pressure difference across the system, L_{11} represents hydrodynamic conductance, L_{22} represents the electrical

conductance, L_{21} represents electrohydraulic conductance, and L_{12} represents the hydroelectric conductance or in view of Onsager relations, both are water-electric interaction coefficients and equal each other.

Using another form of phenomenological coefficients we can write

$$q = J_w = L_p + L_I I \quad . \quad . \quad . \quad . \quad . \quad . \quad (21a)$$

$$I = J_e = L_q q + L_e E \quad . \quad . \quad . \quad . \quad . \quad . \quad (21b)$$

As we have salt moving in the system, we should include another equation and another factor in each equation. In dilute solution, however, such as we used, it has been shown that the flow of salts may have negligible influence on water flow (Michaeli and Kedem, 1961).

The coefficients in equations (21) are related to those in equation (20) as follows

$$L_p = L_{11} - \frac{L_{12}\, L_{21}}{L_{22}} = L_{11}\,(1-L_c) \text{ where } L_c = \frac{L_{12}\, L_{21}}{L_{11}\, L_{22}}$$

$$, \quad L_e = L_{22} - \frac{L_{12}\, L_{21}}{L_{11}} = L_{22}\,(1-L_c)$$

$$, \quad L_q = \frac{L_{21}}{L_{11}} \text{ and } L_I = \frac{L_{12}}{L_{22}} .$$

Electrokinetic coupling

Electrokinetic coupling is the effect of the linkage between electrokinetic potential and the rate of water flow, i.e. the coefficient L_{12} in equation (20a). This is sometimes referred to as electrokinetic blocking, since it may oppose the flow of water

caused by a hydraulic pressure difference.

Hydraulic flow rates, q, through the sand permeant bed can be expressed as equation (20a) or (21a). The term $L_I(I)$ or $L_{12}(E)$ is the contribution of electrokinetic coupling to the flow. It will be convenient, in order to visualize that effect, to express it as related to the contribution of the hydraulic pressure to the flow rate. This can be done as follows:

If q_p is the rate of flow that would exist in the absence of coupling, then from equation (20a) $q_p = L_{11} P$, and

$$\frac{q_p - q}{q_p} = \frac{L_{12}}{L_{11}} \frac{E}{P} \qquad . \quad . \quad . \quad . \quad . \quad . \quad (22)$$

which, under condition of no electrical current (I = o) will be equal to $\frac{L_{12}L_{21}}{L_{11}L_{22}}$ by equation (20b). From equations (21) it will also be equal to $\frac{L_I}{L_p} \cdot \frac{I}{P}$. This term $\frac{L_{12}L_{21}}{L_{11}L_{22}}$ has been referred to previously as L_c, which is another form of electrokinetic coupling.

So, in order to evaluate any form of electrokinetic coupling, one should determine the three phenomenological coefficients ($L_{12} = L_{21}$, L_{11} and L_{22}). After having determined those coefficients from experimental results the influence of electrokinetic coupling on hydraulic flow rate may then be evaluated from equation (22).

Assumptions and conditions

In applying the phenomenological relationships and analysis herein to our system, several assumptions and conditions should be met. Assumptions inherent in the derivations and the proof of the theory of irreversible processes have been discussed in detail by Overbeek (1953). The following two conditions are discussed in here

because of their particular concern with the system under study:

(a) Fluxes are linearly related to driving forces; if they are not, then equations (20), (21) and (22) need to be expanded to the non-linear case.

(b) Only hydraulic and electrical gradients cause flows; if other forms are acting, then additional terms must be included in the above derivations.

The requirements that the forces and fluxes be linear were checked for each run and substantiated (Figures 25, 26 and 27). In each case the relation between the discharge q and pressure was shown to be linear the same as for the discharge and streaming potential.

The requirement that only hydraulic and electrical gradients cause the flow was met by the experimental conditions. The two side chambers were kept at equal temperature (the apparatus was placed and the whole procedure was run in the constant temperature room). The chambers also had equal ionic concentrations as there was no significant difference in conductivity of water samples taken from the two chambers (see Derjaguin and Duckin, 1960). Thus, there were only electric and hydraulic gradients across the system.

Evaluation of the phenomenological coefficients

Phenomenological coefficients of equation (20) are evaluated by relating them to the experimental results as shown in Appendix. Those in equation (21) could be evaluated either by comparing them to the former ones or by relating them to the experimental results. However,

one of these two could be used as a check on calculations. Tables 2 and 3 show a summary of these coefficients with their calculated values and their dimensions. Conversion factors between experimental results and the quantities required for computations of these coefficients are shown in Table 1.

CHAPTER IV

EXPERIMENTAL APPARATUS AND PROCEDURE

Apparatus

The experimental apparatus is shown in Figures 2 and 3. Details of different parts are shown in Figures 4 and 5. The apparatus consists of three main parts: streaming cells, flow system and pressure manometers and the electrical circuit and electronic equipment for measurement and recording of the streaming potential.

Streaming cell

Two identical streaming cells were used, one fitted with silver-silver chloride electrodes and the other with platinized platinum electrodes. Each consisted of a lucite tube of 8.85 cm inside diameter with a cross sectional area of 61.48 cm^2. The porous plug column 7.70 cm long, through which flow took place, was confined between two identical porous plates 6.2 mm in thickness and 90 mm in diameter sealed to the two side solution compartments each 10.16 cm long. The plates were kept in full contact with the porous sample by screwing in the two side compartments into a rubber "O" ring at the edges of the cell. The whole streaming cell unit was held together with brass bolts which were inserted through corresponding holes. Two electrodes (platinum or silver silver chloride) were fitted to the end of the porous plug and coupled with the electronic circuit as shown in Figure 6.

Flow system

Deionized (conductance) water and salt solutions were stored in an elevated pyrex reservoir. The liquid then flowed to the side tank which was kept at a desired constant position on the stand by bolting its support into the corresponding holes at equal distances into the stand. To keep the head constant in the tank, the flow was approximately controlled by the screw clamp and the outflow was wasted through an outflow system near the top of the tank. The tanks have provisions so that thermometers and conductivity cell electrodes can be fixed through the top of the tank. The flow connections are also arranged such as to allow for spot samples to be drawn during flow into or out of those tanks. Spot samples could be obtained also from the outflow system. Solutions from the tank were conveyed to the two side compartments (of either cell) through the flow control switchboard, which directs the flow to pass under a constant head to either cell in either direction, right left or left right as desired (see Figure 4). Each side compartment has an opening at the top for introducing solutions and is connected from the bottom—just before and after the two edges of the cell—to the manometer tubes. The difference in head (in inches of H_2O) was read on graduated scale from difference in water rise in the piezometeric tubes.

Electrical circuit and electronic equipment

A Keithly electrometer (model 150A) was used to measure the streaming current and streaming potential simultaneously. It has the range from one volt to one microvolt and from one microamper to 0.10 millimicroamper (10^{-10}) full scale on a zero-center meter. The

output from the electrometer was fed into the y axis of a time base recorder Model HR-96 where the x axis was an adjustable time of sweep. The recorder has a range from .05 in/sec to 20 in/sec in steps with a chart that provides 7 x 10 inches of plotting area.

Resistance and conductivity of the porous plug column were measured with a general radio impedance bridge (model 1650-A). The specific resistance and conductivity of the permeant solution were measured by dip in a conductivity cell model RC 16B2.

Details of Procedures

Preparation of sample water and solutes

Ottowa sand C109 and C190, grain size distribution curves shown in Figure 42, was leached repeatedly in boiling concentrated hydrochloric acid until no discoloration of the acid was observed. The sand was then washed with distilled water until the filtrate was free of chloride ion. This was achieved when the supernatant gave no coloration on the addition of drops of dilute silver nitrate solution. The material was then washed and stored under double distilled water which had specific conductance of less than 10^{-6} mhos.

Deionized water (conductance water) and distilled water were used for pure water measurements and conductance water was used for preparation of all salt solutions. Conductivity of the deionized water varied from 1.5 - 1.0 x 10^{-6} ohm^{-1} cm^{-1}. The water was deaerated in the lab by warming it to a 50°C and then boiling under reduced pressure then left to cool under vacuum. Deaeration will prevent air in the solutions from being entrapped in the soil sample

through the porous plate. Also, no trace of air would be formed on the electrode which might cause change in the electrode potential. Very few workers (Goring and Mason, 1950) concerned themselves with the deaeration of water, yet proper deaeration is essential in obtaining reproducible results and its importance cannot be too strongly emphasized. Chemical reagents used were purified crystal reagents.

Electrodes

Silver-silver chloride electrode. Silver-silver chloride electrodes were prepared from a perforated light platinum disc two inches in diameter and one millimeter thick. The disc had 144 perforations per square inch, each .032 inch in size. The face of the disc was covered with 80 mesh platinum gauze spot welded to it. A platinum wire was electrically spot welded to the back of the perforated disc. Electrical contact with the external circuit was made from a brass terminal and copper wire which was soldered (thermal free solder) to the platinum wire. The electrodes were boiled in concentrated nitric acid then washed for two hours under running water. Directly before silver plating, the electrodes were cleaned by anodizing in concentrated nitric acid for one hour with a current of 1 milliampere. The electrode was then washed with distilled water. For silver plating, two 250 ml beakers were used as anode and cathode compartments. An inverted U shaped tube was used as the salt bridge. The cathode compartment was mechanically stirred with a magnetic stirrer and platinum wire served as anode in the circuit. Potassium cyanide solution was used for silver plating. The concentration of the solution used (Ives and Janz, 1961) was approximately

10 gm ($K\ Ag\ (CN)_2$) potassium silver cyanide per litre. The salt was prepared after the procedure of Basset and Corbette: add 41 gm of silver cyanide to an aqueous solution of 20 gm potassium cyanide. When the silver plating solution was used for more than one time, it was freed from the free cyanide by adding dilute silver nitrate solution until no discoloration was observed. Silver deposition was continued for six hours at (0.4 ma cm^2) 81 ma. When the plating was finished, the electrodes were soaked in concentrated ammonium hydroxide (NH_4OH) for three hours and washed with water for two days. The same cell vessels were used in chloridizing the electrode with the electrode as anode in the circuit and electrodeposition. This process was performed in the dark by turning the light off and covering the anode vessel with black. The current density was the same ($.4$ m.a/em^2) for about 30 minutes using 0.1 N hydrochloric acid (HCl) as electrolyte solution. The electrodes were then washed in conductance water (deionized water) for two days. The color of the fresh electrode was sepia, yet after washing period the color changed to a pink shade. When the electrodes were fixed into the cell they gave a potential difference of 0.94 m.v. in 10^{-3} N KCl. This potential is sometimes referred to as no flow potential (Zuker, 1959; Korpi, 1960) or asymmetry potential and was isolated from measurements of the true values which were recorded.

Platinized platinum electrode. Platinized platinum electrodes were prepared from an 80 mesh platinum gauze two inches in diameter. Platinum wire was welded to the back of the gauze and electrical contact with the circuit was made as before (see Ag-AgCl electrode).

The gauze was briefly immersed in a dilute aqua regia (cleaning mixture made of three volumes of 12 N HCl, one volume of 16 N nitric acid and four volumes of water). The electrode was then treated with warm concentrated nitric acid and washed in conductance water. Immediately before platinization, the electrodes were cathodically electrolized in dilute (0.01 N) sulfuric acid for 10 minutes and 30 m.a. The electrodes were then washed with double distilled water and then platinized in the previously discussed electric cell filled with a two per cent solution of commercial platinum chloride in 2 N hydrochloric acid. The current density was 300 m.a. ($\approx$15 ma/cm^2) for 15 minutes. The whole procedure was then repeated while the electrometer was positioned to the current measurement. The deposition was hardly visible grey and the no flow potential was about 2 m.v. in conductance water.

Measurements of streaming potential and streaming current

The elevated pyrex reservoir 18 litre capacity was filled with the desired solution (distilled water, conductance water, salt at different concentrations or simulated natural waters). The head container was fixed on the stand to give the desired constant pressure head. The pressure head was kept constant by controlling the flow in and out of it by the screw clamps. The electrometer was then switched to the voltage measurements and its output connected to the time base recorder. The electrometer range was positioned together with the recorder attenuator control to give the desired sensitivity for the expected values. The sensitivity was then further adjusted

and the chart calibrated by adjusting the vernier control located in the center of the attenuator control. The multiple pole multiple throw electric switch was then switched to the desired cell (Ag-AgCl and platinum electrode cells) simultaneously. The flow switch board was then switched to let the solution flow from right to left through the sample. The streaming potential recorded continuously on the recorder chart. When the steady state condition for both the potential and pressure head was reached the manometer readings were recorded and the flow stopped. The flow was then reversed to flow from left to right and the previous process repeated. This whole procedure was then repeated at six to eight different pressures yielding several sets of data at different values of streaming potential. In the first preliminary runs the cell resistance was measured for each pressure and found to be fairly constant over the period during which the set of measurements was obtained and measurement at an intermediate pressure was sufficient. A potential difference was then applied to the porous plug under zero pressure and the corresponding current was recorded. Sample example of the recorded data is shown in Figures 7 and 8.

Measurements of discharge (flux) and other flow parameters

In the preliminary runs the fluid velocity was measured by introducing an air bubble into the outflow capillary tubes connected to the solution side chambers. The capillary tube was calibrated to give the discharge directly from the air bubble velocity of sweep. However, it was found that the flow was relatively high (ranging from

4.0 to 13 cm^3/sec) and the bubbles moved relatively fast to be followed especially at high discharges. So it was decided to measure the flow by collecting and measuring the value of the outflow—at the steady state—in a graduated cylinder for a certain time interval. Dividing the value of the outflow by the time interval gives discharge in cm^3/sec. The other items of the flow parameters were obtained by calculation.

Measurements of the cell constant

In the initial experiments the cell constant was determined with 0.1 N potassium chloride after the method of Briggs and subsequent workers (Briggs, 1928; Bull and Gortner, 1931; Jones and Wood, 1944; Korpi, 1961; Zuker, 1959; and Feurestenau, 1956). It is supposed that at about 0.1 N concentration, the surface conductance ceases to influence the bulk conductance of the pore liquid. However, Parriera and Schulman (1961) used 0.02 N KCl solution, Goring and Mason (1950) used .05 N KCl solutions for the determination of the cell constant. In order to obtain a reliable concentration to be used in our experiments, a series of experiments were conducted to determine the optimum concentration of electrolyte necessary to eliminate surface conductance effects in connection with Ottowa sand. Progressively stronger solutions of potassium chloride, KCl, in distilled water were used as the permeant liquid in the plugs and the normality of each solution was predetermined. The conductivity of the effluent liquid was determined using a dip in conductivity cell.

The variation of the plug cell constant, C, with concentration of potassium chloride is summarized in Tables 5 and 6 and shown in

Figure 43. For distilled water and diluted solutions of KCl, the specific conductivity of the plug was compared to that of the bulk liquid thus indicating a large surface conductance. With increasing concentration of electrolyte, surface conductance effect becomes less and the greater part of the conductivity becomes due to bulk liquid.

The cell constant, C, (C = conductivity of the liquid x bulk resistance of the plug) therefore decreased until the normality reached such a value that surface conductance was no longer significant; C then remained almost constant. From Figure 43 it is evident that, for the plug, the cell constant, C, is effectively constant for the range of normality = 5×10^{-5} through 2×10^{-2}. So a value for C = 0.85 was taken as a representative constant for the first sample 1 and C = 0.510 for sample 2.

Flow (asymmetry) potential

The change in streaming potential is usually confused by the presence of another potential difference which usually persists even when the liquid flow is stopped. Much of the disagreement among streaming potential workers appears to be due to this other potential which was referred to as "asymmetry potential" by Hunter and Alexander (1962) and as "flow potential" by Modi (1957), Li H. C. (1958), Zuker (1959) and Korpi (1960).

This extraneous potential was observed by many investigators and was thoroughly investigated by Zucker as the primary subject of his Doctoral dissertation. He concluded that this "flow potential" is not a function of the plug material electrolyte, electrical instrumentation or cell construction, but it was found to be associated

with the electrodes. He also concluded that this extraneous potential is made up of two phenomenons, one associated with the flow and the other with polarization. However, polarization could be in turn connected to the flow conditions. The fact that polarization potential may stay constant during flow but may change once flow has stopped indicates that connection. Thus one can conclude that the electrode contributes an arbitrary EMF to the streaming potential which continues for a period after the flow has stopped.

Previous methods of obtaining streaming potential

Although electrode potentials (flow, polarization) had been noticed some time ago, it was not until recently (Zuker, 1959; Korpi, 1960) that thorough investigations have been made. Most of the previous workers tried to eliminate the electrode effects or render them insignificant—in order to obtain the true streaming potential—by one or more of the following methods:

(a) Limit salt concentrations ($<10^{-4}$ N) and use freshly plated reversible electrodes to decrease polarization effects especially in connection with platinum electrodes.

(b) Use a very high pressure (rate of flow) to make that effect relatively small. In these cases the assumption that the flow should be laminar may be violated and the flow might sometimes be turbulent. Also, the flow effects (which were not understood until later after Zuker) were also affected by the flow.

(c) Feurestenau and subsequent workers (Modi, 1957; Li, 1958) used a procedure in which solutions flowed first in one direction

under a known almost constant pressure and the streaming potential was read, then the flow was stopped and readings were taken after sixty seconds. Next with the flow in the opposite direction the streaming potential was measured. The no flow potential (reading after sixty seconds from the flow stoppage) was added or subtracted as correction to the reading depending on the direction of the flow.

This procedure produced a straight line relationship between E_{str} and the pressure, P, for solutions of very low concentrations. Yet it produced anomalous curves for solutions with concentration greater than 10^{-3} N. Also, the corrected streaming potentials in both directions do not seem to agree and produce two separate lines for E-P relationships not passing through the origin, a case which is not supported by the electrokinetic phenomena.

Korpi used a procedure—which was the primary object of his thesis—in which he tried to eliminate the arbitrariness of the potential corrections after the flow stopped by continuously recording the streaming potential on a recorder. Using the same principle, Parriera (1965) developed an automatic recording apparatus for measurements of the streaming potentials. Korpi's procedure will be discussed together with suggested modifications in the following sections.

The steady state condition

Two factors have been overlooked by the previously mentioned investigators. The first is the fact that experimentally, when the liquid flow commences, the streaming potential will increase until the steady state. It is only at this steady state (stationary)

condition that the convection current, I_{str}, is balanced by the conduction current (counter current), I_C, and then the total flow of electricity will be zero; $I_{str} + I_C = 0$. It is when this condition prevails that one should stop or start the flow and record the readings which will be the actual streaming potential.

Secondly, the electrode contribution to the streaming potential is embodied in the streaming potential readings and prevails for a period after the flow is stopped (Zuker, 1959). That contribution is related to the flow and proved to be directional. So when the flow is suddenly stopped or started, the sudden increasing or decreasing ordinate is not only the streaming potential but will also be the flow potential added or subtracted to the streaming potential depending on the flow direction.

Modifications in the recommended procedure

In the procedure used in this investigation the streaming potential was recorded simultaneously with the streaming current for the same constant pressure and discharge on a time base recorder. An example of these recordings given in Figures 7 and 8 shows the actual form in which the data was obtained from the recorder. Referring now to Figure 9, at a, the solution starts flowing from right to left through the plug. When the steady state was reached—under constant head and rate of flow—at b, the flow was stopped. The potential E_b is the sum of the streaming potential E_{st}, the flow potential (electrode potential) E(el) and the polarization potential E(Pol). E_d is the polarization potential at steady state for no flow, so we can assume that $(E_b - E_d) = E_{st} + E_{d_{el}} = b$. Also, $(E_f - E_h) = E_{st} - E_{}$

= a. The actual streaming potential will then be $\frac{a + b}{2}$. Korpi's method when used will give an erroneous value either $(E_b - E_c)$ or $(E_f - E_g)$. Those two values will algebraically include, rather than the electrode potential, the effect of the response of the recorder. This factor was observed by Korpi and suggested as a source of error in his recorded values. As it could be seen from Figures 10 and 11, for 10^{-4} N KCl and 10^{-3} N KCl if Korpi's method were used, then streaming potential in one direction will be 25 per cent to 100 per cent more than that in the other direction (compare ordinate 1 and 2 of the figures). The efficiency of our procedure is appreciated for the cases of relatively high concentration and low pressure (rate of flow). In these cases the error effect using the Korpi method may be more than the actual readings, and the ordinate considered by Korpi may give negative values.

CHAPTER V

RESULTS AND DISCUSSIONS

Reliability of Experimental Data

There are some sources of test errors that could affect the measured data, namely streaming potential, streaming current and flow and pressure measurements.

With the method used in this study, the results were observed from Ag-AgCl electrode cell and platinized platinum electrode cell. The two cells were identical in size, length and shape. The solution and system were also the same (see the procedure). Typical values of streaming potential and streaming current obtained from the two electrodes for conductivity water and NaCl solution are shown in Figures 12, 13 and 14. Figure 15 shows α , where $\alpha = \frac{E}{q}$ in $\frac{\text{m.V. sec}}{\text{cm}^3}$ vs normality of KCl solution permeating through S, for Ag-AgCl and Pt-Ptl cells. From these figures it can be seen that the results obtained from Ag/AgCl electrodes are identical to those obtained from the platinum electrodes for streaming potential and streaming current for both sizes of sand used.

The significance of this reproducibility is that the platinum electrodes fitted in a separate cell and with electrode potential completely different gave almost the same results as did Ag-AgCl electrodes fitted into another separate identical cell. This indicates that despite the difference in behavior of the two electrodes, it was possible to obtain similar values for streaming potential and

streaming current induced due to the same differential pressure head.

Most of the results obtained produced a straight line relationship between both E and I and the effective differential pressure or discharge. These lines passed by the origin in agreement with the electrokinetic phenomena and the analytical developments.

Flow and pressure measurements were found to be sufficiently consistent for repeated runs at steady state conditions. Errors from these sources, if any, are within the precision of the test measurements.

Experimental Results

Summary of the complete results from the experimental investigations is given in Figures 25 to 41. Only concluding results are presented here which illustrate the principal features of the streaming current, streaming potential, rate of flow and effective pressure relationships.

Electrolyte solutions used were primarily conductance water, distilled water, NaCl and KCl solution at different salt concentrations. In reporting the results S_1 will denote sand plug with 0.23 millimeter of effective diameter and effective porosity of 31 per cent. Also S_2 will appreviate sand plug with effective diameter of 0.575 millimeter and effective porosity of 28 per cent.

Typical results on an actual recording chart are shown in Figures 7 and 8. Procedure for interpretation and obtaining the actual streaming potential and current following our modified procedure are shown in Figure 9.

Experimental results are presented here under the following headings: (a) Plug resistance, (b) Rate of flow and applied differential pressure, (c) Phenomenological coefficients and electrokinetic couplings, (d) Rate of flow and developed streaming potential and streaming current, (e) Salt concentration and particle size effects, (f) Temperature effects, (g) Zeta potential, (h) Practical considerations.

Plug resistance

The plug resistance of the cell was measured for each run and results are shown in Figure 16. In this figure log plug resistance is plotted against log electrolyte concentration (normality) in the permeating solution are tabulated. From the graph it can be seen that all resistances are below 10^5 ohms for concentrations greater than 10^{-4} N.

Measurements of resistance were made by both general radio impedance bridge and by a lab made impedance bridge. Similar values were obtained all the time and values reported are the average of the two readings, one on each apparatus for each setting of the flow.

As we know, ohms law, $R = \frac{E}{I}$ does not hold for transport current, but did hold for conductance current at zero flow. Figure 16 shows values of resistance measured by the bridge and $(\frac{E}{I})_{q=o}$ values. From the figure there is no significant difference between the two readings.

Rate of flow and applied differential pressure

Flow rate means flow rate per unit time, i.e. cm^3 per second. For calculation of seepage velocity in cm/sec, it must be divided by a factor equal to the cross-sectional area multiplied by the porosity. For S_1 this factor will be equal to 19.06 and for S_2 it is equal to 17.20. The applied differential pressure here is the pressure between the ends of the sample in centimeters of water, for pressure per unit length it has to be divided by 7.70. Each point on the graphs shown is the average of two readings, one with solutions flowing left to right and the other with solutions passing right to left through the plug for all values measured.

Values for the rate of flow in cm^3/sec are plotted as a function of applied pressure in cm of water on Figures 25, 26 and 27 for conductance water, sodium chloride and potassium chloride solutions respectively. Values shown are both while measuring streaming current and streaming potential. An increase in applied differential pressure resulted in an increase in the rate of flow and a straight line relationship was obtained between the rate of flow, q, and the pressure p. For all cases this line passed through the origin. This indicates a linear relationship between p and q with a constant coefficient of proportionality (coefficient of permeability). From the Kozeny formula, the coefficient of permeability K is given by

$$K = \beta \frac{d^2}{\eta} \frac{\sigma^3}{(1-\sigma)^2} \quad . \quad . \quad . \quad . \quad . \quad . \quad (14)$$

And from Darcy's law, $v = K \frac{p}{L}$

The discharge rate q will then be

$$q = K \frac{p}{L} \cdot A$$

$$= \frac{\beta d^2}{\eta} \frac{\sigma^3}{(1-\sigma)^2} \cdot A \cdot \frac{p}{L} \quad . \quad . \quad . \quad . \quad . \quad . \quad (23)$$

for S_1 $d = 0.023$ centimeters, $\sigma = 31\%$ and $\beta = 5.50$, and

for S_2 $d = 0.0575$ centimeters, $\sigma = 28\%$ and $\beta = 6.12$

and

$$\frac{(\frac{q}{p}) \text{ for } S_1}{(\frac{q}{p}) \text{ for } S_2} = 0.20$$

From the previous experimental results reported in this study (Figures 25, 26 and 27), $\frac{q}{p}$ for S_1 is on the average = 0.485, and for $S_2 = 2.20$.

then

$$\frac{(\frac{q}{p})_{S_1}}{(\frac{q}{p})_{S_2}} = \frac{0.485}{2.20} = 0.22$$

which is in agreement with the expected value of 0.20. This suggests that Kozeny formula could fit the experimental data. This is in agreement with the conclusion given by Wylie and Spangler (1952), that is for the ranges of the coarse sand, in a range similar to the one in this study, Kozeny formula will fit the flow data with β taken usually as 5.0. To detect the effect of counterelectro-osmosis—due to the developed streaming potential—on the flow, values for q are plotted versus p while measuring streaming current, and while measuring the streaming potential. From the figures it is

clear that there was no significant difference in the p vs q relationship due to counterelectro-osmosis. This means that $(\frac{p}{q})_{E=o}$ will be the same as $(\frac{p}{q})_{I=o}$. The effect of salt concentration of the pore fluid on the rate of flow showed in general that there was no effect on the pressure discharge relationship due to change in electrolyte concentration for both samples and solutions tested.

Phenomenological coefficients and electrokinetic couplings

Phenomenological coefficients were determined from experimental results together with equations (20) and (21) and calculated values are summarized in Tables 2 and 3. As these equations involved both electrical and mechanical units it was necessary to convert the experimental results into cgs units. These required conversion factors are tabulated in Table 1. After having determined those coefficients, the influence of electrokinetic coupling on the hydraulic flow rate was computed using equation (22). This was done for all runs and the calculated results are given in Tables 2 and 3, which express in per cent the amount by which the flow rates were reduced due to electrokinetic couplings, relative to the flow rate that would exist in the absence of coupling. As seen from these results, these values were of negligible amount and could be ignored.

From the phenomenological analysis (see also Overbeek, 1953b, and Henniker, 1952) a conclusion was drawn that the hydrodynamic resistance is smaller when short circuited electrodes connect the two ends of the sample (while measuring I_{str}) than when no electric current is allowed in an outside circuit (while measuring E). This

means $\left(\frac{q}{p}\right)_{E=o} > \left(\frac{q}{p}\right)_{I=o}$. Also, as we have salt moving with the system, then it is expected that the flux of salt would affect the rate of flow (Taylor, 1964). The experimental result, however, has shown neither. This is due to the fact that, in case of saturated coarse sand, the linkage transfer coefficients are very small with respect to the direct ones. Also, in dilute solution such as the ones used, it has been shown that (Michaeli and Kedem, 1961) the flow of salts has negligible influence. This means that the flow of solution is determined only by the effective pressure, and this is what was actually observed.

Rate of flow and developed streaming potential and streaming current

The values for streaming potential, E, for different samples considered ranged from 30×10^{-6} to 240×10^{-3} volts. Streaming current values varied from 12×10^{-9} to 1.0×10^{-6} amperes. Values for both E and I were influenced by both the size of the soil particles and the salt concentration of the percolating solutions.

Streaming potential and current values are plotted as a function of their corresponding rate of flow for pure water (conductance and distilled water) and for electrolyte solutions at different salt concentrations (Figures 28 to 41). For all solutions and both soil samples used, an increase in the rate of flow resulted in a linear increase in the developed E and I. This line generally passes through the origin irrespective of solutions and sample used.

Since the charge carried per second (I_{str}) by the liquid in any cross section of the sample is a function of the local velocity v

and the charge density ρ

as $$I_{str} = P_s \int v \rho \, dx \qquad . \; . \; . \; . \; . \; . \quad (24)$$

one would expect it to be influenced by both ρ and v. Hence, an increase in the rate of flow (consequently v) keeping ρ and P_a constant (and the flux is laminar) would increase the speed by which the charge is conveyed and the streaming current will directly increase with the rate of the flow. As the liquid flow commences, a potential difference will be set up between the ends of the sample, which in turn will cause an electric conduction current opposite in sense to the streaming current. This potential will increase until the steady state conditions prevail (Figure 9), then it remains fairly steady and the streaming current is balanced by the conduction current. Thus an increase of the speed of the charge convection is expected to increase the rate of change in E. Consequently, if the conductivity of the system is kept constant, E would be expected to increase linearly with q, as

$$(E) \cdot (\text{conductivity}) = I_c, \text{ and at steady state}$$

$$I_c = - I_{st} .$$

This is in agreement with the experimental results reported for all cases and in agreement with the electrokinetic phenomena.

Salt concentration and particle size effects

An increase of soluble salt concentrations (normality of the solutions) resulted in a decrease in both E and I. A sharp decrease is seen in case of streaming potential, whereas a gradual decrease is observed for the case of streaming current. When the slope

$\alpha = \frac{E}{q}$ in millivolt-sec/cm^3 was plotted as a function of salt concentration N in the percolating fluid a straight line was obtained on a log-log scale (Figure 17). In the case of streaming current, a straight line relationship was obtained between β (where β is the slope $\frac{I}{q}$ in milliamper-sec/cm^3) and the log salt concentration in the percolating solutions, N (Figure 18). Similar relationships were also obtained for KCl solutions (Figures 19 and 20). Plots of α against salt concentration in the percolating fluid is shown in Figure 21. In this case, α values are for both KCl and NaCl solutions. It is clear from the values obtained for all salt concentrations tested that E and I values—for the same soil sample at a specified discharge—are affected by salt concentration, N, and less affected by the type of ions in the solutions.

To show the effect of the size of the sand particles, a comparison between S_1 and S_2 is shown in Figures 17 and 19 for α against salt concentration N. In these plots α was presented as a function of N with the size of sand particles as a parameter. As shown in the figures, values of α were always higher for S_1 than for S_2 for both NaCl and KCl solutions. Hence, plots of α against N on a log-log scale are a function of the size of the soil particles. As shown in Figures 17 and 19 in the range of the concentration tested the two lines for S_1 and S_2 are not parallel but approach each other as the salt concentration N in the permeant solution increases. This suggests a linear relationship between α and N in the form of $\log \alpha = a \log N + b$ where b is constant value related to the size of the solid particles and a as a factor related to the salt

concentration. Similar relationship in the form of $\beta = c \log N + d$ where d is another constant value for each size and c related also to the salt concentration. This could be seen from Figures 18 and 20. In this case the two lines approach each other in a similar manner.

The conveyance of charges is limited only to the diffuse part of the double layer, i.e. to the liquid that can flow with respect to the surface. The potential within such layer decreases practically in exponential manner (see Figure 1). This diffuse double layer has no sharply defined end point but slowly becomes negligible. It is nevertheless convenient to assign to it a thickness designed usually by δ . This thickness changes greatly with the normality of the solution. Hence, when the salt concentration in the permeating solution increases it suppresses the double layer, especially its diffuse part. This compaction of the double layer would shift the suppressed diffuse part nearer to the wall where it will be conveyed at relatively lower velocity. Potential at the wall, also, cannot remain the same but must decay faster (Ham, 1940). The slipping plane may be also changed (Kruyt, 1952). Consequently smaller values for ζ would be expected.

If, as is usually the case, the thickness of the double layer is extremely thin compared to pore diameter, then the gradient of the velocity $\frac{dv}{dx}$ can be assumed to be constant inside this layer, and the change in i_{str} due to lower conveyance would be linear. A straight line was always found when log ζ was plotted against log salt concentration in the permeating solution. As I_{st} is affected

by both v and ζ then one would expect it to vary linearly with log salt concentration. The reason for more rapid decrease of streaming potential E (than streaming current I) due to increase in salt concentration may be due to the fact that E is proportional to both I and the conductivity of the bulk solution. Hence, rather than being proportional only to η and the conveyance, it is also affected by change in the conductivity. The latter is found also to be proportional to log salt concentration. Therefore, one would expect log α ($\alpha = \frac{E}{q}$) to be proportional to log normality of the bulk solution.

According to classical derivations (Helmoholtz and Smowlowsky) the size and shape does not affect streaming potential. The conventional equation

$$E = \frac{1}{4\pi} \frac{D}{\eta} \frac{P}{k} \zeta \qquad . \quad . \quad . \quad . \quad . \quad . \quad . \quad (25)$$

where E is the streaming potential, P the applied pressure drop, D the dielectric constant, k is the average specific conductance of the liquid in the capillary and ζ is the zeta potential and η is the dynamic viscosity—gives E as independent of size and shape, a conclusion not supported by many experimental results. Debye and Huckle criticized that conclusion contending that the constant $\frac{1}{4\pi}$ should vary with the capillary's shape and that $\frac{1}{4\pi}$ is valid only for cylindrical tubing. Henry and Mooney (1931) in later analysis advocated Huckle's conclusion. Wood (1946b) introduced—in an analytical derivation—what he termed the "radius effect" which indicates the effect of the size of the capillary on the streaming potential. He supported his conclusion by noting some experimental results by Bull and Gortner (1932) who investigated particle size

effects on the zeta potential. However, it was pointed out later by Ghosh, Rakshit and Chattoraj (1953) that Wood's "radius effect" counts only for a small portion of the zeta variation with change in particle size. They attributed that variation to the change in surface conductivity. Similar conclusions have been presented by Ghosh, Choudhyry and De (1954) for pyrex glass.

The problem could be better visualized, however, if it is realized that the streaming potential is affected by the hydrodynamic conditions of the system as well as by the surface area of the solid liquid interface. Equation (18a) gives $\frac{E}{q}$ as

$$\frac{E}{q} = \zeta \cdot \frac{D}{8\pi} \cdot \frac{(1-\sigma)^2}{\beta d^2 \sigma^2} \cdot \frac{R}{c} = \zeta \cdot \frac{D}{8\pi} \cdot \frac{1}{K_o} \cdot \frac{R}{c}, \text{ where}$$

$$K_o = \frac{\beta d^2 \sigma^2}{(1-\sigma)^2}$$

So provided that $\frac{R_1}{c_1} = \frac{R_2}{c_2}$

$$\frac{(\frac{E}{q}) \text{ for } S_1}{(\frac{E}{q}) \text{ for } S_2} = \frac{\zeta_1}{\zeta_2} \cdot \frac{(K_o)_2}{(K_o)_1} = \frac{\alpha_1}{\alpha_2}$$

Assume ζ_1 equal to ζ_2, then from experimental results $\frac{(K_o)_2}{(K_o)_1} = \frac{\alpha_1}{\alpha_2}$ would be equal to 4.10 and the two lines for S_1 and S_2 on Figure 18 would be expected to be parallel, with their ordinates in the ratio of 4.10. From the figures, however, the two lines approach each other as the salt concentration in the permeating solution increases. This change is certainly due to change in ζ. When ζ was calculated using the procedure of this study, values for S_2 were larger than those for S_1 in a manner shown in Figure 22. When values for $\frac{\zeta_2}{\zeta_1}$ were multiplied by $\frac{1}{4.10}$ and calculated ratios (shown in Table 4)

were multiplied by α_1 and the resulted values were plotted on Figure 19 together with the experimental results, a close agreement was obtained. The difference between calculated and observed values, however, is thought to be due to the difference between $\frac{R_1}{c_1}$ and $\frac{R_2}{c_2}$. This difference was actually about 10 per cent.

Temperature effects

By temperature effects it is meant the effects of change in temperature of the sample and the percolating solutions on the resulting streaming potential provided that all other factors are kept constant. All the experimental results reported in these have been obtained by keeping the whole apparatus in the constant temperature room with the liquid solutions always left in the room until their temperature was the same as that of the room, i.e. at 80 $\pm$ 1°F. However, two special runs were made with the temperature in the room kept constant at two different temperatures, namely at 85 $\pm$ 1°F and the other at 62 $\pm$ 1°F. The developed streaming potential E was plotted as a function of q with the temperature as a parameter (Figure 23). From the graph it is clear that $\frac{E}{q}$ is higher for 62°F than for the 85°F. This indicates that temperature would have an appreciable effect on the experimental results if temperature of the experimental apparatus was not controlled. This trend needs more investigation before any firm conclusions can be made about the detailed nature of the temperature effect.

Temperature effects on the electrokinetic potential were also observed by Buchanan and Heymann (1952). They reported an increase in ζ potential with decreasing temperature with $\frac{d\zeta}{dT}$ being in the

order of -0.20 millivolt/^{o}C. Variations due to temperature effects may be related to the increasing thickness of the double layer with the increase in temperature. It also could be due to changes in dielectric, D, and viscosity η with change in temperature. As shown previously in Chapter III, $\frac{dD}{dT} = -.30$ was reported for conductance water.

Zeta potential

Of paramount importance in the quantitative study represented here is the evaluation of the zeta potential ζ. As mentioned before, ζ is the potential at the plane of shear (Figure 1), that is the potential at the boundary between the solvent adhering to the particles at rest and that which moves with respect to it.

Streaming current is given previously as

$$I = \frac{D\zeta}{8\pi} \frac{(1-\sigma)^2}{\rho d^2 \sigma^2} q \qquad . \quad . \quad . \quad . \quad . \quad . \quad (15a)$$

If I is measured in ampers, q in cm^3/sec, d in centimeters and ζ in millivolts and D taken as 80 (Guggenheim, 1940; Wood, 1946a; Hunter, 1961) then we have

$$I = 3.54 \times 10^{-12} \zeta \frac{(1-\sigma)^2}{\rho d^2 \sigma^2} q \qquad . \quad . \quad . \quad . \quad . \quad (26)$$

For S_1, ζ will be

$$\zeta_1 = 1.75 \times 10^9 \frac{I}{q} \qquad . \quad . \quad . \quad . \quad . \quad . \quad . \quad (27)$$

And for S_2, it will be

$$\zeta_2 = 8.60 \times 10^9 \frac{I}{q} \qquad . \quad . \quad . \quad . \quad . \quad . \quad . \quad (28)$$

Calculated values for ζ_1 and ζ_2 for KCl are tabulated in Table 4 and were plotted as a function of KCl concentrations (Figure 22). As shown in this figure, ζ decreased linearly with the logarithm of the salt concentrations with ζ values higher for S_2. Two separate lines fitted the calculated values for ζ_1 and ζ_2 . These two lines are not parallel but approach each other as salt concentration decreases.

Helmoholtz-Smowluchowski classical formula is usually used in calculating ζ potential from streaming potential measurements. This equation has been amended by several authors (Briggs, 1928; Rutgers, 1940) and there is a general agreement now (Buchanan and Heymann, 1949c) to use the equation

$$\zeta = \frac{4\pi\eta}{D} \frac{Ek}{p} \qquad \ldots\ldots\ldots \quad (29)$$

where all items as defined before, for the calculation of ζ denoted usually in the literature by ζ_a. The term k in this equation represents the effective specific conductivity (total conduction). This will include both specific and surface conductance. It is common practice now to compute k from the actual resistance R and the cell constant c as $k = \frac{c}{R}$. The accuracy of such procedure, however, depends upon determining the cell constant with sufficient precision in a manner which avoids errors due to surface conductance.

Another problem with this equation is that, in well conducting system, E may be too small for accurate determination. Therefore it was suggested by some workers (Buchanan and Heyman, 1949c; Davis and Rideal, 1961) to use the streaming current measurements instead of streaming potential for the determination of ζ . This approach is

considered to avoid surface conductance problems. Buchanan and Heyman suggested the function

$$\zeta = \frac{4\pi\eta}{D} \frac{Ic}{p}$$

where all variables as defined before. The equation still includes c, which would affect the precision of calculation. The Davis and Rideal relation is applicable only for capillaries and needs to be adjusted to be used for porous materials.

In our procedure we use

$$\zeta = \frac{8\pi}{D} \frac{\beta d^2 \sigma^2}{(1-\sigma)^2} \frac{I}{q} \qquad . \quad . \quad . \quad . \quad . \quad . \quad (30)$$

This is believed to constitute a satisfactory method of finding ζ. Besides avoiding conduction problems, it points out the effect of both size and shape of the media on ζ. Our calculated values for ζ for 10^{-4} N KCl is 190 m.v. This is in close agreement with the values given by Rutger and Desmet (1945 and 1947) and by Jones and Wood and Wood and Robinson (1945 and 1946a) for jena glass capillaries (200 m.v.) and quartz capillaries (177 m.v.). These two values were determined using both streaming potential and electro-osmosis methods.

Practical considerations

A main objective of this study is to present an approach for a new method to evaluate quantitatively the flow rate through porous material. Dissolved salts in the permeant solutions have a remarkable effect upon the interpretation and evaluation of the experimental results obtained with this suggested method. Soluble salts found in ground water originate primarily from solution of rock

material. Sedimentary rocks are more soluble than igneous rocks. Because of their high solubility combined with their abundance in the earth's crust, they furnish a major portion of the soluble constituents to ground water. Out of the commonly added cations due to sediment rocks sodium, Na, and calcium, K, have the highest possibilities. Bicarbonates, carbonates and sulfates are the corresponding anions. Chloride, Cl, also occurs to a certain amount, with sewage, connate waters and intruded sea water as its major contributing source (Foster, 1942; Todd, 1960).

For the experimental results reported in this study, two salts (NaCl and KCl) were used as solute in the test solutions. For each run, one at a time each of the two salts at a specified concentration was used. The normality of the solutions was used to express their salt concentrations. Therefore, it was felt necessary to test the validity of the procedure used in this study for cases with solutions similar to naturally existing percolating ground water.

For that purpose, solutions were prepared in the lab to simulate some selected ground water samples reported in the literature (Doneen, 1950). These solutions were then used as permeant solutions in our experimental apparatus using the same experimental procedure described before. The chemical analysis for these solutions is given in Table 7. Streaming potential and current obtained for these solutions were then plotted as a function of their corresponding rate of flow (Figures 33, 34, 40 and 41). For all cases, these plots produced straight line relationships similar to those obtained before for solutions with one salt as a solute in the percolating

solutions. This suggests the feasibility of the use of this procedure for naturally existing ground water with dissolved combined salts as well as solutions with one soluble salt.

Considering the difficulties connected with the determination of the normality of these natural waters, an alternative method to the normality was thought to be used to express the concentration of solutions. This is done by measuring the electrical conductance of the solutions. When the experimental results (for E, I and q) for these simulated natural ground waters were compared to those for NaCl and KCl solutions tested before, comparable results were obtained provided that conductance of the solutions was taken as a parameter (Figure 24).

CHAPTER VI

CONCLUSIONS AND SUGGESTIONS FOR FURTHER RESEARCH

Conclusions

Analytical derivations and analysis of the experimental investigations, together with the subsequent interpretation and discussions of the results from this study, suggest the following conclusions with respect to streaming current and streaming potential induced by water flow through porous media.

1. The flow through samples tested followed Darcy's law and the ratio of permeability coefficients of different samples agreed with Kozeny-Carreman equation.

2. There was no significant difference in flow versus pressure relationship due to counter-electro-osmosis (electrokinetic coupling) or changes in electrolyte concentrations in the ranges of the experiments in this study.

3. A modified procedure is recommended for the measurements of both streaming current and streaming potential through porous materials. This recommended modified procedure is important for cases of relatively high concentration and low pressures.

4. Streaming current and streaming potential induced by flow through porous material were directly proportional to the rate of the flow. An increase in the rate of the flow at a constant salt concentration and soil particle diameter resulted in an increase in the developed streaming potential and current. Emperical equations

in the form of $I = C_1 q$ and $E = C_2 q$ are suggested in which C_1 and C_2 are dependent upon salt concentration and particle size diameter.

5. Both streaming current, I, and streaming potential, E, were affected by salt concentration (normality N) and less affected by the type of ions in the solution. An increase of soluble salt concentration resulted in a decrease in both E and I. A sharp decrease was observed in case of streaming potential whereas a gradual decrease was observed in the case of streaming current.

6. Increase in soil particles effective diameter, at a constant salt concentration, caused a decrease in both α and β, where $\alpha = \frac{E}{q}$ and $\beta = \frac{I}{q}$. This decrease was more for dilute solutions. These relationships may be expressed by log α = a long N + b and β = c long N + a where a and c related to salt concentration, b and d related to particle size.

7. Temperature changes would have an effect on the developed streaming potential and current.

8. The procedures used in this study are suggested to be used for naturally existing ground waters with dissolved combined salts as well as solutions with one soluble salt in the range tested in this study.

9. Comparable results were obtained for simulated natural waters and NCl and KCl solutions, provided that the conductance of the solution was taken as a parameter.

10. Although electrokinetic coupling has but a negligible effect on the rate of flow samples tested in this study, the phenomenological coefficients procedure presented seems to be a reliable and

easy procedure for cases where such effect is of a significant amount.

11. Analytical relationships developed together with the experimental work could probably be used as the basis of reliable method for measuring the rate of flow through porous materials.

Suggestion for Further Research

Experimental investigations in this study were limited only to sand samples of effective diameters of 0.230 and 0.575 millimeters. Permeating solutions tested were conductance water, sodium chloride and potassium chloride solutions. Combination of salts as solutes in the permeating solutions were tested in order to determine the practicality of the proposed procedure for naturally existing waters. In view of these experimental limitations complete information on the practical aspects of the flow, streaming potential and streaming current relationships could not be obtained. On the basis of the analytical findings and experimental experience gained in this investigation, it is believed that improvements have been made in the experimental procedure especially in connection with streaming current and streaming potential measurements. From the analytical derivations obtained in this study, a basic relationship has been evolved which makes a reliable basis for additional experimental investigations beyond this study.

With this in mind, a few suggestions are presented below as extensions of this research. It is hoped that these will help to encourage some other experimental studies that should be pursued in order to present the full picture of the flow, streaming current and

streaming potential relationship, as a tool for evaluating the rate of the flow through porous materials.

1. Measurements should be made of the streaming current and potential for flow through finer and coarser sand samples. This should be done keeping all parameters but the size of the sand particles constants. This will give more tests for the analytical relationship suggested in this study in connection with the size effects.

2. The possibility of replacing the concentration of salt solutions with the conductivity of the solution is worth more investigation over a wider range of salt solutions, with cations different in nature and valence. If such substitutions were always possible, it paves the way for practical application of the suggested procedure. Many simplified procedures now used for determining conductivity of permeating solutions in situe will be a helpful tool to our procedure.

3. It would be useful to check the effect of changes in temperature of the sample and percolating solutions on the resulted E and I provided all other factors are kept constant. This should be done in a wide range that should include the freezing temperature range.

4. Attempts should be made to test the viewpoint considering the retardation of flow due to electrokinetic coupling to be responsible for non-Darcy behavior of the flow through fine materials, especially clayly soils. This was not possible in this study due to the fact that the samples tested were coarse and

electrokinetic coupling effect was negligible.

5. Some studies should be devoted to different problems that will be encountered in the field use of the suggested procedure. Two of these problems will be:

(a) To develop a reliable procedure for placing electrodes in sites without disturbing the media through which rate of flow is to be determined;

(b) To isolate particular strata fitted to these electrodes without disturbing the general flow pattern of the flow.

6. Utilization of the suggested procedure for determining the direction of the flow should be experimentally evaluated. This could be done by placing similar electrodes at different positions in a sample through which liquid is flowing. It is expected that the highest induced E or I would be recorded between the two electrodes placed perpendicular to the main direction of the flow provided that the media is isotropic and homogeneous.

7. It may be interesting to use an approach to relate E, I and rate of flow through unsaturated soil samples similar to the one suggested in here for saturated soil samples. In such case, the flow functions governing flow through unsaturated soils should be utilized.

LITERATURE CITED

Abramson, H. A. 1934. Electrokinetic phenomena and their application to biology and medicine. American Chemical Society. Monograph series, 66:17.

Adamson, A. W. 1960. Physical Chemistry of Surfaces. Interscience Publishers, Inc., New York, p. 179.

Alexander, Jerome. 1946. Colloidal Chemistry Theoretical and Applied. Reinhold Publishing Corporation, New York, p. 523.

Anonymous. 1951. Two monographs on electrokinetics. Engineering Research Institute, University of Michigan, Ann Arbor, p. 101-158.

Biefer, G. J., and S. G. Mason. 1959. Electrokinetic streaming viscous flow and electrical conduction in inter-fibre networks, Transaction of the Faraday Society 55:1239.

Biekerman, J. J. 1940. Electrokinetic equation and surface conductance. A survey of the diffuse double layer theory of colloidal solutions. Transaction of the Faraday Society 36:154.

Biekerman, J. J. 1958. Surface Chemistry, Second Edition. Academic Press Inc. Publishers, New York, p. 405.

Bier, M. 1959. Electropheresis. Academic Press, New York, p. 431-438.

Binder, G. J., and J. E. Cermak. 1963. Streaming potential fluctuations produced by turbulence. The Physics of Fluids 6(8):1192.

Bocquet, P. E. 1954. Streaming Potential Concept. Ph.D. dissertation, University of Michigan, Ann Arbor, 324 p.

Bocquet, P. E., C. M. Sliepcevich, and D. F. Bohr. 1956. Effect of turbulence on the streaming potential. Industrial and Engineering Chemistry 48(2):197.

Briggs, D. R. 1928. Determination of the potential on cellulose A-method. Journal of Physical Chemistry 46:641.

Buchanan, A. S., and E. Heyman. 1948. Notes on the electrokinetic potential of cellulois and electrokinetic equation. Transaction of the Faraday Society 44:318.

Buchanan, A. S., and E. Heyman. 1949a. The electrokinetic potential of barium sulphate. Proceeding of the Royal Society of London 195A:152.

Buchanan, A. S., and E. Heyman. 1949b. Electrokinetic potential of sparingly soluble sulfates. Journal of Colloidal Science, Part I, II, 4:137, 151.

Buchanan, A. S., and E. Heyman. 1949c. Determination of electrokinetic potential in concentrated solutions by the streaming current method. Journal of Colloidal Science 4:157.

Bull, H. B., and R. A. Gortner. 1932. The effect of particle size on the zeta potential. Journal of Physical Chemistry 36:111.

Burgreen, D., and F. R. Nakache. 1963. Electrokinetic flow in capillary elements. Aeronautic System Division Technical Documents Report 63-243.

Burgreen, D., and F. R. Nakache. 1964. Electrokinetic flow in ultrafine capillary slits. Journal of Physical Chemistry 68: 1084.

Butler, J. A. V. 1951. Electrical phenomena at interfaces. The Macmillan Company, New York, p. 30.

Cermak, J. E., and L. V. Baldwin. 1963. Measurements of Turbulence in Water by Electrokinetic Transducer. Fluid Mechanics Symposium, 56th Annual Meetings of American Institute of Chemical Engineers, Houston.

Chattoraj, D. K., and H. B. Bull. 1959. Electrophoresis and surface charge. Journal of Physical Chemistry 63:1809.

Davies, J. T., and E. K. Rideal. 1963. Interfacial Phenomena. Academic Press, New York and London, p. 108.

DeGroot, S. R., P. Mazur, and J. Th. G. Overbeek. 1952. Non equilibrium thermodynamics of sedimentation potential and electropheresis. Journal of Chemical Physics 20:1825.

Derjaguin, B. V., and S. S. Duckin. 1960. Electrokinetic phenomena controlled by diffusion. Third International Congress of Surface Activity, Cologne, 2:324.

Donnen, L. D. 1950. Analysis of Irrigation Waters. California Agriculture 4(11):6, 14.

Dulin, C. I., and A. H. Elton. 1952. Determination of electrokinetic charge and potential by the sedimentation method. Journal of Chemical Society Part 1:286.

Dulin, C. I., and A. H. Elton. 1953. Determination of electrokinetic charge and potential by the sedimentation method. Part III. Silica in some aqueous chloride solution. Journal of Chemical Society Part 2:1168.

Foster, H. D. 1942. Chemistry of Ground Water in Hydrology (O. E. Meinzer, ed.). McGraw-Hill, New York, p. 646-655.

Fuerstenau, D. W. 1953. Streaming potential studies on quartz. Sc.D. thesis. Massachusetts Institute of Technology.

Fuerstenau, D. W. 1956. Streaming potential studies on quartz in solutions of ammonium acetates in relation to the formation of hemimicells at the quartz solution interface. Journal of Physical Chemistry 60:981.

Gaudin, A. M., and D. W. Fuerstenau. 1955. Quartz floatation with anionic collectors. American Institute of Mining and Metallurgical Engineers 202:66-72.

Ghosh, B. N., B. K. Choudhyry, and P. K. De. 1954. Evaluation of true zeta potential of the particles of glass forming a diaphragm from measurements of streaming potential. Transaction of the Faraday Society 50:955.

Ghosh, B. N., S. C. Rakshit, and C. Chattoraj. 1953. The evaluation of true zeta potential of quartz particles of different size from measurements of streaming potential. Journal of Indian Chemical Society 30:601.

Gibbings, J. C., and E. T. Hignett. 1966. Dimensional analysis of electrostatic streaming current. Electrochimica Acta 11:815.

Glasstone, S. 1946. Textbook of Physical Chemistry. Van Nostrand, New York, p. 1220-1224.

Glueckauf, E. 1964. Bulk dielectric constant of aqueous electrolyte solutions. Transaction of Faraday Society 60, Part 9:1637.

Goring, D. A. I., and S. G. Mason. 1950. Electrokinetic properties of cellulose fibers II zeta-potential measurements by the stream compression method. Canadian Journal of Research 28(B):323.

Guggenheim, E. A. 1940. Preamble electric dimensions. Transaction of Faraday Society 36:139.

Guggenheim, E. A. 1957. Thermodynamics. North Holland Publishing Company, Amsterdam, p. 453.

Gurney, R. W. 1953. Ionic processes in solution. McGraw-Hill, New York.

Haggis, H., J. B. Hasted, and A. S. Buchanan. 1952. Dielectric depression caused in water by addition of electrolyte. Journal of Chemical Physics 24:575.

Ham, A. J., and E. D. M. Dean. 1940. An examination of electrokinetic charge as a function of the thickness of the double layer. Transaction of the Faraday Society 36:53.

Harr, M. E. 1962. Ground Water and Seepage. McGraw-Hill Company, New York, p. 4.

Hasted, J. B., D. M. Robinson, and C. H. Collie. 1948. Dielectric properties of aqueous ionic solutions pat 1 Part 11. Journal of Chemical Physics 16:1.

Helmoholtz, H. 1879. Ann. Physik Vol. 7, Part 3, p. 337; "Gesammte Abhanglungen," Vol. 1, p. 85, 1882; traced by P. E. Bocquet, 1952.

Henniker, J. E. 1952. Retardation of flow in narrow capillaries. Journal of Colloidal Science 7:443.

Hignett, E. T. 1963. Static electrification arising from fluid dynamic causes. Ph.D. thesis, University of Liverpool.

Hignett, E. T., and J. C. Gibbins. 1965. The entry correction in the electrostatic changing of fluid flowing through pipes. Journal of Electroanalytical Chemistry 9:260.

Hoydon, D. A. 1960. The significance of zeta potential of emulsion droplet. Third International Congress of Surface Activity, Cologne 2:341.

Hunter, R. J. 1961. Dielectric constant in the equations of electrokinetics. Journal of Colloidal Science 16:19.

Hunter, R. J. 1966. The interpretation of electrokinetic potentials. Journal of Colloidal and Interface Science 22:231-239.

Hunter, R. J., and A. E. Alexander. 1962. Some notes on the measurements of electrokinetic potential. Journal of Colloidal Science 17:781-788.

Ivez, D. J. G., and G. J. Janz. 1961. Reference Electrodes Theory and Practice. Academic Press, New York, p. 179.

Jones, G., and L. A. Wood. 1945. The measurement of potentials at the interface between vitreous silica and solutions of potassium chloride by the streaming potential method. Journal of Chemical Physics 13(3):106.

Jumkis, A. B. 1962. Soil Mechanics. University series in Civil Engineering and Applied Mechanics. D. Van Norstrand Company Inc., Princeton, New Jersey, p. 226.

Korpi, G. K. 1960. Measurements of streaming potential. M. Sc. thesis, Massachusetts Institute of Technology.

Kraemer, E. O. 1942. Advances in Colloid Science. Edited by E. O. Kraemer, Floyd E. Bartel and others. Interscience Publishers, New York, p. 44.

Kruyt, H. R. 1952. Colloidal Science, Vol. 1. Irreversible system. Elsiever Publishing Company, New York, p. 204.

Leibenzon, L. S. 1947. The flow of natural fluids and gases in porous medium. State Press for Technology, Moscow.

Li, H. C. 1958. Adsorption of organic and inorganic ions on quartz. Sc.D. thesis, Massachusetts Institute of Technology.

Martinez, E., and G. L. Zucker. 1960. Asbestos ore body minerals studied by zeta potential measurements. Journal of Physical Chemistry 64:924.

Michaels, A. S., and C. S. Lin. 1955. Effect of counterelectro-osmosis and sodium ion exchange on permeability of kaolinite. Industrial and Engineering Chemistry 47:1249.

Michaeli, I., and O. Kedem. 1961. Description of the transport of solvent and ions through membranes in terms of differential coefficients. Part 1. Phenomenological characterization of flows. Transaction of the Faraday Society 57:1185.

Modi, H. J. 1957. Streaming studies on corundum. Sc.D. thesis, Massachusetts Institute of Technology.

Mysels, K. J. 1959. Introduction to colloidal chemistry. Interscience Publishers, Inc., New York, p. 315.

Neale, S. M. 1946. Revised theory of the streaming potential. Transaction of the Faraday Society 42:474.

Neale, S. M., and R. H. Peters. 1945. Electrokinetic measurements with textile fibres and aqueous solutions. Transaction of the Faraday Society 42:478.

Oldham, I. B., F. J. Young, and J. F. Osterle. 1963. Streaming potential in small capillaries. Journal of Colloidal Science 18:328.

Olsen, H. W. 1961. Hydraulic flow through saturated clays. Ph.D. dissertation, Massachusetts Institute of Technology.

Olsen, H. W. 1966. Simultaneous fluxes of liquid and charge through saturated kaolinite. Soil Science Society of America Meetings, August 1966, p. 49.

Overbeek, J. Th. G. 1953a. Colloidal Science. Vol. I, Chap. 5 (ed. Kruyt) Elseiver, Amsterdam, p. 194.

Overbeek, J. Th. G. 1953b. Thermodynamics of electrokinetic phenomena. Journal of Colloidal Science 8:420.

Overbeek, J. Th. G., and P. W. O. Wigga. 1946. On electro-osmosis and streaming potential in diapragms. Recueil des Travaux Chimiques 65:556.

Parriera, H. C. 1965. Automatic recording apparatus for measurements of streaming potentials. Journal of Colloidal Science 20:1.

Parriera, H. C., and V. H. Schulman. 1961. Streaming potential measurements on paraffin wax. Advanced Chemistry Series 33:160.

Partington, J. R. 1949. An Advance Treatise on Physical Chemistry, Vol. 5. Longman's, London, New York, Toronto, p. 287-291.

Polubarinova-Kochina, P. VA. 1962. Theory of ground water movement. Princeton University Press, Princeton University, p. 16-17.

Rice, C. L., and R. Whitehead. 1965. Electrokinetic flow in narrow cylindrical capillary. Journal of Physical Chemistry 69:4017.

Rutgers, A. J. 1940. Streaming potential and surface conductance. Transaction of the Faraday Society 36:69.

Rutgers, A. J. 1954. Physical Chemistry. Interscience Publishers, Inc., New York, p. 403.

Rutgers, A. J., and M. DeSmet. 1945. Researches on electro endo-osmosis. Transaction of the Faraday Society 41:758.

Rutgers, A. J., and M. DeSmet. 1947. Electro-osmosis, streaming potential and surface conductance. Transaction of the Faraday Society 43:102.

Rutgers, A. J., M. DeSmet, and G. DeMyer. 1957. Influence of turbulence upon electrokinetic phenomena. Transaction of the Faraday Society 53:393.

Schulman, T. H., and H. C. Parriera. 1963. Report No. 1, Office of Naval Research Contract ONR 2259(63).

Scott, R. F. 1963. Principles of Soil Mechanics. Addison and Wesley, Reading, Massachusetts, p. 54.

Smoluchowski, M. 1921. Elektrische endosmuse bend stromungstronne. Handbuch der Elektrizitat und des Magnetismus. Vol. 11, Graetz (ed.), Barth; tr. by P. E. Bocquet, Two monographs on electrokinetics, University of Michigan Engineering Research Bulletin 33 (1951).

Staverman, A. J. 1952. Non equilibrium thermodynamics of membrane processes. Transaction of the Faraday Society 38:176.

Stern, O. 1924. Zeitschrift fur Electrochemie 30:508; cited by Kruyt, 1952.

Stewart, P. R., and N. Street. 1961. Streaming potential and turbulence. Journal of Colloidal Science 16:193.

Taylor, S. A., and J. W. Cary. 1960. Analysis of the simultaneous flow of water and heat or electricity with the thermodynamics of irreversible process. Seventh International Congress of Soil Science, Madison, Wisconsin, U.S.A., p. 80.

Taylor, S. A. 1963. Simultaneous flow in soils and plants. Part 1. Non-equilibrium thermodynamics in soils and plants. Utah State University, p. 3-13. (Mimeographed)

Taylor, S. A. 1964. Physics of Irrigated Soils. Soil Plant Water Relations. Utah State University Bookstore, p. 209.

Todd, D. K. 1959. Ground Water Hydrology. John Wiley and Sons, New York.

White, H. L., F. Urban, and E. A. Van Atta. 1932. Streaming potential and surface conductance. Journal of Physical Chemistry 36:3152.

White, H. L., F. Urban, and E. T. Krick. 1932. Streaming potential determination on capillaries of various sizes. Journal of Physical Chemistry 36:120.

White, H. L., F. Urban, and B. Monaghan. 1941. The magnitude of surface conductivity at aqueous glass interface. Journal of Physical Chemistry 45:560.

Wood, L. A. 1946a. The measurement of the potential at the interface between vitreous silica and pure water. Journal of Chemical Physics 68:437.

Wood, L. A. 1946b. Derivation of streaming potential equation. Journal of Chemical Physics 68:432.

Wood, L. A. 1946c. An analysis of the streaming potential method of measuring the potential at the interface between solids and liquids. Journal of American Chemical Society 68:432.

Wood, L. A., and L. B. Robinson. 1946. The electrical potential at the interface between vitreous silica and solutions of barium chloride. Journal of Chemical Physics 14(4):251.

Wylie, M. R. J., and M. B. Spangler. 1952. Application of electrical resistivity measurements to problems of fluid flow in porous media. Bulletin of American Association of Petroleum Geologist 36:359-403.

Zaslavsky, D., and I. Ravina. 1965. Review and some studies of electrokinetic phenomena. Symposium on moisture equilibrium and moisture change in soils beneath covered areas. Butterworth and Company, Australia, p. 55-69.

Zuker, G. L. 1959. A Critical Evaluation of Streaming Potential Measurements. Sc.D. thesis, Columbia University.

APPENDIX

Evaluation of Phenomenological Coefficients

The phenomenological coefficients in equations (20) and (21) have been evaluated by relating them to the experimental results. In each set of these equations we have four experimental quantities—I, E, q and p—and two equations. So we need a third independent equation before we can arrive at a definite relation between two of the variables. The third equation generally specifies that one of the variables held equal to zero. However, in our experimental measurements we measured both streaming potential and streaming current for the same run. This gives us an additional information that will help us to solve for the four phenomenological coefficients as follows. Also, Onsager's relation $L_{21} = L_{12}$ was established experimentally by Saxen and recently checked for accuracy (Rutger and de Smet, 1947).

Evaluation of L_q, L_{11} L_{21}

As the two electrodes are short circuited all the convection current induced by the flow—during the measurements of streaming current—will return back through the outside circuit (and not conducted back as conduction current through the system). So, no potential difference will be developed across the system and E will be equal to zero.

From equation (20b)

$$I = L_{21}p \text{ and } L_{21} \text{ will be equal to } \left(\frac{I}{p}\right)_{E=o}$$

From equation (20a)

$q = L_{11}p$ and $L_{11} = \left(\frac{q}{p}\right)_{E=o}$ = slope of q vs p relationship which is equivalent to Dary's law where L_{11} is the hydraulic conductivity or hydrodynamic conductivity of the first kind.

From equation (21b)

$$I = L_q\, q \quad , \text{ and}$$

$L_q = \left(\frac{I}{q}\right)_{E=o}$ = slope of the q vs I straight line relationship

Compared to our derivations (see previous derivations) equation L_q will be comparable to $\frac{D\zeta}{8\pi}\,\frac{(1-\sigma)^2}{\beta d^2\,\sigma^2}$ and L_{11} will be comparable to $\frac{\beta d^2}{L\eta}\,\frac{\sigma^2}{(1-\sigma)^2}\,A_o$

$\frac{L}{p}$

When measurements are made for streaming potential and no current is allowed to flow outside the system and the convection current is balanced at the steady state by the conduction current, the total current, I, would be equal to $I_{str} + I_{cond} = o$.

From equation (21a), then

$$L_p = \left(\frac{q}{p}\right)_{I=o}$$

In this case L_p is the hydrodynamic conductivity of the second kind.

It is interesting to note that hydrodynamic conductivity in the case when E = o, will be smaller than that when I = o by the correction factor L_c. This difference will then be equal to $\left(\frac{q}{p}\right)_{E=o} - \left(\frac{q}{p}\right)_{I=o}$ which is due to the electrokinetic couplings.

L_e

From streaming potential measurements E, q and p are experimentally evaluated. At steady state $I_{total} = o$, and

$$L_e = L_q \frac{q}{E} = \frac{I}{q} \times \frac{q}{E} = \left(\frac{I}{E}\right)$$

Incidentally in this case $\frac{L_q}{L_e}$ will be comparable to C_2 in equation (18b) (see previous derivation) as

$$\frac{L_q}{L_e} \cong \frac{D\zeta}{8\pi} \frac{(1-\sigma)^2}{\beta d^2 \sigma^2} \frac{R}{c}$$

Another way of calculating L_e is by applying potential to the system under zero flow conditions and measuring I. So from equation (2b), as $q = o$

$I = L_e E$ and $L_e = \frac{I}{E}$ which is the conductance of the system comparable to $\frac{R}{c}$. This seems to be one way of comparing the results.

L_{22} is computed directly from equation (20b) as

$$I = L_{21} p + L_{22} E$$

at $p = o$

$$L_{22} = \left(\frac{I}{E}\right)_{p=o}$$

Dimensions

If q is measured in cm^3/sec per cross sectional area per cm length of the soil sample, p is measured in dyne per cross sectional area per cm length of the soil sample, E is measured in stat volts per cm length and I is measured in stat coulomb per cm length of the soil sample, then phenomenological coefficients should have the following units

$$L_{11} \equiv \frac{cm^3}{\text{dyne sec}}$$

$$L_{22} \equiv \frac{\text{stat coulomb}}{\text{stat volts. sec.}}$$

$$L_{12} \equiv \frac{cm}{\text{stat volt-sec}}$$

$$L_{21} \equiv \frac{\text{stat coulomb } cm^2}{\text{dyne. sec.}}$$

$$L_p \equiv \frac{cm^3}{\text{dyne. sec}}$$

$$L_e \equiv \frac{\text{stat coulomb}}{\text{stat volts. sec.}}$$

$$L_q \equiv \frac{\text{stat coulomb}}{cm}$$

$$L_I \equiv \frac{cm}{\text{stat coulomb}}$$

Table 1. Conversion factors

To convert experimental results	In	Into	Multiply by
q	$cm^3\ sec^{-1}$	sec^{-1}	2.112×10^{-3}
p	cm of H_2O	$dyne/cm^3$	1.267×10^{2}
I	ampers	$\frac{\text{stat coulomb}}{\text{sec. cm length}}$	3.90×10^{8}
E	volts	$\frac{\text{stat volts}}{\text{cm length}}$	4.364×10^{-4}
$\frac{q}{p}$	$\frac{cm^2}{sec}$	$\frac{cm^3}{\text{dyne sec}}$	1.667×10^{-5}
$\frac{I}{p}$	$\frac{\text{coulomb}}{\text{cm of } H_2O \text{ sec}}$	$\frac{\text{stat coul. } cm^2}{\text{dyne sec}}$	3.067×10^{6}
$\frac{I}{q}$	$\frac{\text{coul.}}{cm^3}$	$\frac{\text{stat coul.}}{\text{cm}}$	1.846×10^{11}
$\frac{I}{E}$	$\frac{\text{ampers}}{\text{volts}}$	$\frac{\text{stat coul.}}{\text{stat volts sec.}}$	8.92×10^{11}

Table 2. Phenomenological coefficients and electrokinetic couplings (equation 20).

Sample	Solution	Normality	L_{11} in $\frac{cm^3}{dyne\ sec.}$	L_{12} in $\frac{cm}{stat\ volt\text{-}sec}$	L_{21} in $\frac{stat\ coul.cm^2}{dyne\ sec.}$	L_{22} in $\frac{stat\ coul.}{stat\ volt\ sec.}$	Electrokinetic coupling $\frac{q_p - q}{q_p}$ %
	Cond.	Water	8.335×10^{-6}	139.5×10^{-3}	139.5×10^{-3}	4.06×10^{6}	.0648
	NaCl	5×10^{-4} N	8.25×10^{-6}	160.5×10^{-3}	160.5×10^{-3}	8.1×10^{7}	.00383
		10^{-3}	8.49×10^{-6}	140	140	15.9×10	.00154
S_1		5×10^{-3}	8.20	47.6	47.6	63.3	
		10^{-2}	7.98	28.2	28.2	98.1	
	KCl	10^{-4} N	8.20×10^{-6}	125×10^{-3}	125×10^{-3}	2.24×10^{7}	.0085
		5×10^{-4}	8.38	97.5×10^{-3}	97.5	8.05	.00141
		10^{-3}	8.42	84.5	84.5	15.1	
		5×10^{-3}	8.10	48.0	48	55.5	
		10^{-2}	7.80	26.20	26.20	141.0	
	Cond.	Water	3.60×10^{-5}	203×10^{-3}	203×10^{-3}	6.15×10^{6}	.0188
	NaCl	10^{-4} N	3.74×10^{-5}	210×10^{-3}	210×10^{-3}	3.24×10^{7}	.00337
		5×10^{-4}	3.58×10^{-5}	174	174	9.46	
		10^{-3}	3.60×10^{-5}	152	152	20.1	
S_2		5×10^{-3}	3.62×10^{-5}	93.8	93.8	66.4	
		10^{-2}	3.73×10^{-5}	36.8	36.8	135.0	
	KCl	10^{-4} N	3.42×10^{-5}	136×10^{-3}	136×10^{-3}	2.76×10^{7}	.00198
		5×10^{-4}	3.33×10^{-5}	114	114	14.0	
		10^{-3}	3.33×10^{-5}	104.5	104.5	26	
		5×10^{-3}	3.60×10^{-5}	92.0	92.0	107	
		10^{-2}	3.84×10^{-5}	73.0	73.0	182	

Table 3. Phenomenological coefficients and electrokinetic couplings (equation 21).

Sample	Solution	Concent.	L_p in $\frac{cm^3}{dyne\ sec.}$	L_q in $\frac{stat\ coul.}{cm}$	L_I in $\frac{cm}{stat\ coul.}$	L_e in $\frac{stat\ coul.}{stat\ volt\ sec.}$	Electrokinetic coupling $\frac{q_p - q}{q_p}$ %
	Cond.	Water	8.35×10^{-6}	22.2×10^{3}	3.44×10^{-8}	4.10×10^{6}	.07
S_1	NaCl	5×10^{-4} N	8.30×10^{-6}	20.7×10^{3}	1.98×10^{-9}	8.1×10^{7}	.00393
		10^{-3} N	8.50×10^{-6}	15.7×10^{3}	8.80×10^{-10}	16.0	.00138
		5×10^{-3} N	8.22	7.75	7.55×10^{-11}	62.5	
		10^{-2} N	7.92	3.70	2.87×10^{-11}	89.2	
	KCl	10^{-4} N	8.20×10^{-6}	15.70×10^{3}	5.60×10^{-9}	2.28×10^{7}	.00875
		5×10^{-4} N	8.31×10^{-6}	11.75	1.21×10^{-9}	8.25	.00142
		10^{-3}	8.35	9.80	5.60×10^{-10}	15.10	
		5×10^{-3}	7.95	4.07	8.65×10^{-11}	64.5	
		10^{-2}	7.70	3.51	1.85×10^{-11}	144.0	
	Cond.	Water	3.74×10^{-5}	57.8×10^{2}	3.3×10^{-8}	6.18×10^{6}	.019
	NaCl	10^{-4}	3.80×10^{-5}	57.2×10^{2}	6.5×10^{-9}	2.63×10^{8}	.00372
		5×10^{-4}	3.74	48.1	1.74×10^{-9}	9.8×10^{7}	
		10^{-3}	3.80	30.5	7.55×10^{-10}	20.9×10^{7}	
S_2		5×10^{-3}	3.58	22.2	1.41×10^{-10}	64.0×10^{7}	
		10^{-2}	3.68	8.7	2.75×10^{-11}	138.0×10^{7}	
	KCl	10^{-4}	3.36×10^{-5}	40.8×10^{2}	4.93×10^{-9}	2.94×10^{7}	.00202
		5×10^{-4}	3.57	35.0	8.12×10^{-10}	13.8×10^{7}	
		10^{-3}	3.50	31.5	4.0×10^{-11}	26.1	
		5×10^{-3}	3.57	26.7	9.15×10^{-11}	98.0	
		10^{-2}	3.68	19.2	4.0×10^{-11}	197.0	

Table 4. Calculated ζ values for different concentrations of KCl for S_1 and S_2.

KCl concentration	ζ_1	ζ_2	ζ_2 / ζ_1	$\frac{1}{4.10} \times \frac{\zeta_2}{\zeta_1}$
10^{-4} N	148.50	190	1.275	$\frac{1}{3.20}$
5×10^{-4} N	112	154	1.37	$\frac{1}{3.00}$
10^{-3} N	93	140	1.51	$\frac{1}{2.70}$
5×10^{-3} N	47.50	120	2.52	$\frac{1}{1.65}$
10^{-2} N	33	094	2.85	$\frac{1}{1.45}$

Table 5. Cell constant measurements, Sample 1

Concentr. KCl	Apparatus	R_s = Resistance of the sample	Conductivity of the sample	Sp. resistance of liquid	C_s Sp. conductance of the liquid	Cell constant $C_s \times R_s$	Average cell constant
Base	1	1.15×10^{5}	8.70×10^{-6}	4.9×10^{4}	20.4×10^{-6}	$20.4 \times 1.15 \times 10^{-1} = 2.34$	2.07
10^{-5} N	2	9.0×10^{4}	1.11×10^{-5}	4.85×10^{4}	20.5×10^{-6}	1.845	
10^{-4} N	1	3.90×10^{4}	2.56×10^{-5}	3.29×10^{4}	3.04×10^{-5}	1.19	1.195
	2	3.95×10^{4}	2.53×10^{-5}	3.3×10^{4}	3.03×10^{-5}	1.20	
5×10^{-4}N	1	1.08×10^{4}	9.25×10^{-5}	1.175×10^{4}	8.568×10^{-5}	.925	0.925
	2	1.11×10^{4}	9.02×10^{-5}	1.20×10^{4}	8.31×10^{-5}	.925	
10^{-3} N	1	6×10^{3}	1.667×10^{-4}	7.0×10^{3}	1.43×10^{-4}	.854	0.862
	2	5.9×10^{3}	1.695×10^{-4}	6.95×10^{3}	1.48×10^{-4}	.870	
5×10^{-3}N	1	1.45×10^{3}	6.89×10^{-4}	1.6×10^{3}	6.20×10^{-4}	.90	0.887
	2	1.38×10^{3}	7.22×10^{-4}	1.575×10^{3}	6.35×10^{-4}	.875	
10^{-2} N	1	6.15×10^{2}	1.62×10^{-3}	7.4×10^{2}	1.376×10^{-3}	0.845	0.855
	2	6.31×10^{2}	1.582×10^{-3}	7.4×10^{2}	1.376×10^{-3}	0.865	
2×10^{-2}N	1	3.66×10^{2}	2.73×10^{-3}	4.45×10^{2}	2.24×10^{-3}	0.815	0.818
	2	3.42×10^{2}	2.93×10^{-3}	4.225×10^{2}	2.370×10^{-3}	0.821	
5×10^{-2}N	1	1.48×10^{2}	6.76×10^{-3}	1.825×10^{2}	5.50×10^{-3}	0.812	0.829
	2	1.50×10^{2}	6.67×10^{-3}	1.775×10^{2}	5.62×10^{-3}	0.845	
10^{-1} N	1	8.4×10^{1}	1.19×10^{-2}	1.05×10^{2}	9.36×10^{-3}	0.750	0.751
	2	7.2×10^{1}	1.39×10^{-2}	0.95×10^{2}	1.05×10^{-2}	0.752	

(1) Impedence Bridge Radio 1650 A.
(2) Self made Impedence Bridge

Table 6. Cell constant measurements, Sample 2

KCl concent.	Apparatus	Resistance of the sample	Conductivity of the sample	Sp. resist. of perm. solution	Sp. cond. of perm. sol.	Cell constant $C_s \times R_s$	Average cell constant
10^{-4} N	1	2.93×10^{4}	3.41×10^{-5}	2.87×10^{4}	3.50×10^{-5}	1.022	1.032
	2	2.94×10^{4}	3.40×10^{-5}	2.82×10^{4}	3.56×10^{-5}	1.040	
5×10^{-4}N	1	6.85×10^{3}	1.46×10^{-4}	1.12×10^{4}	8.92×10^{-5}	0.612	0.610
	2	6.89×10^{3}	1.45×10^{-4}	1.13×10^{4}	8.90×10^{-5}	0.609	
10^{-3}	1	3.51×10^{3}	2.86×10^{-4}	6.10×10^{3}	1.64×10^{-4}	0.575	0.576
	2	3.52×10^{3}	2.85×10^{-4}	6.10×10^{3}	1.64×10^{-4}	0.577	
5×10^{-3}	1	7.42×10^{2}	1.35×10^{-3}	1.32×10^{3}	7.58×10^{-4}	0.562	0.564
	2	7.62×10^{2}	1.32×10^{-3}	1.35×10^{3}	7.55×10^{-4}	0.566	
10^{-2}	1	3.79×10^{2}	2.64×10^{-3}	6.60×10^{2}	1.52×10^{-3}	0.575	0.568
	2	3.82×10^{2}	2.63×10^{-3}	6.80×10^{2}	1.51×10^{-3}	0.562	

Table 7. Chemical analysis of simulated natural waters.

Symbol	EC x 10^6 at 80^oF	Major constituents in Me/ltr						Quality[a] classification
		Ca^{++}	Mg^{++}	Na^{+}	HCO_3	Cl	SO_4	
W_1	255	1.41	0.44	0.89	1.01	1.41	0.48	Good
W_2	770	8.30	0.75	3.96	2.46	2.73	4.47	Permissible
W_3	1200	11.40	5.70	12.90	2.30	2.80	23.00	Doubtful

[a]Based on classification in Todd, 1959

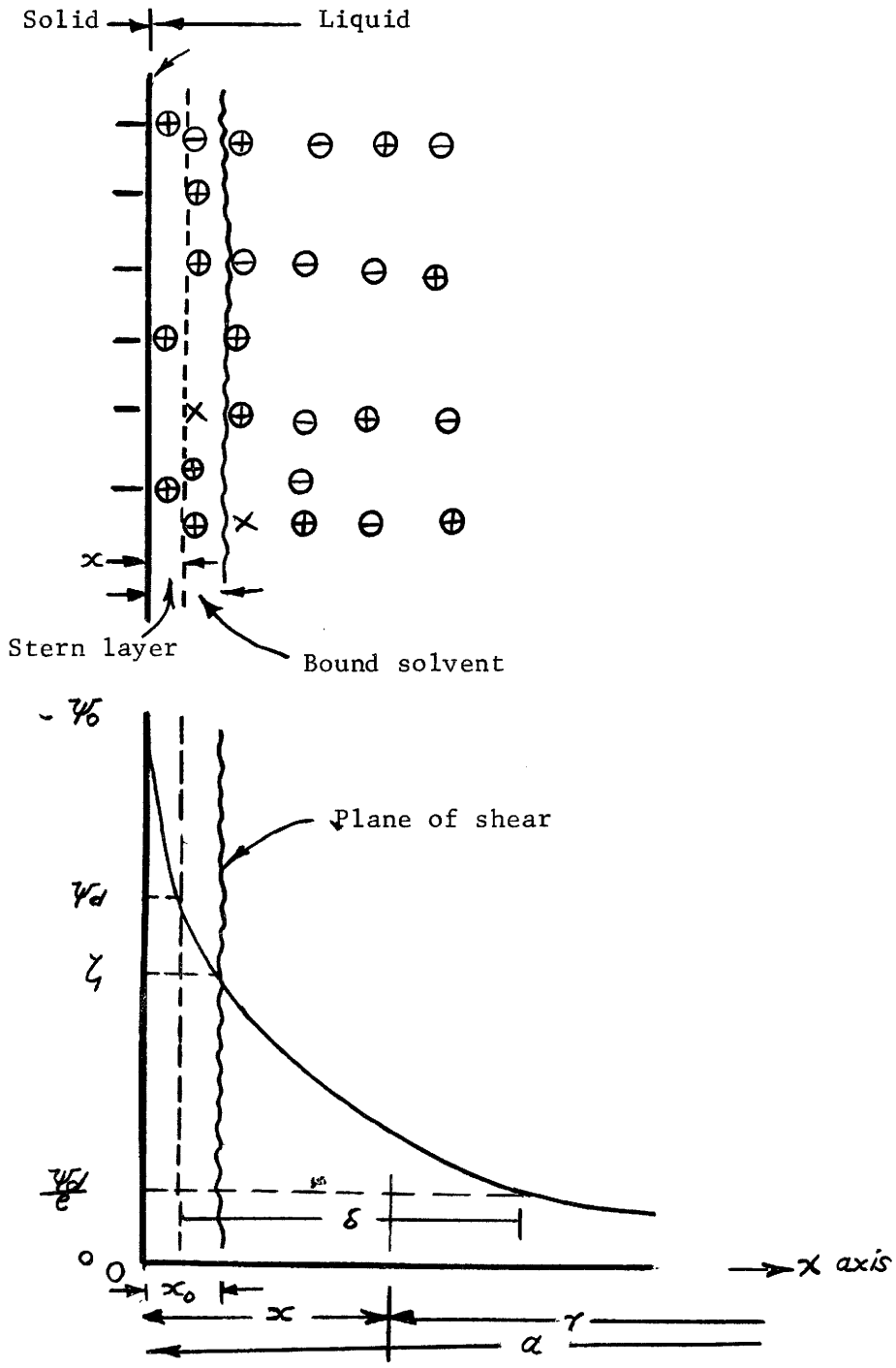

Figure 1. The structure of the double layer and the corresponding potentials. Ψ_o is at the wall, Ψ_d is at the beginning of the diffuse double layer, ζ at the hydrodynamic plane of shear. In the diffuse double layer the potential decays by a factor of $\frac{1}{e}$ over a distance of $\delta = \frac{1}{k}$ for low potentials (after Mysels, 1959).

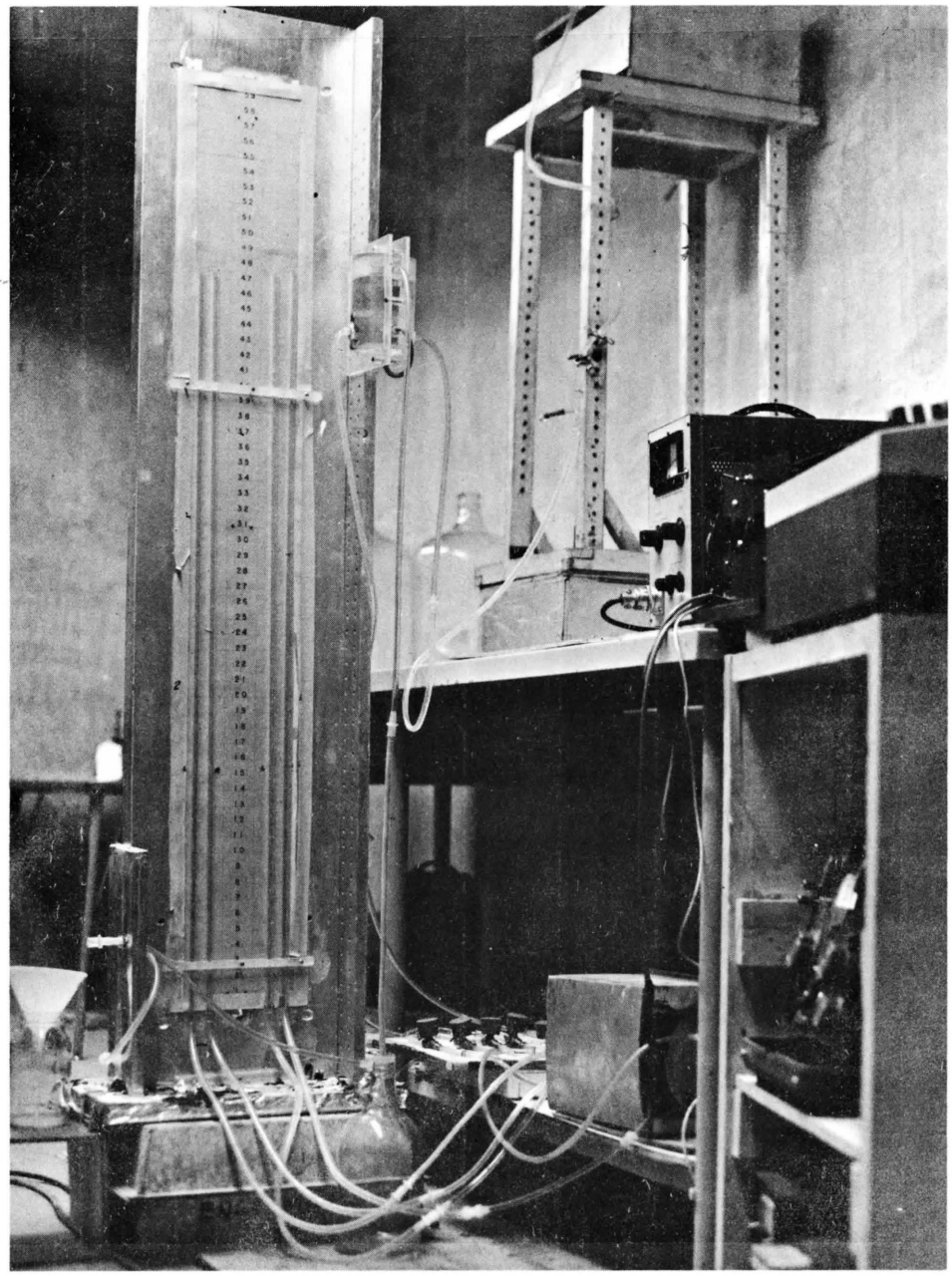

Figure 2: Experimental apparatus — general view.

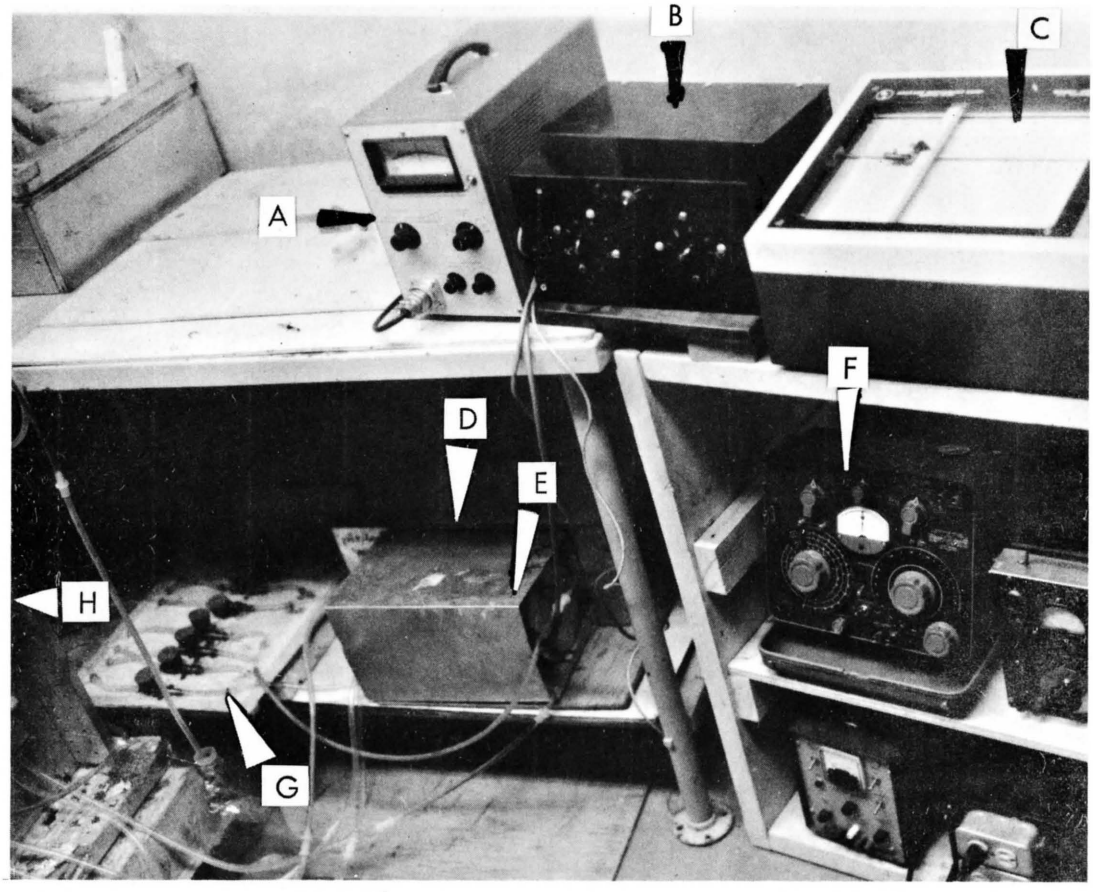

Figure 3: General view of the instrumentation set up.

A. Keithly electrometer model 150A.
B. Multiple connection switch.
C. Time base recorder model HR-96.
D. Ag-agcl. electrode cell inside the shield.
E. Pl-plt. electrode cell inside the shield.
F. General radio impedence bridge 1650A.
G. Flow switch board.
H. Manometer board.

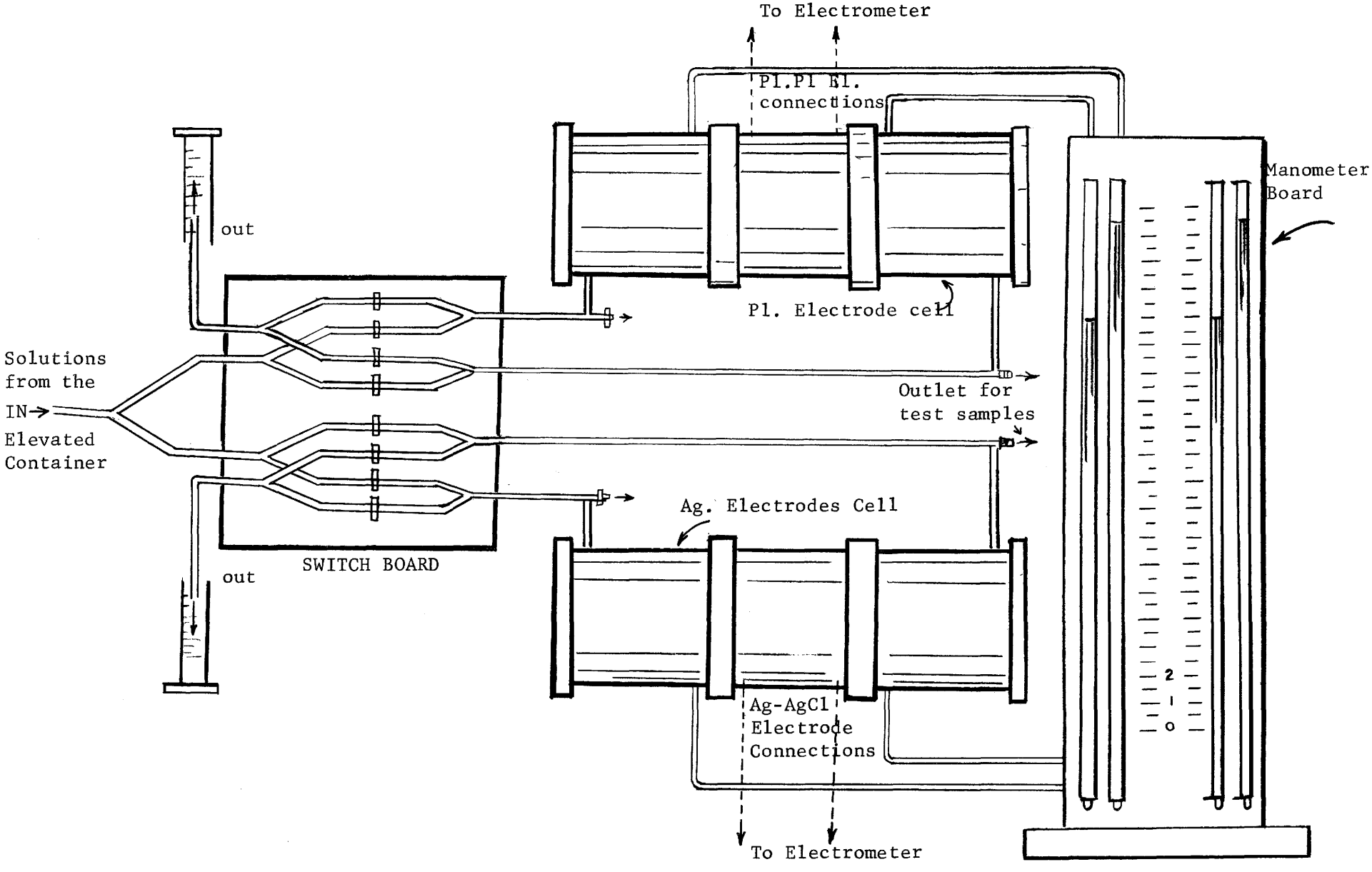

Figure 4. Schematic sketch for the apparatus showing the flow system.

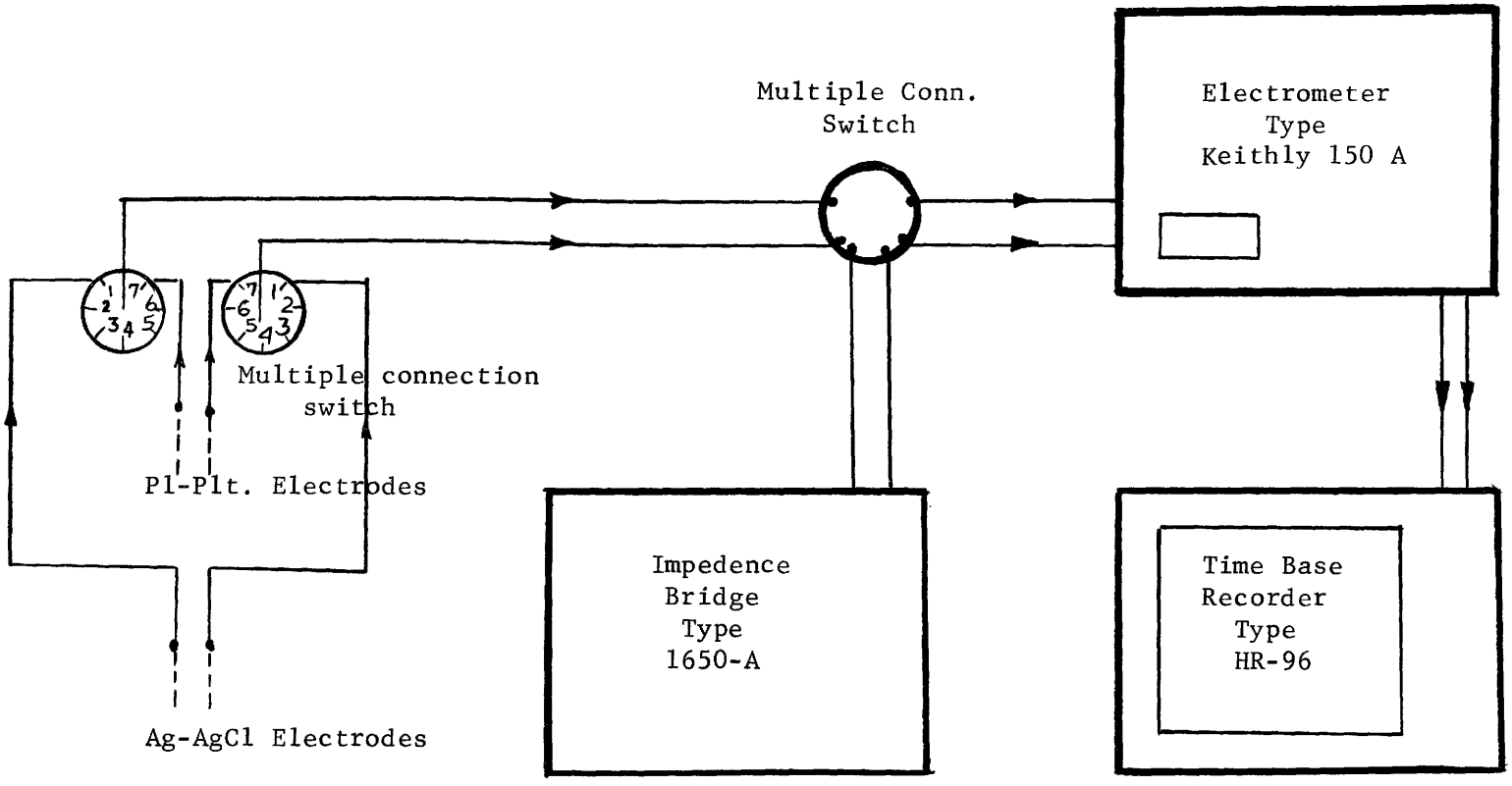

Figure 5. Block diagram of the electrodes and associated electronic instrumentation.

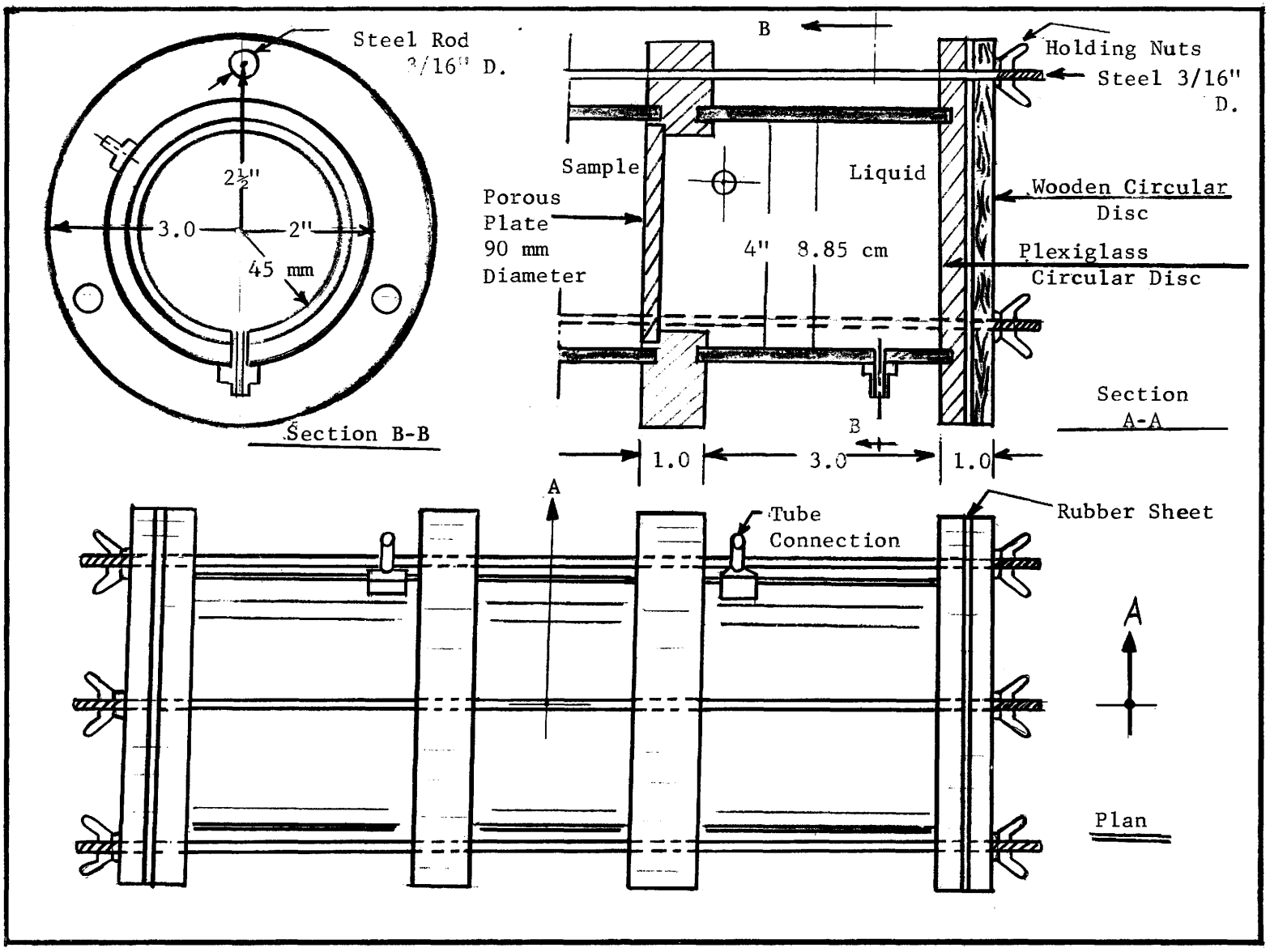

Figure 6. Details of the cell.

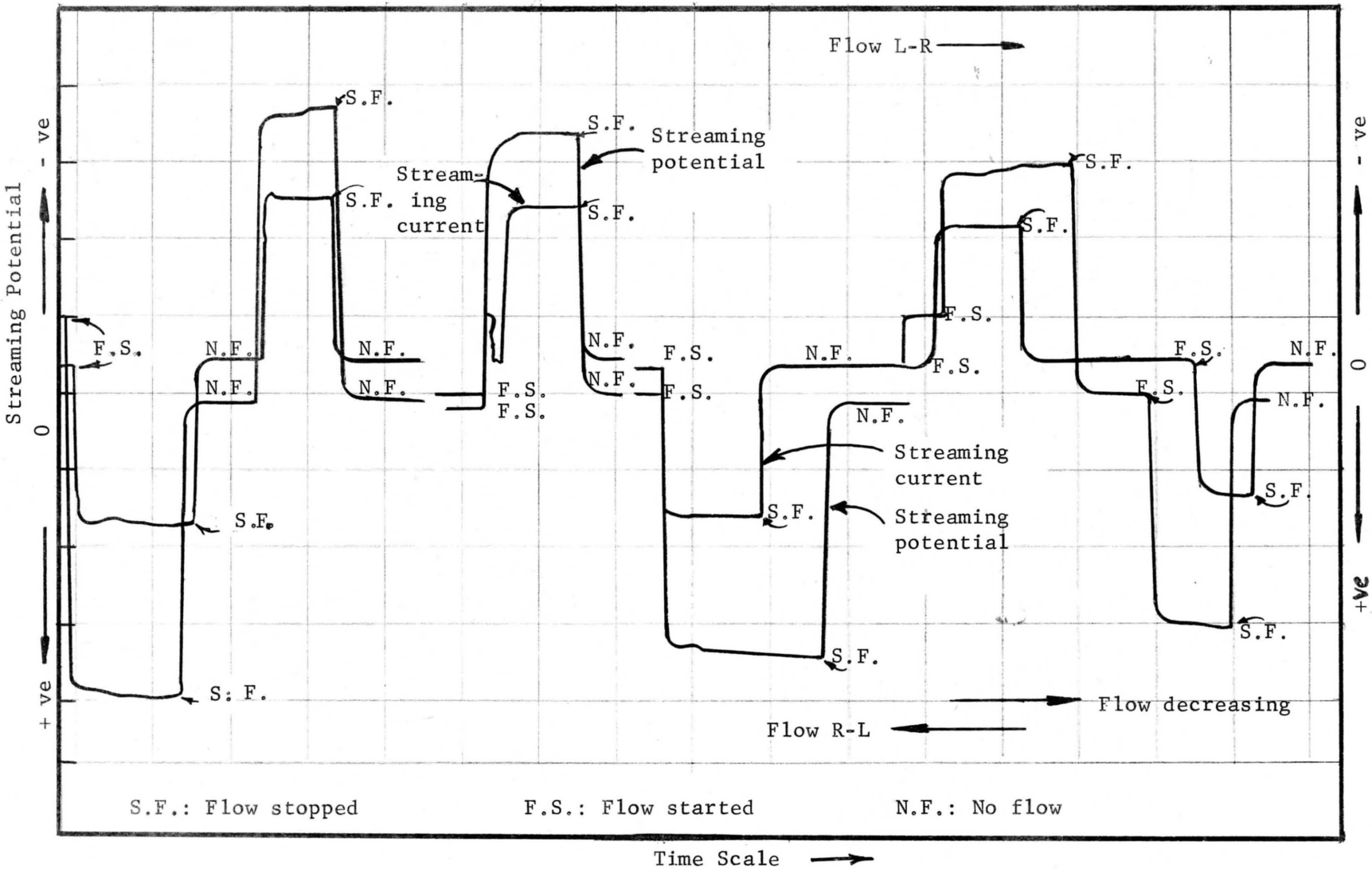

Figure 7. Actual recording data sheet for both streaming current and streaming potential measured simultaneously for the same setting with the flow from left to right and right to left.

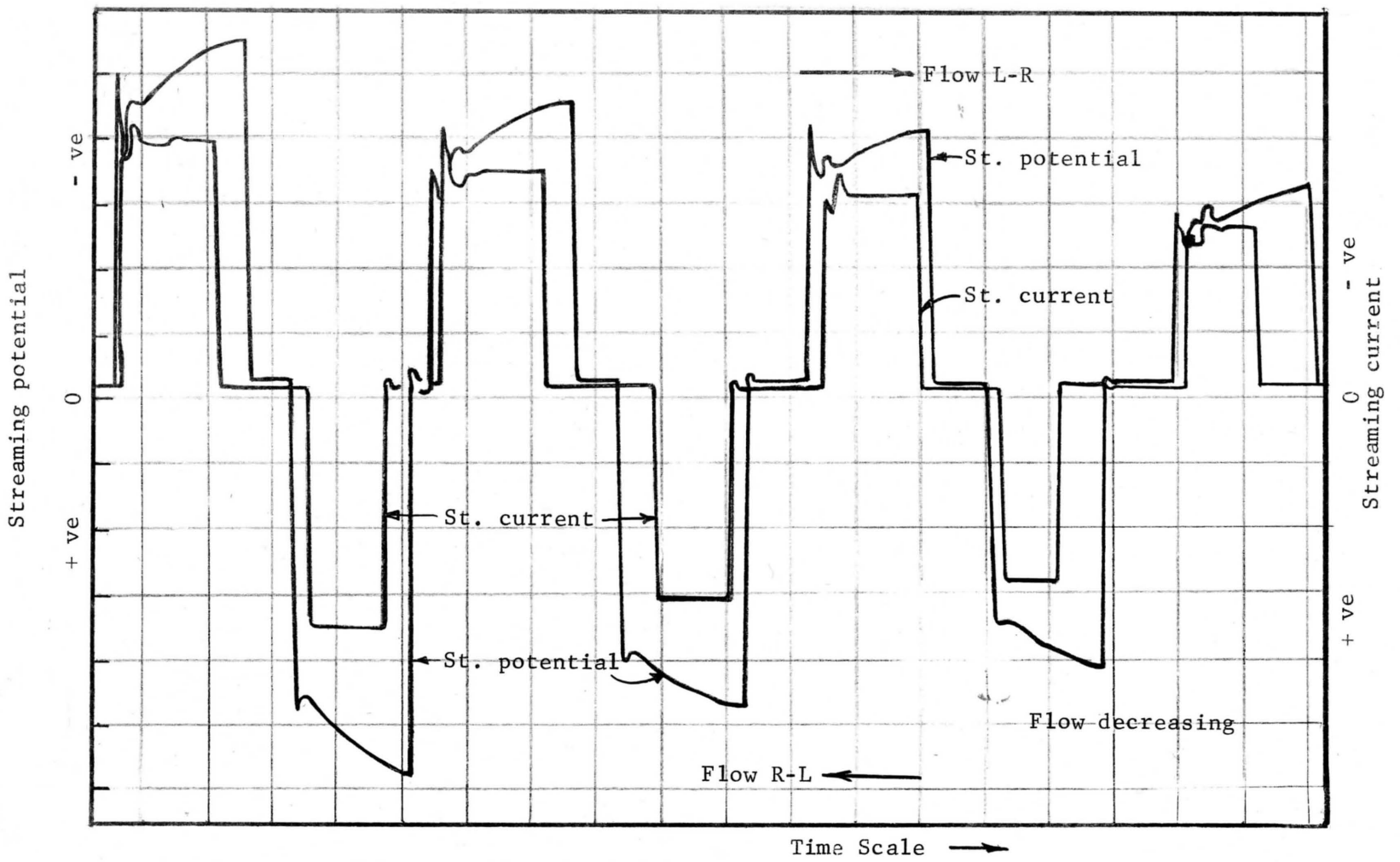

Figure 8. Actual data recording sheet for 10^{-4} KCl permeating through Sample 2.

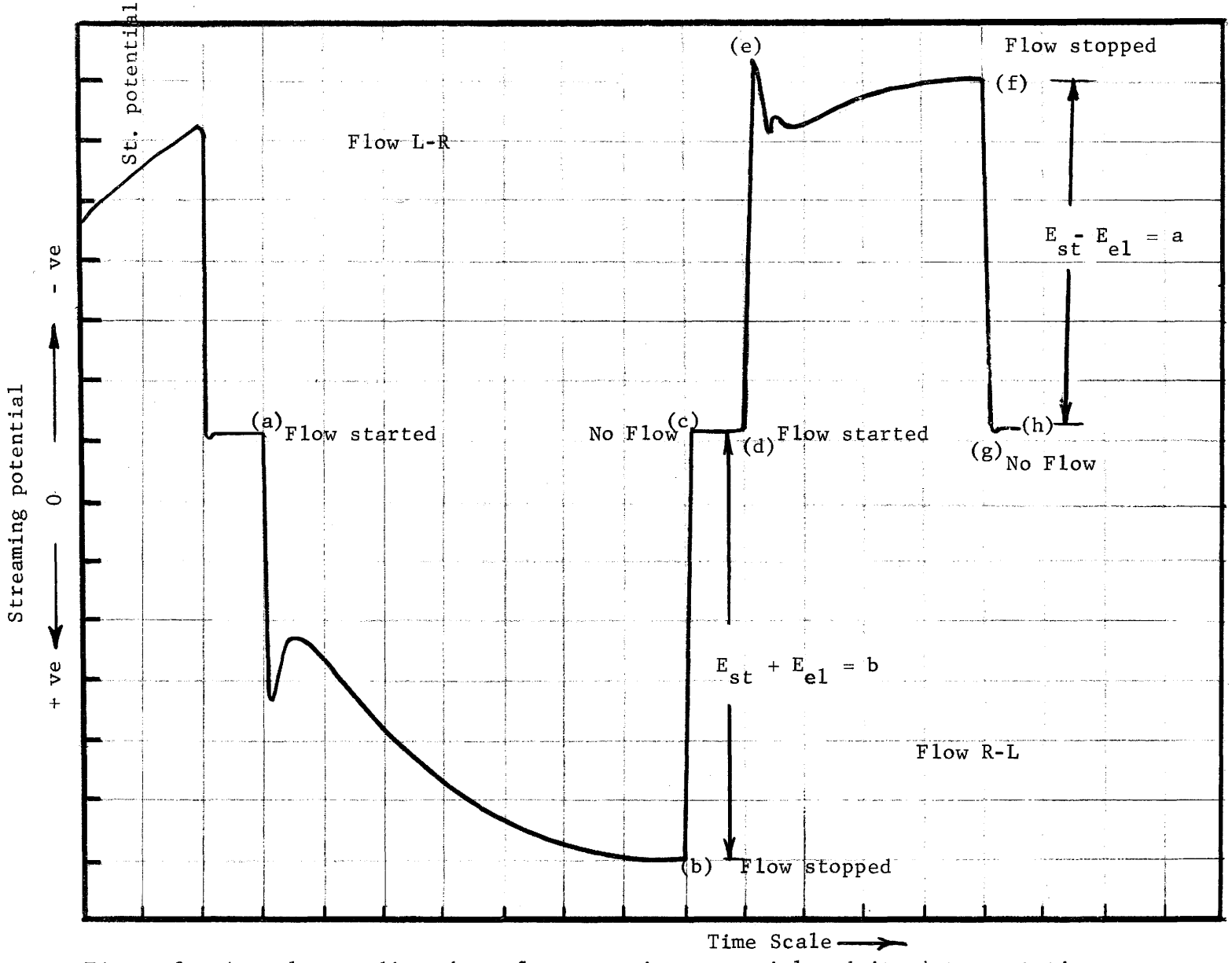

Figure 9. Actual recording chart for streaming potential and its interpretation.

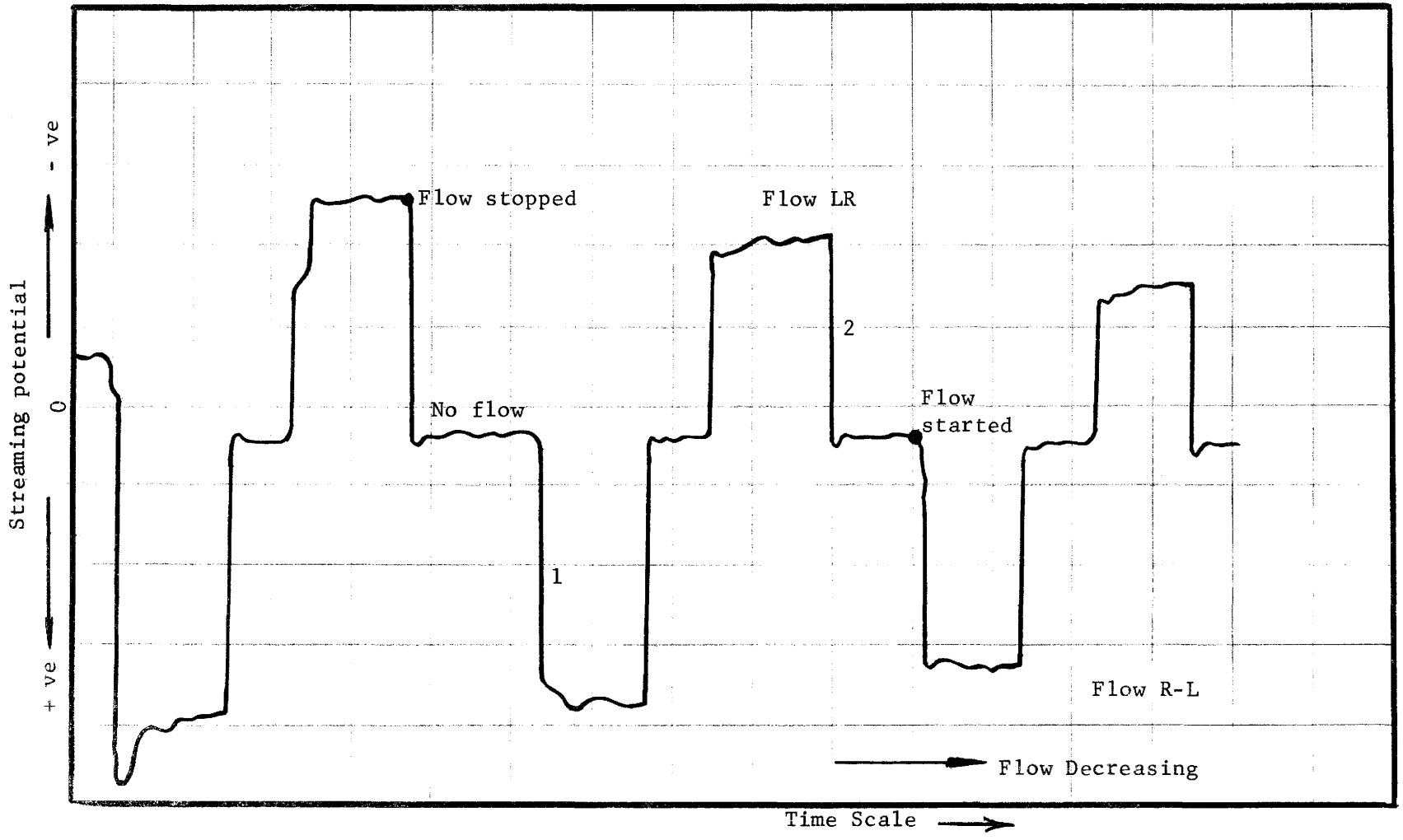

Figure 10. Recording chart for 10^{-4} KCl permeating through S_1

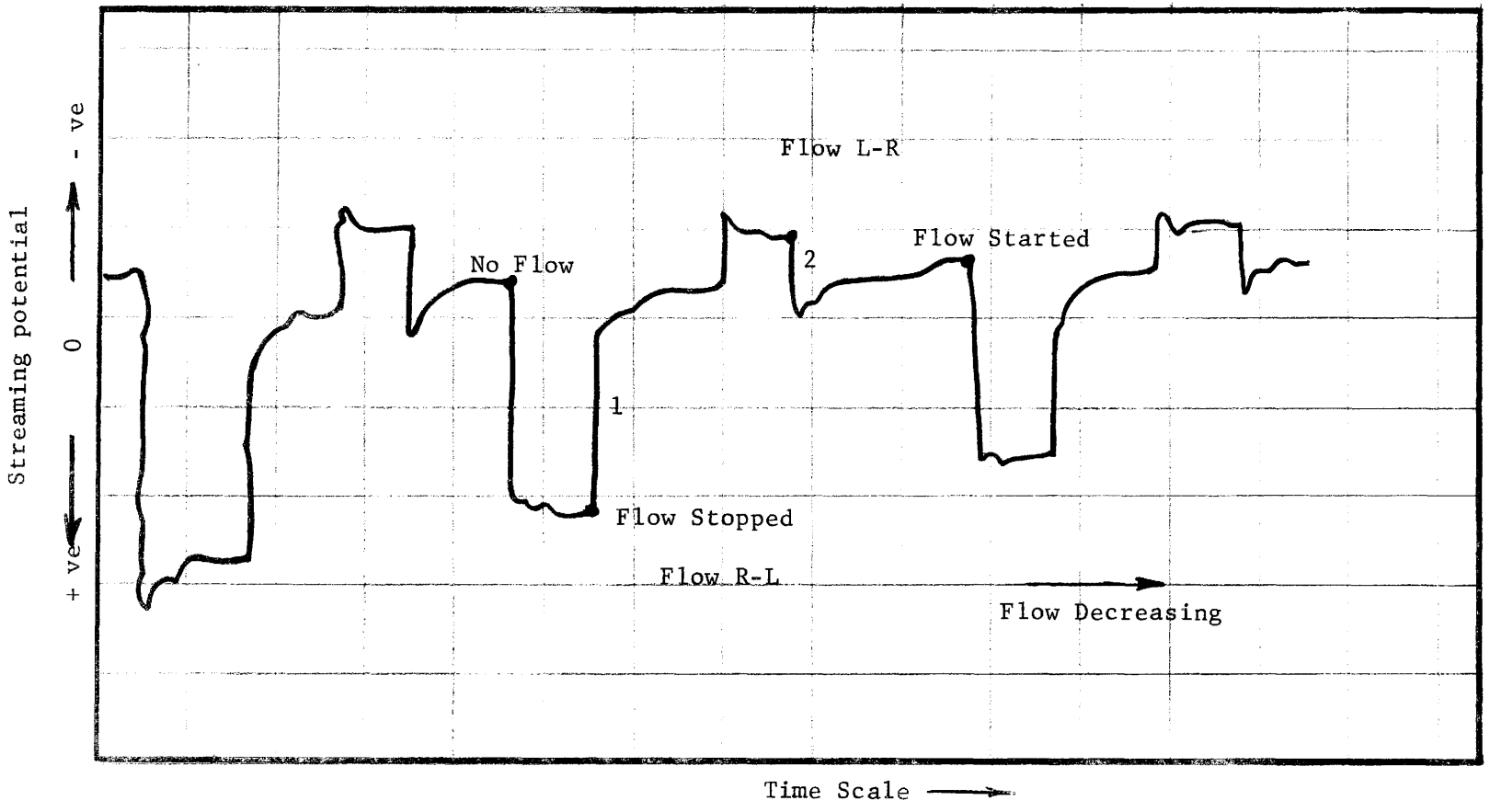

Figure 11. Recording chart for 10^{-3} N KCl permeating through S_2.

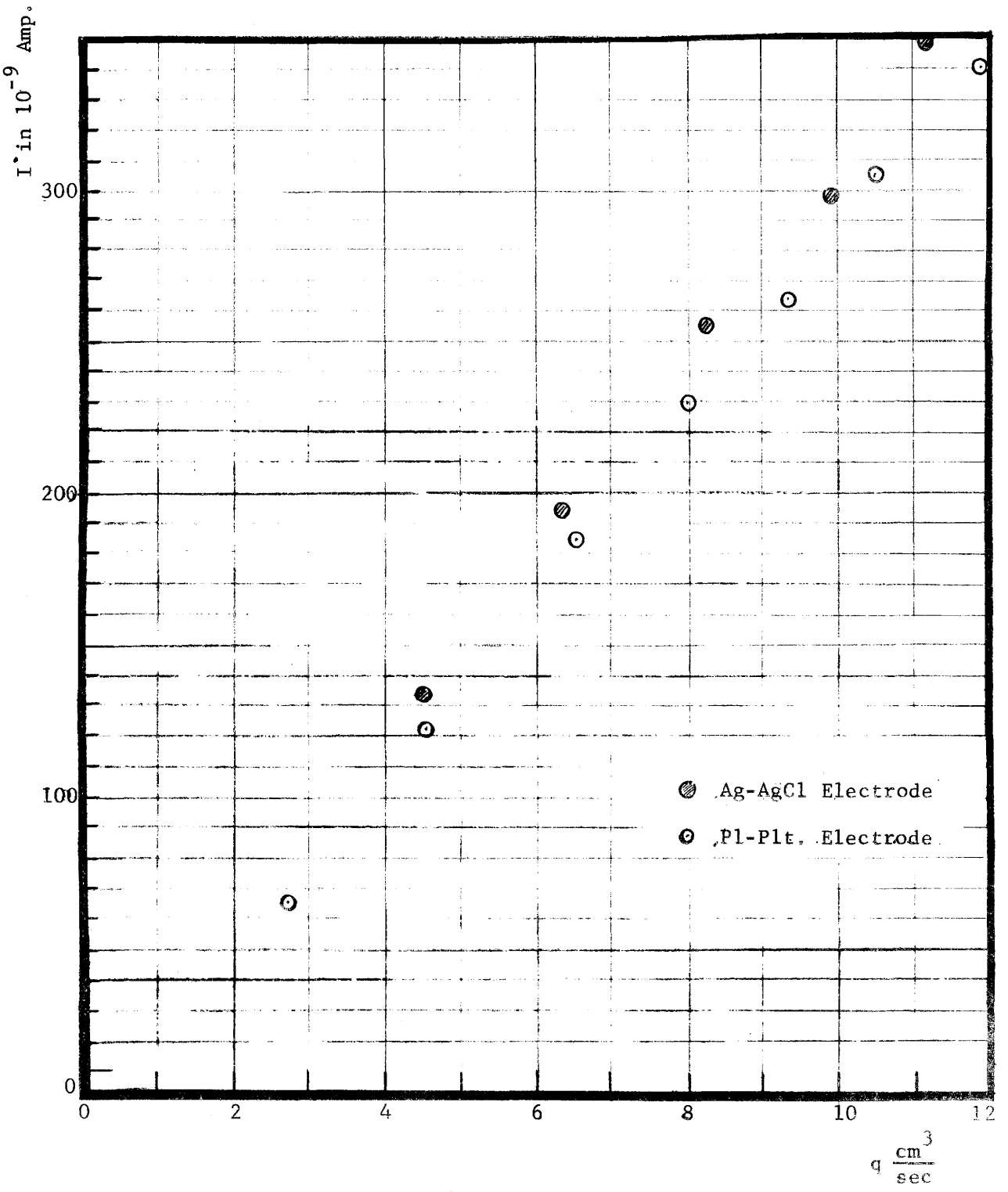

Figure 12. Discharge q in cm^3/sec versus streaming current I x 10^9 in ampers with conductance water permeating through S_2 confined in cells fitted with Ag-AgCl and platinized pl. electrodes.

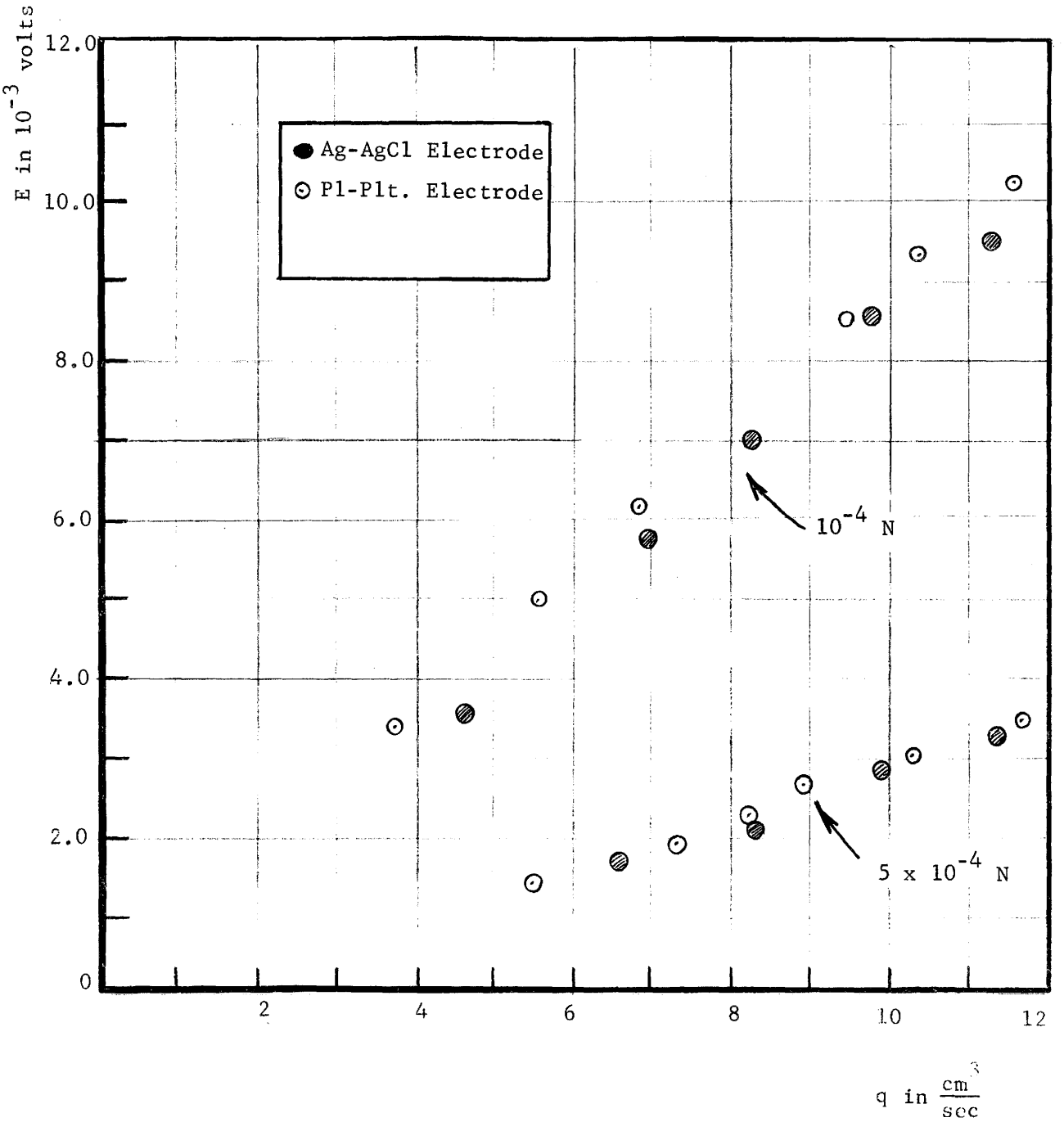

Figure 13. Discharge q in cm^3/sec versus streaming potential, E x 10^3 in volts with NaCl permeating through S_2 confined in cells fitted with Ag-AgCl and platinized pl. electrodes.

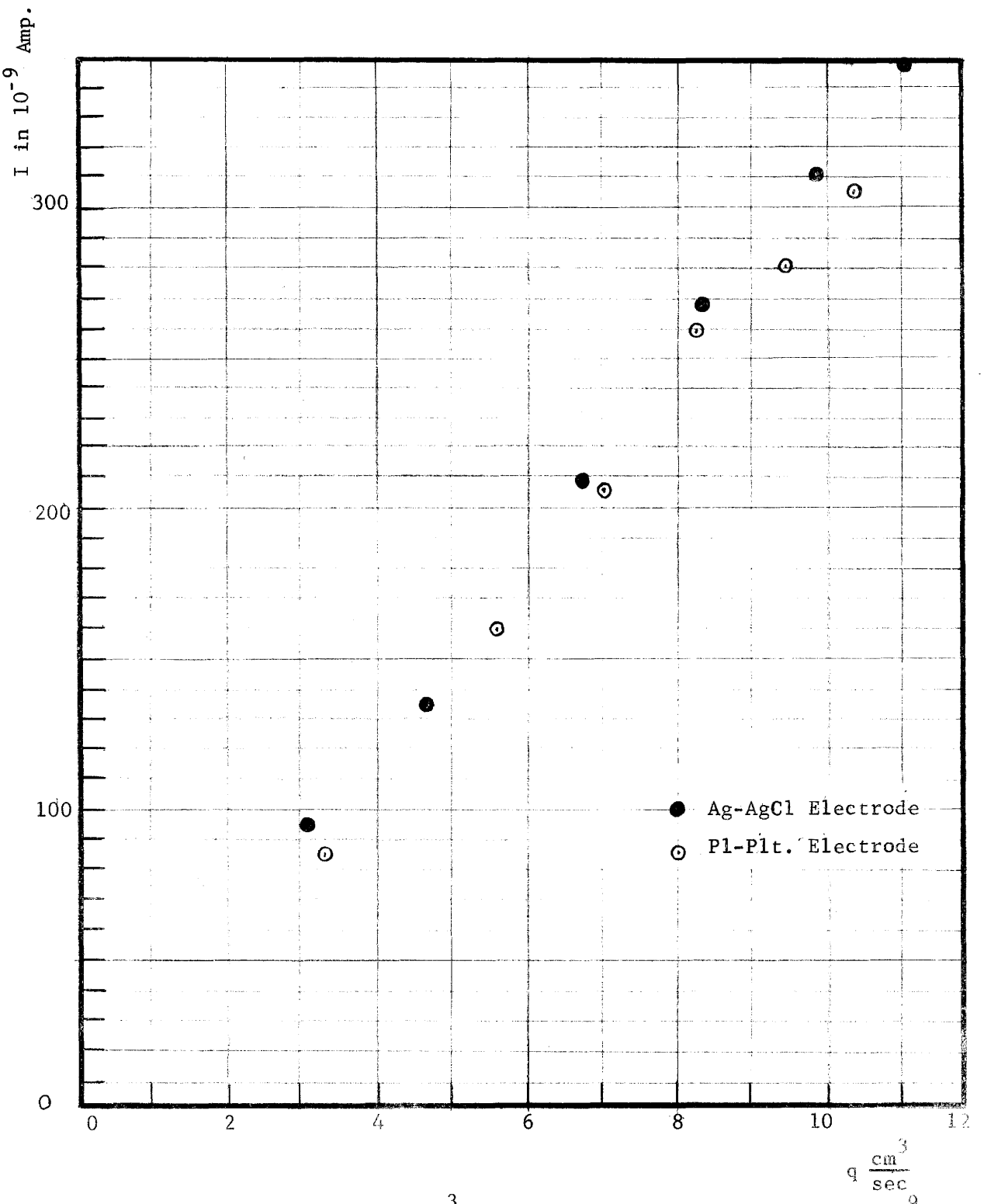

Figure 14. Discharge q in cm^3/sec versus streaming current I x 10^9 in ampers with 5 x 10^{-4} NaCl permeating through S_2 confined in cells fitted with Ag-AgCl and platinized pl. electrodes.

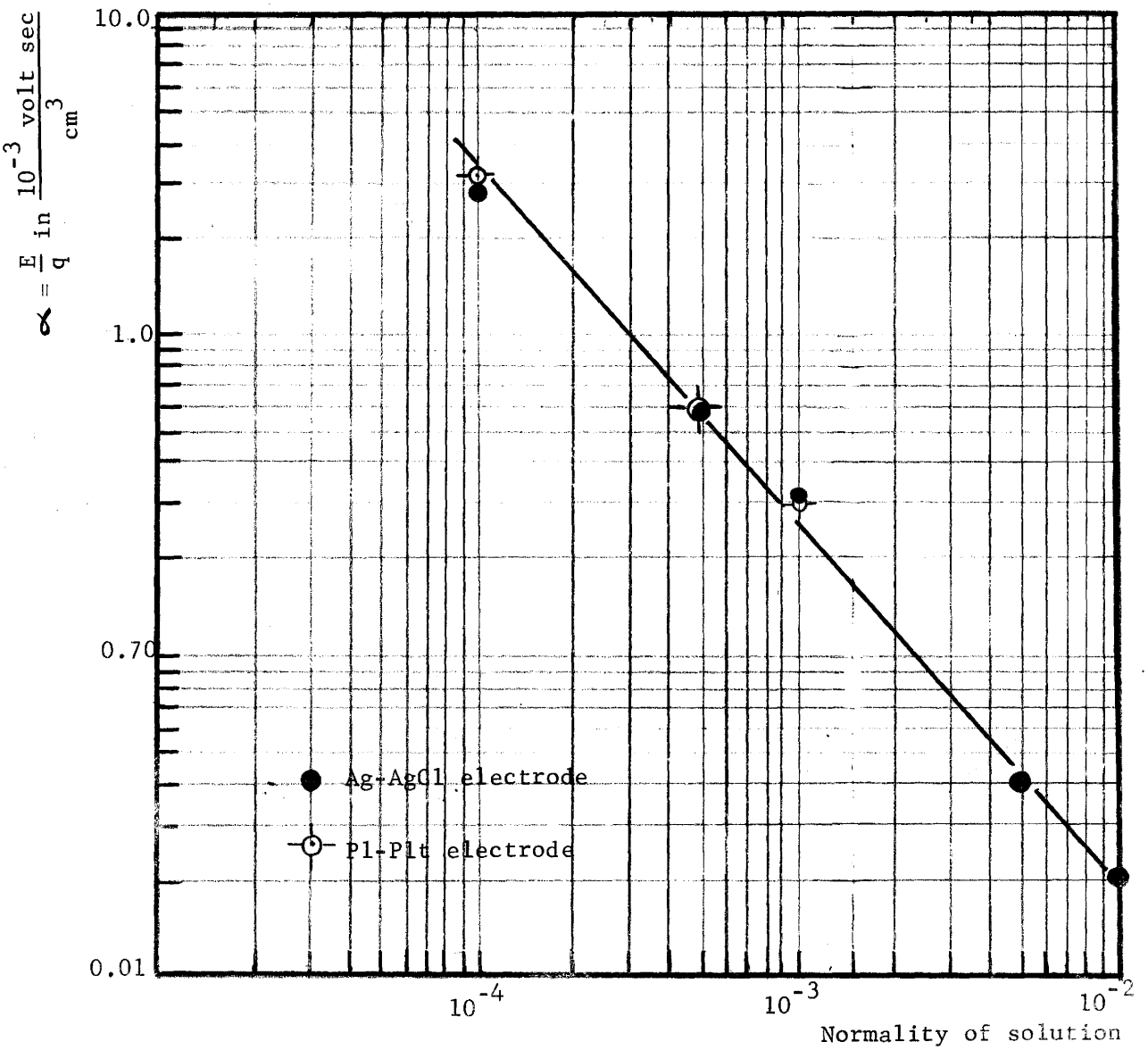

Figure 15. Slope of discharge versus streaming potential, α in $\frac{\text{millivolts x sec}}{\text{cm}^2}$ versus normality of KCl solutions permeating through S_1 confined in cells fitted with Ag-AgCl and platinized pl. electrodes.

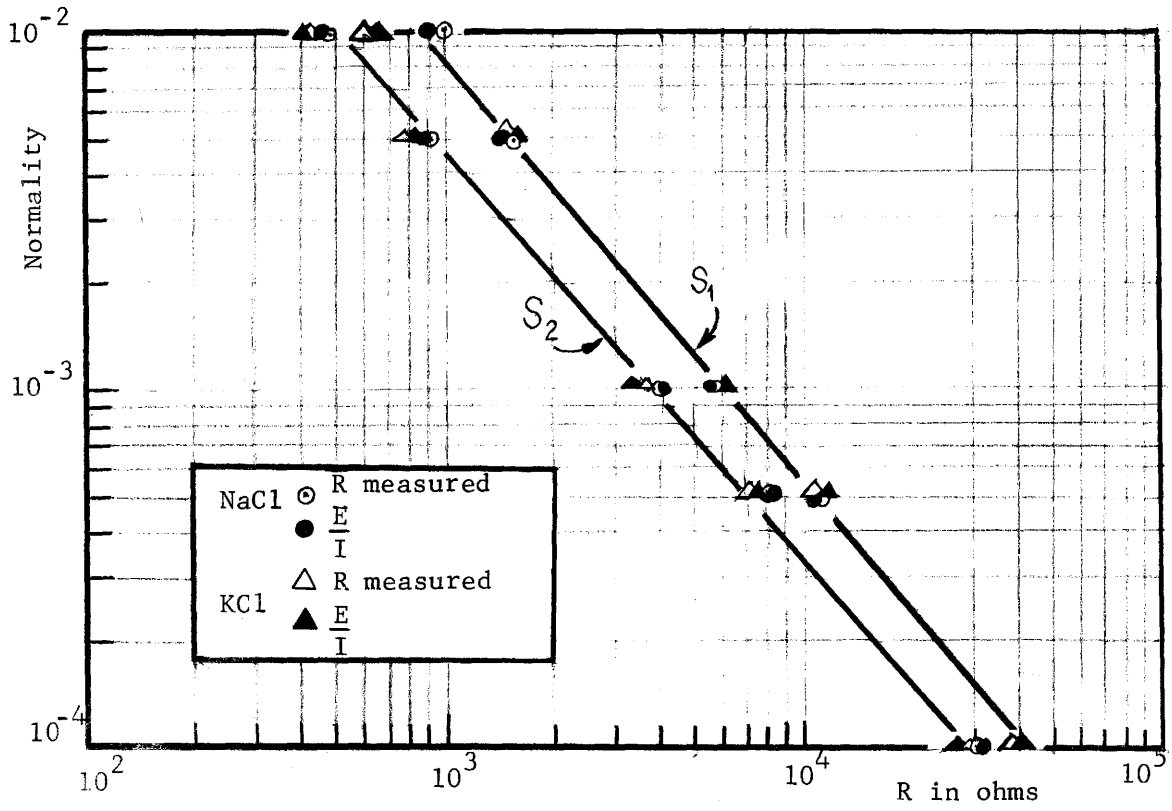

Figure 16. Normality of permeating solution versus the resistance for S_1 and S_2.

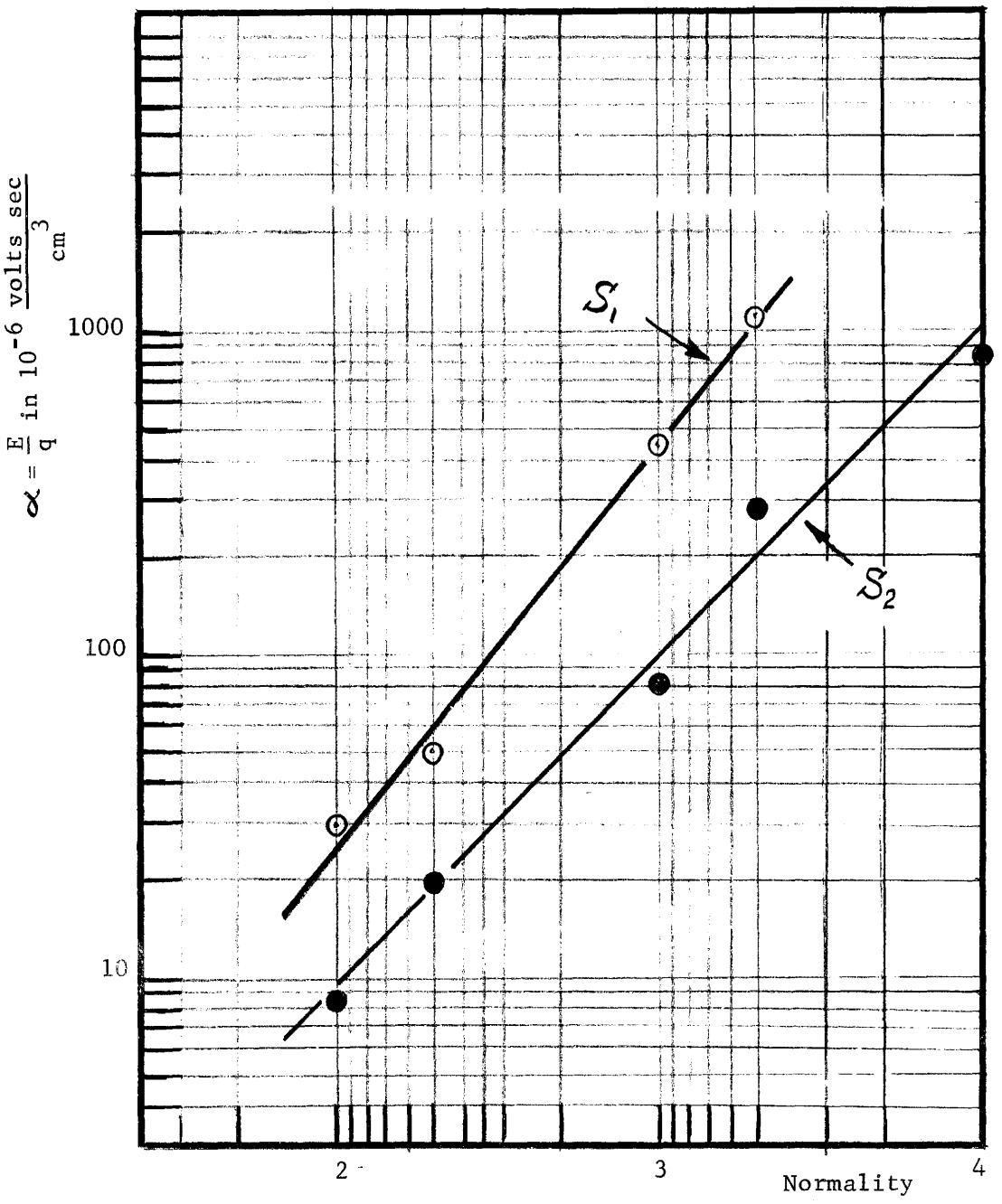

Figure 17. The slope α versus NaCl normality for S_1 and S_2.

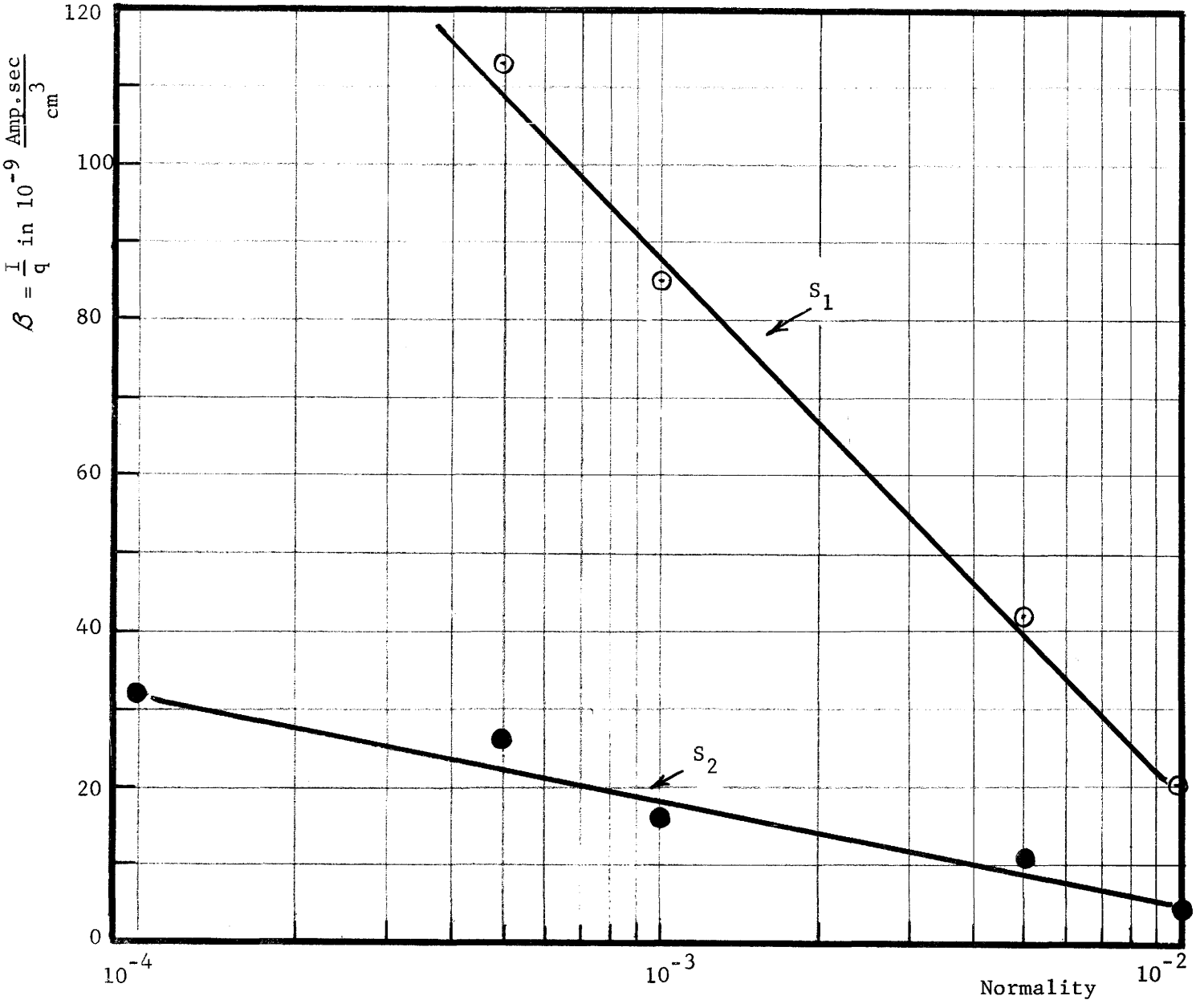

Figure 18. Slope β versus NaCl normality for S_1 and S_2

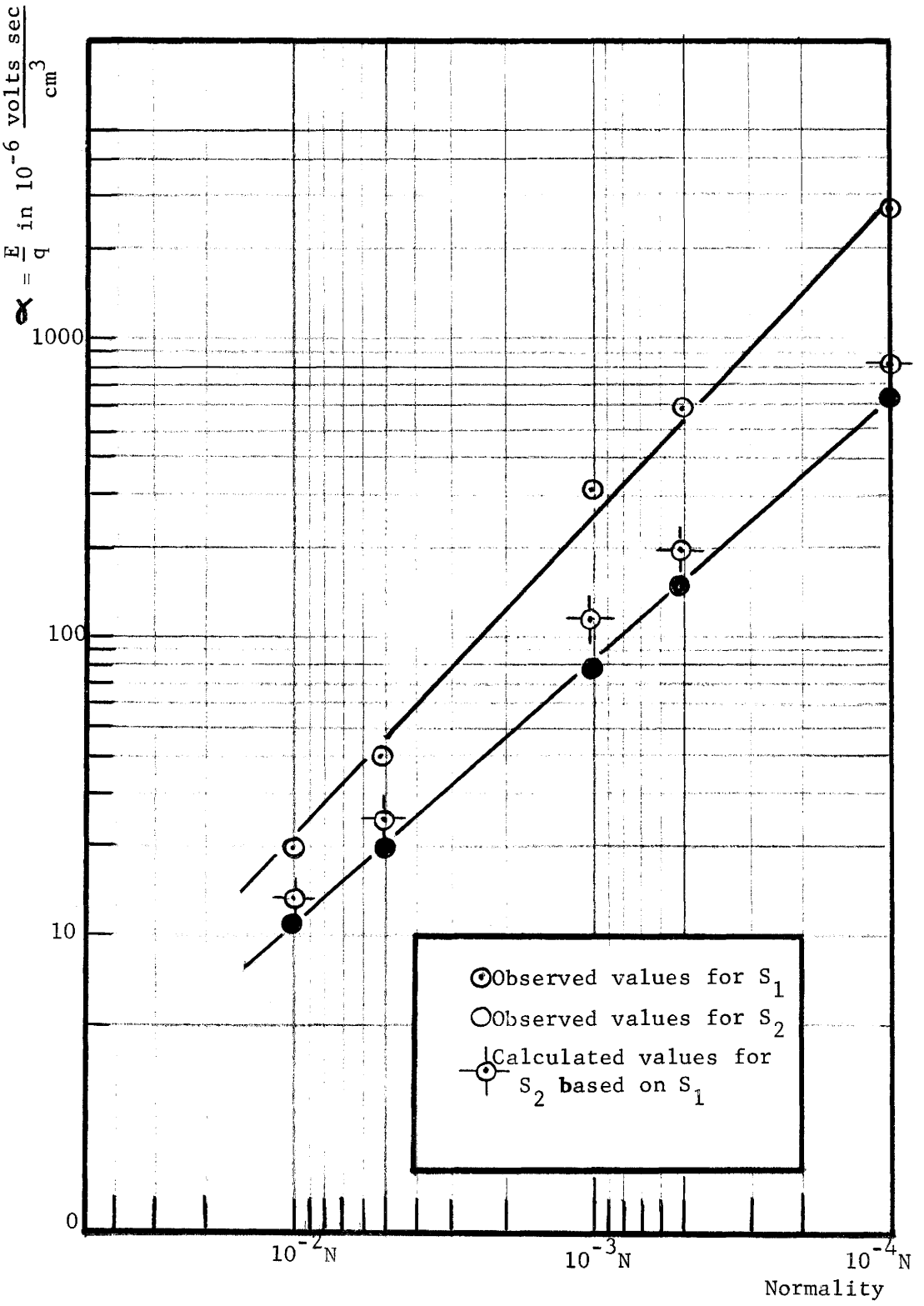

Figure 19. The slope α versus KCl normality for S_1 and S_2.

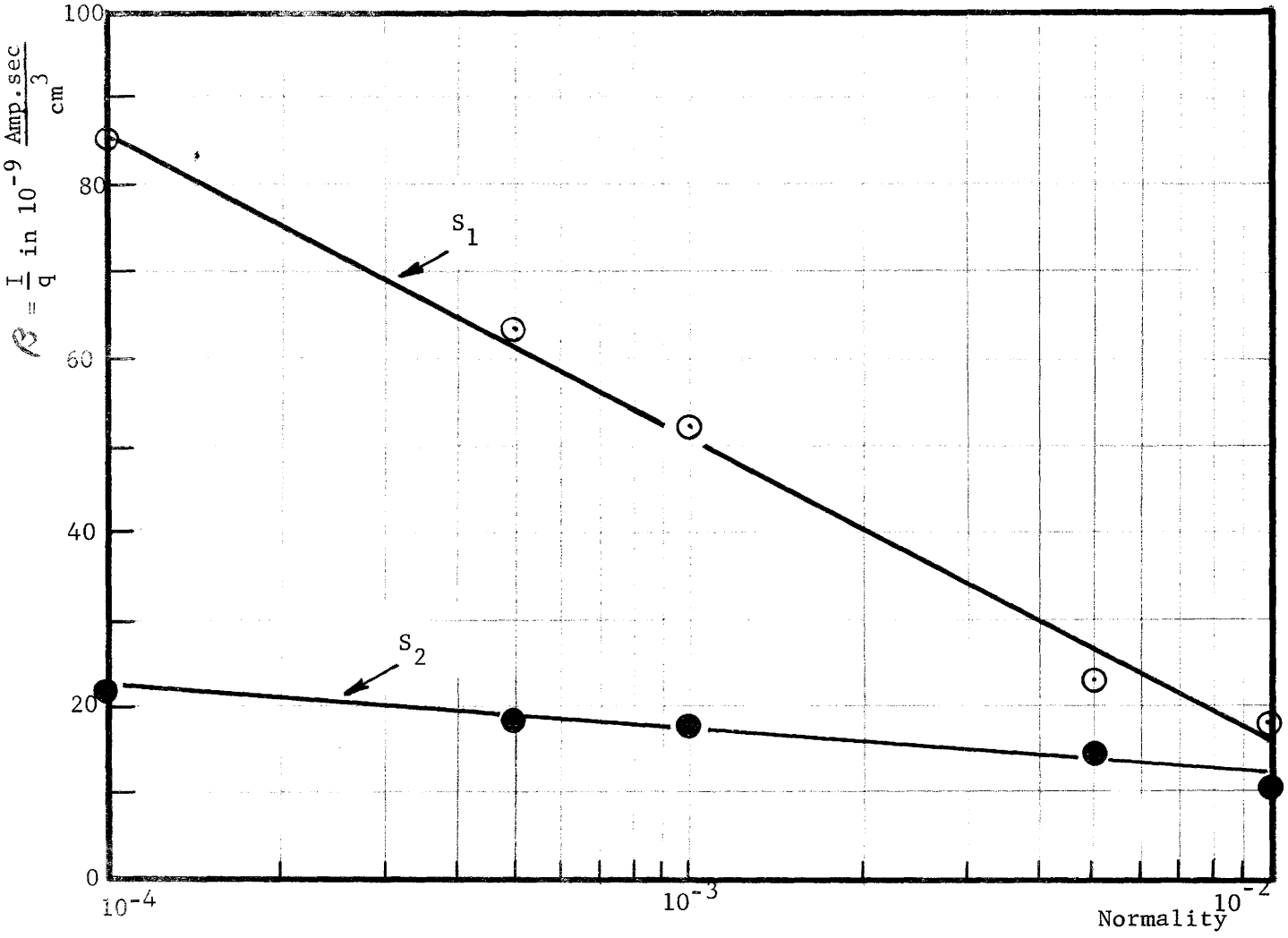

Figure 20. The slope β versus KCl normality for S_1 and S_2.

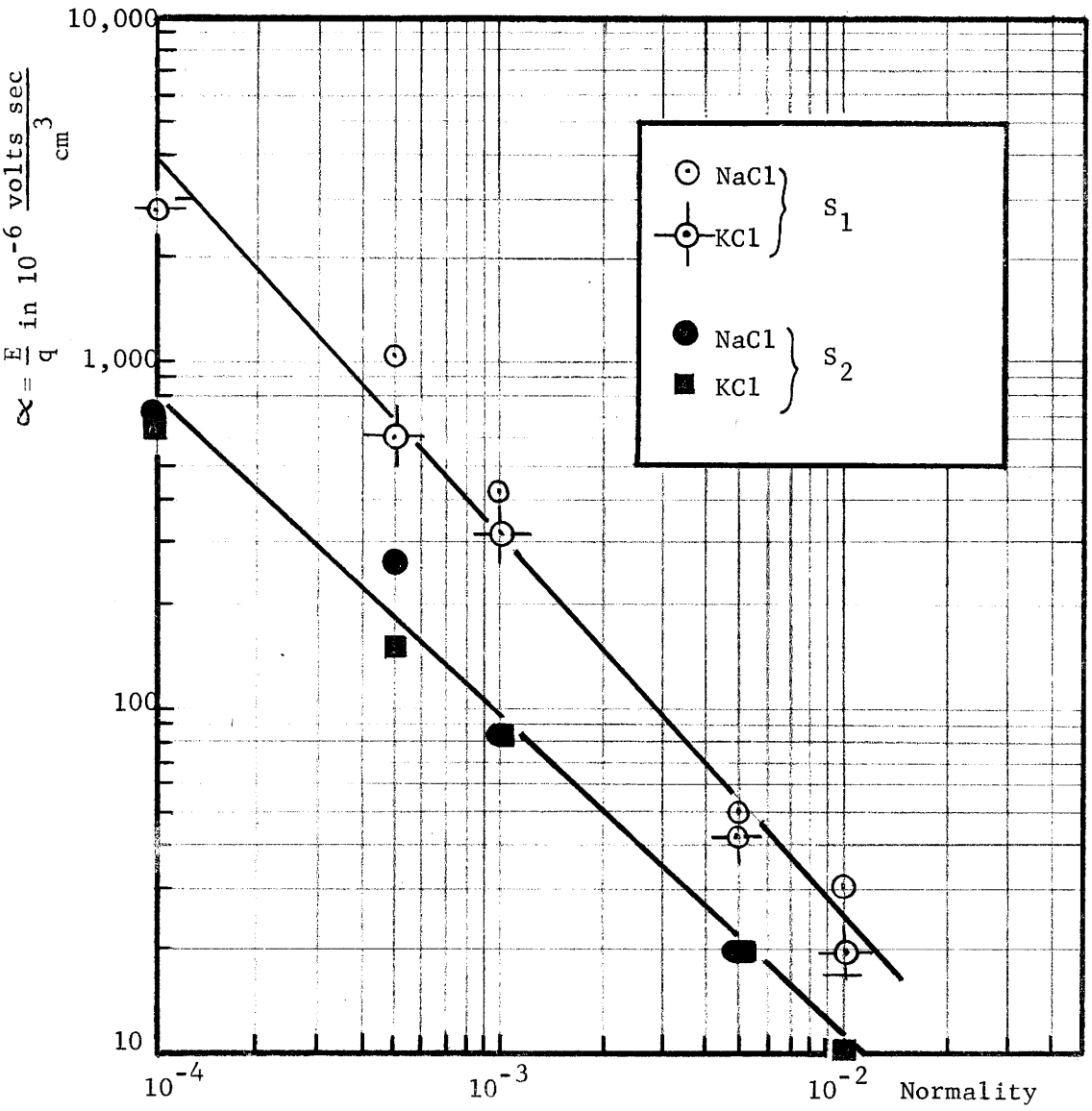

Figure 21. The slope α versus normality of NaCl and KCl for S_1 and S_2.

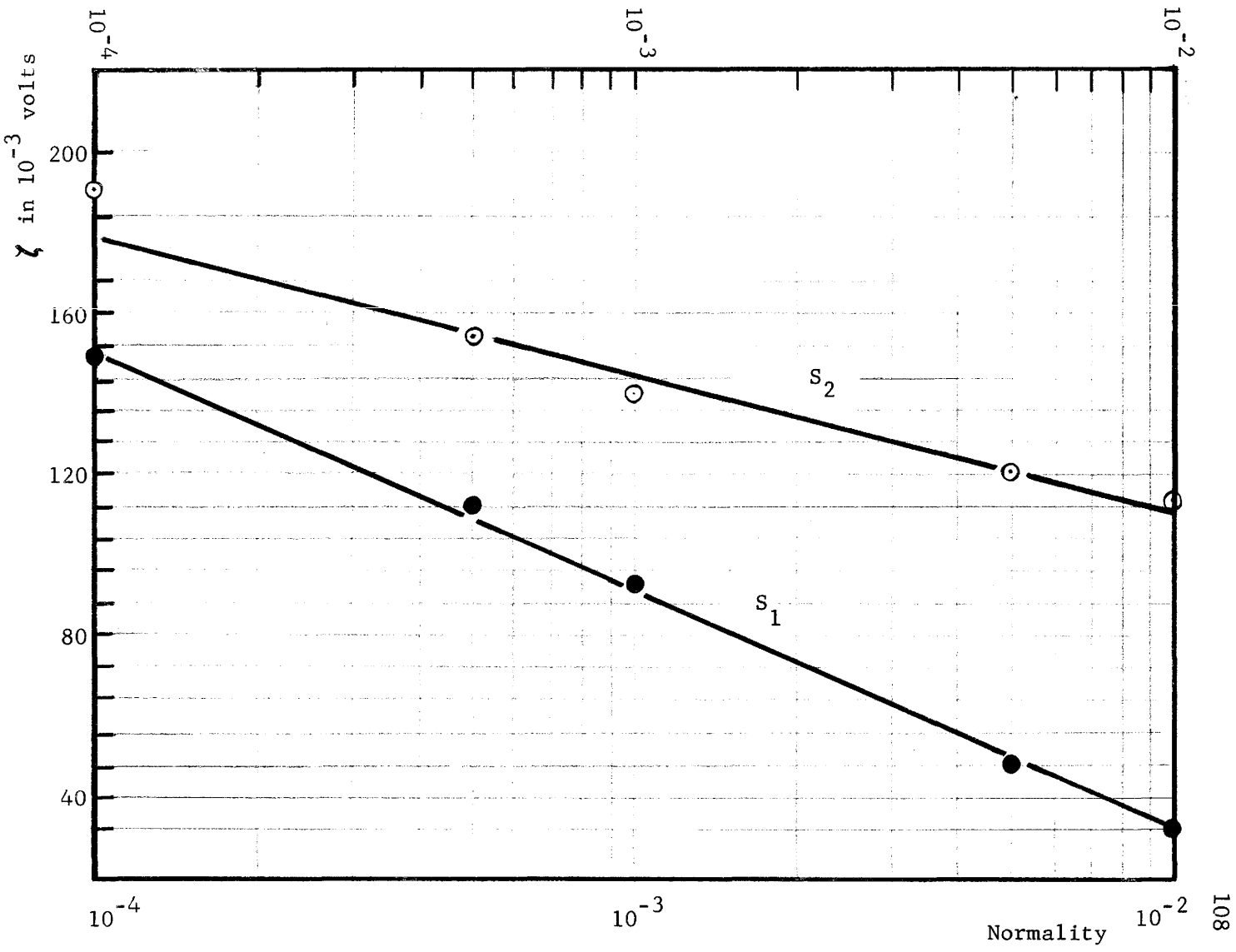

Figure 22. Calculated ζ values versus normality of KCl solutions for S_1 and S_2.

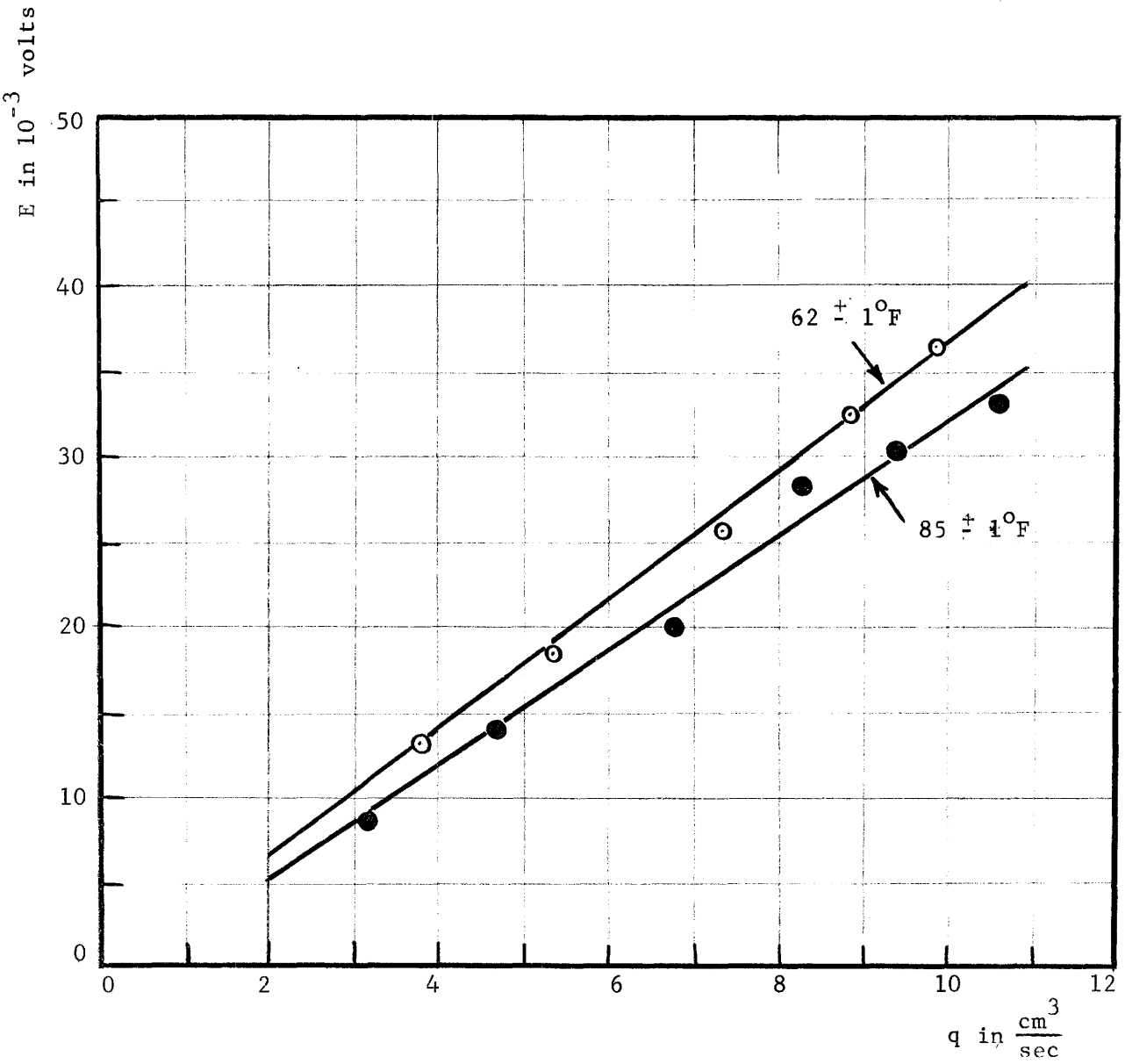

Figure 23. Discharge in cm^3/sec versus streaming potential in millivolts with temperature as a parameter.

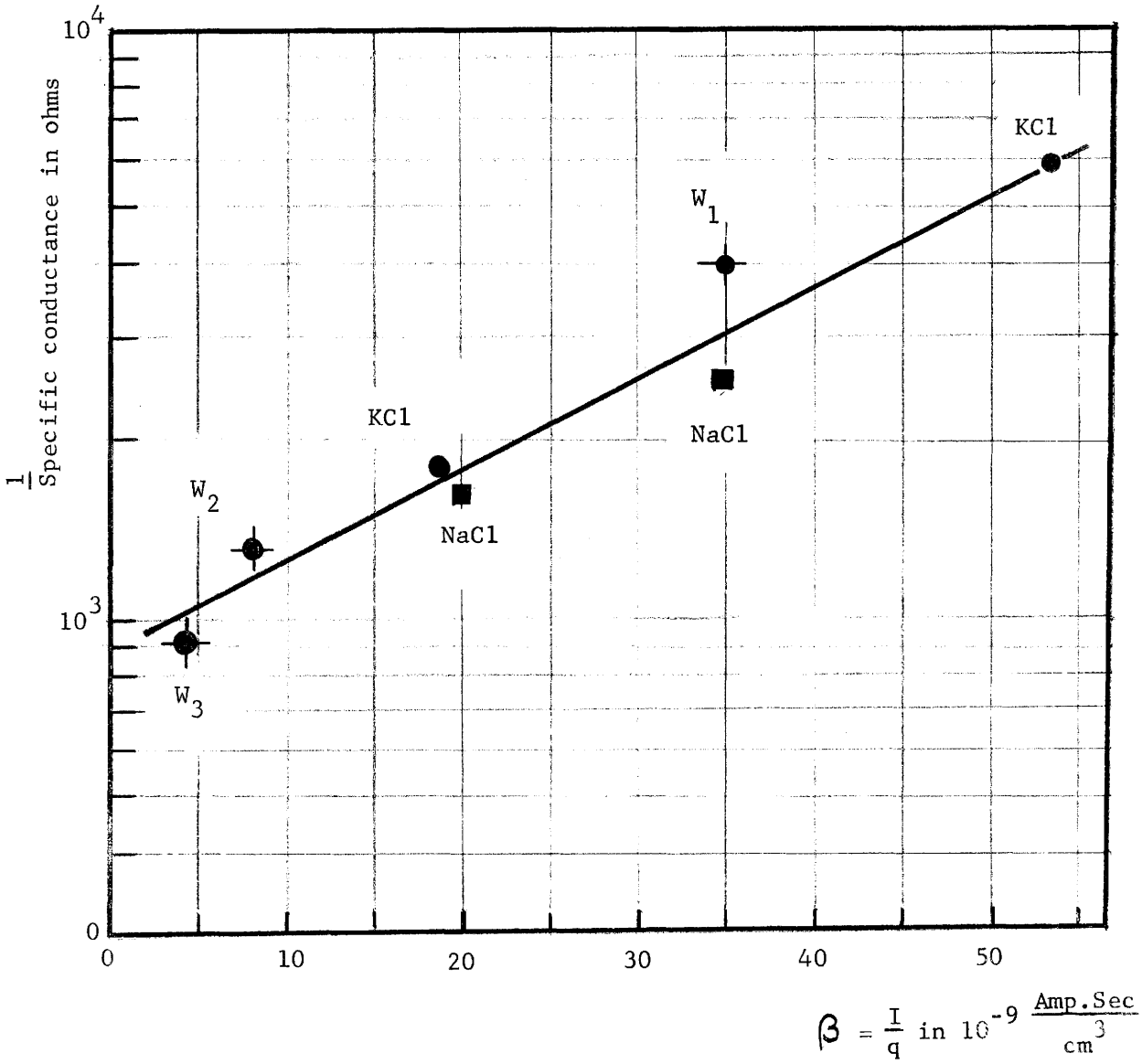

Figure 24. Slope β versus 1/sp. conductance for NaCl, KCl and simulated natural waters, W_1, W_2 and W_3.

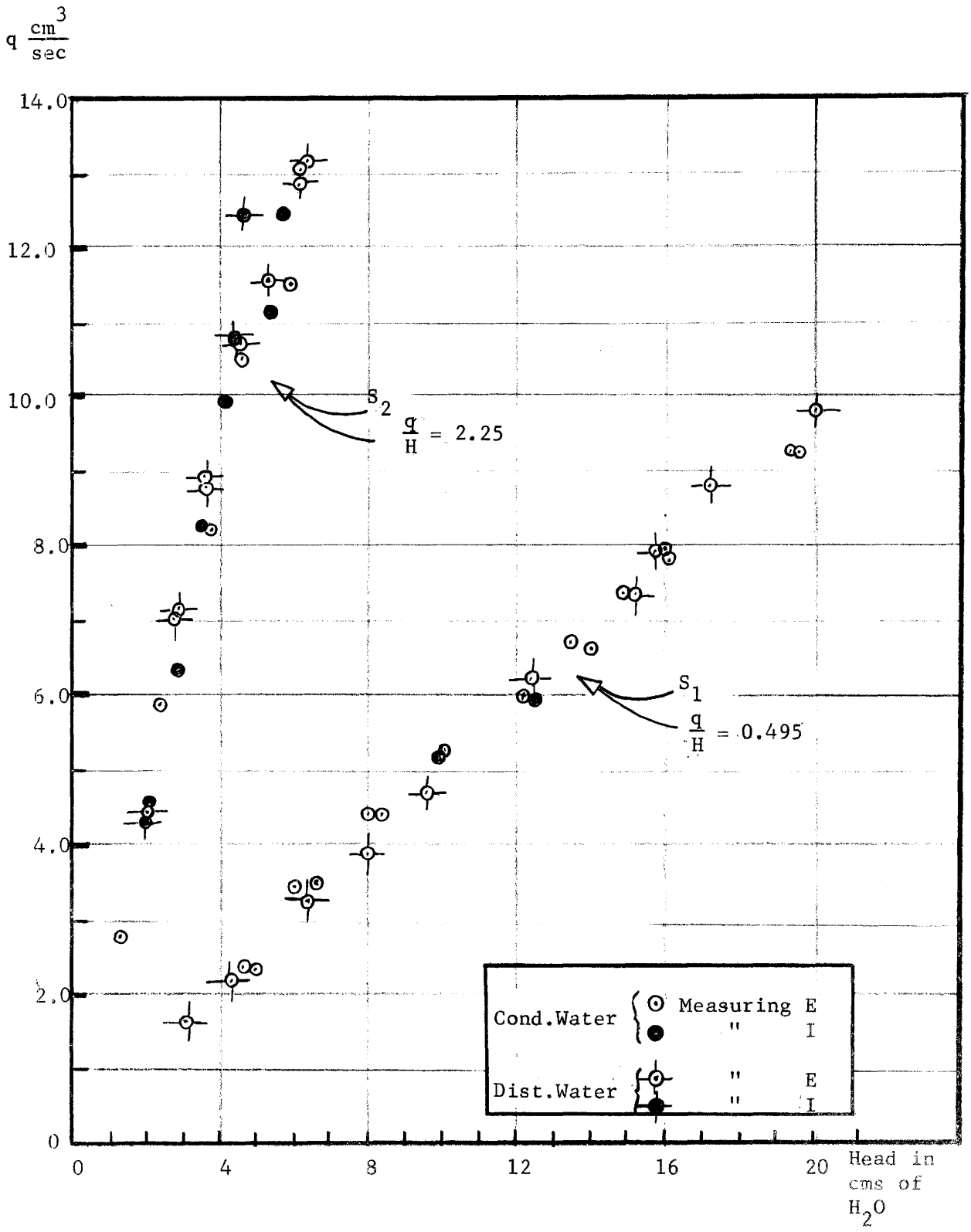

Figure 25. Discharge in cm^3/sec versus applied differential pressure in cms of water for conductance and distilled water permeating through S_1 and S_2.

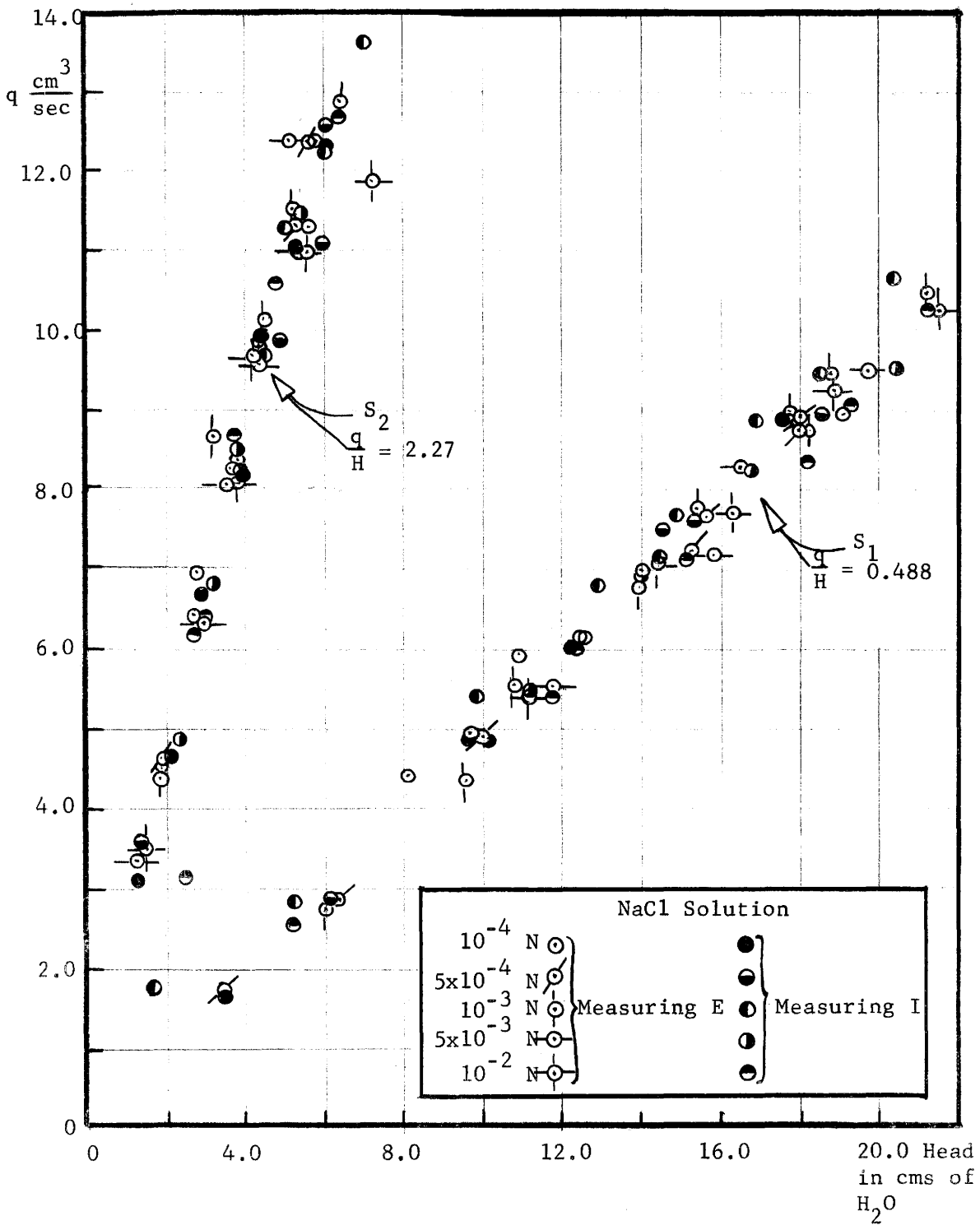

Figure 26. Discharge in cm^3/sec vs. applied differential pressure p in cm of water for sodium chloride solution with different salt concentrations permeating through S_1 and S_2.

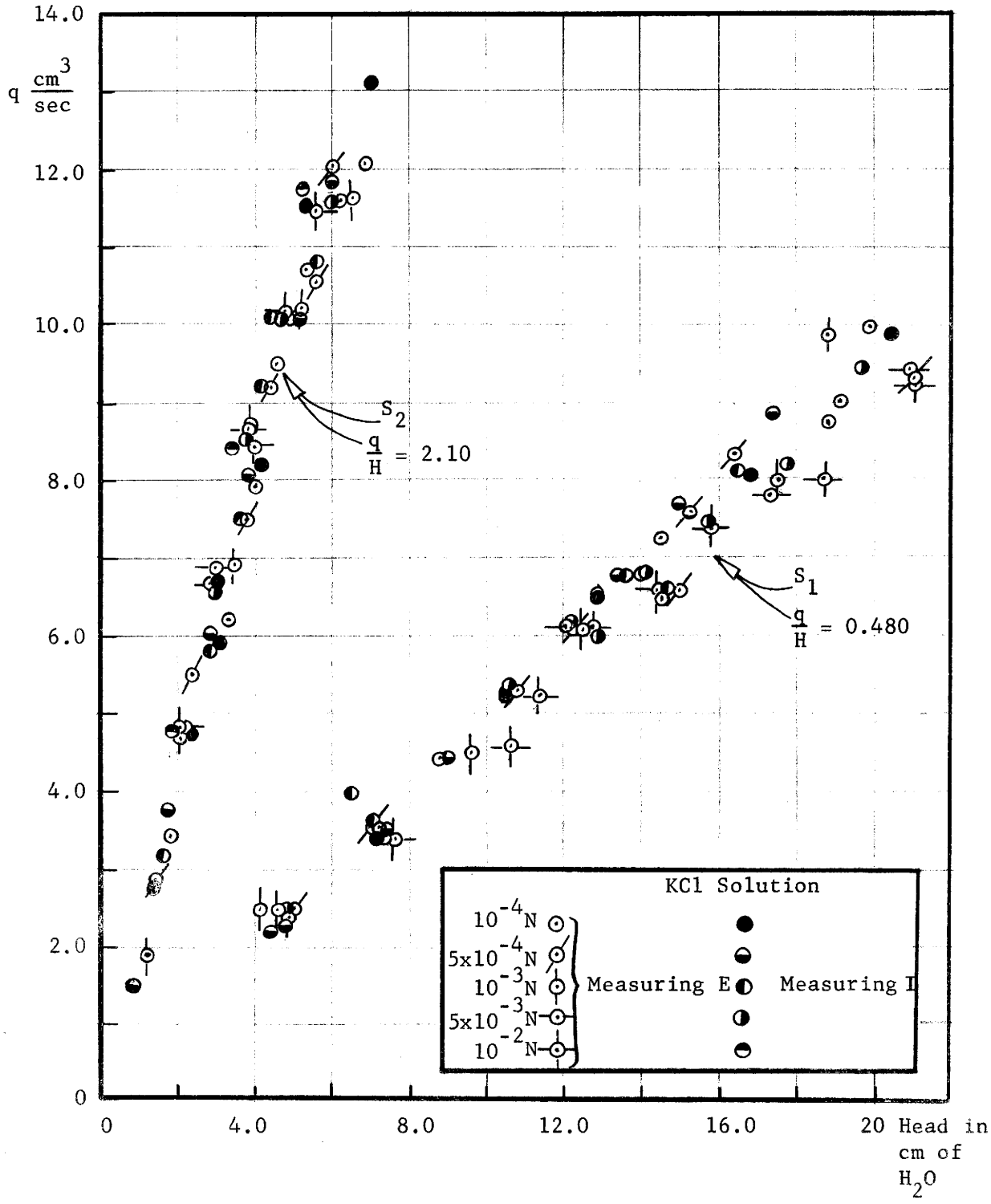

Figure 27. Discharge in cm^3/sec vs. applied differential pressure, H, in cms of water for potassium chloride solution with different salt concentrations permeating through S_1 and S_2.

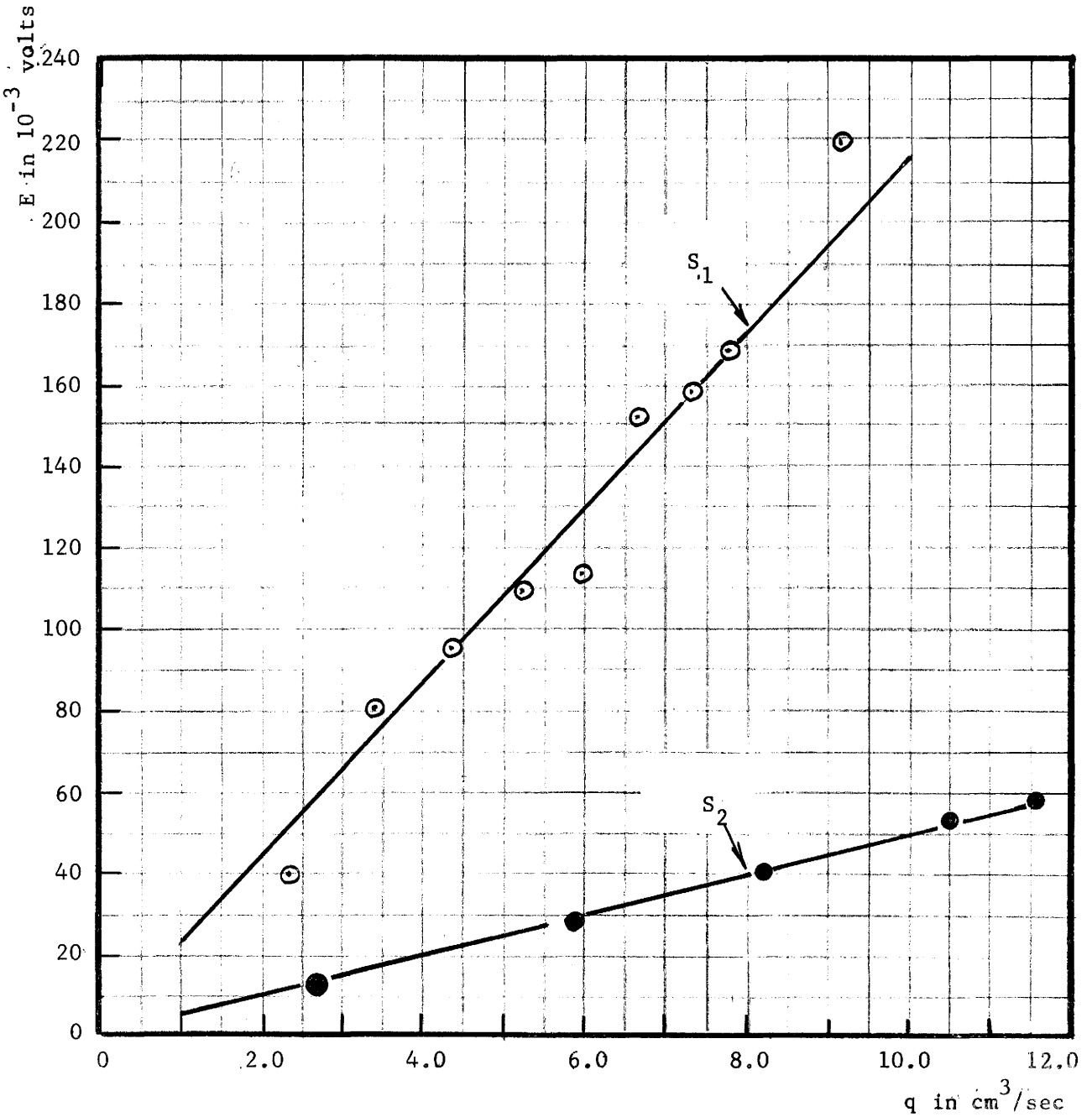

Figure 28. Discharge q versus streaming potential E, for conductance water permeating through S_1 and S_2.

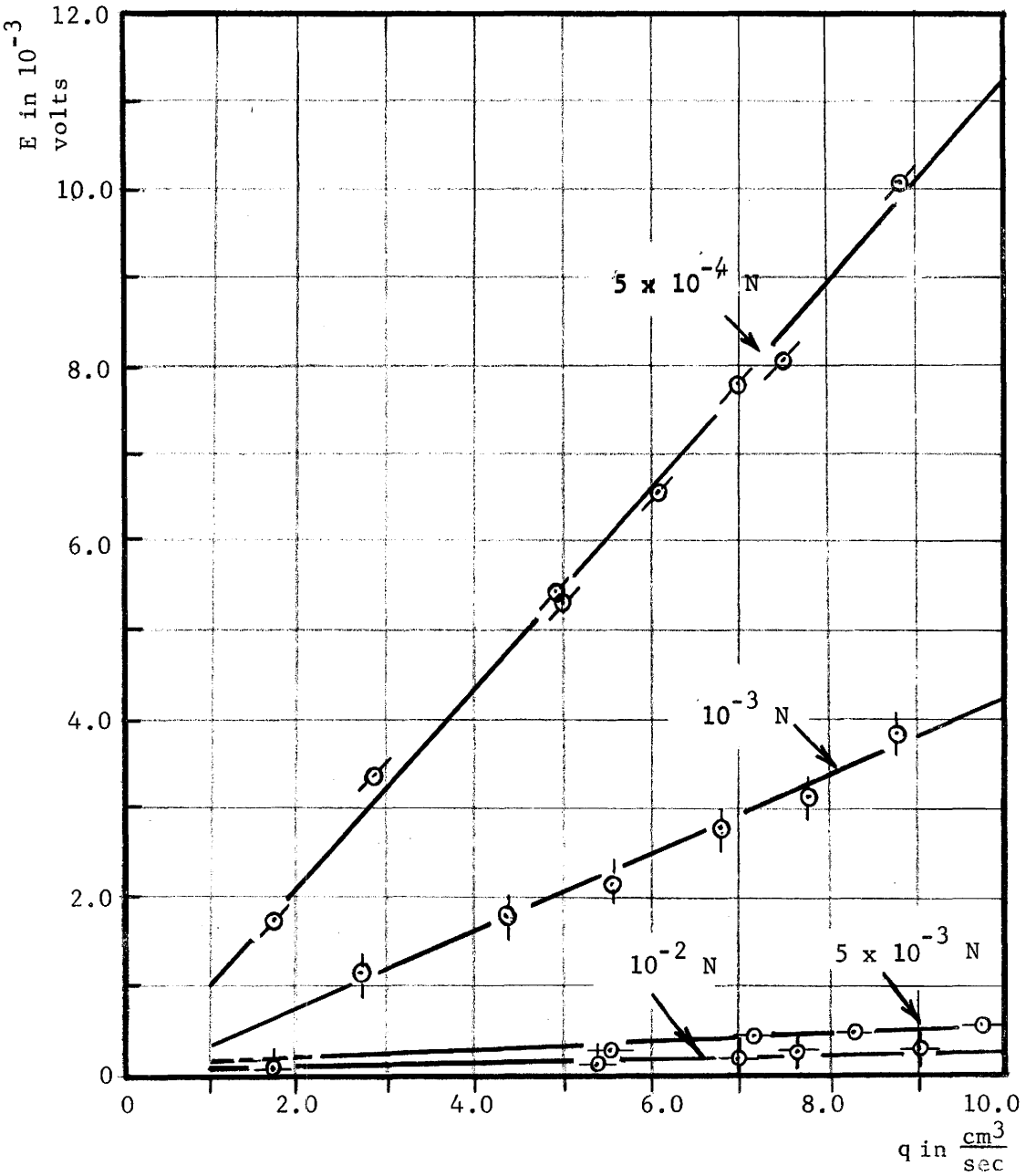

Figure 29. Discharge q versus streaming potential E for NaCl permeating through S_1 at different salt concentrations.

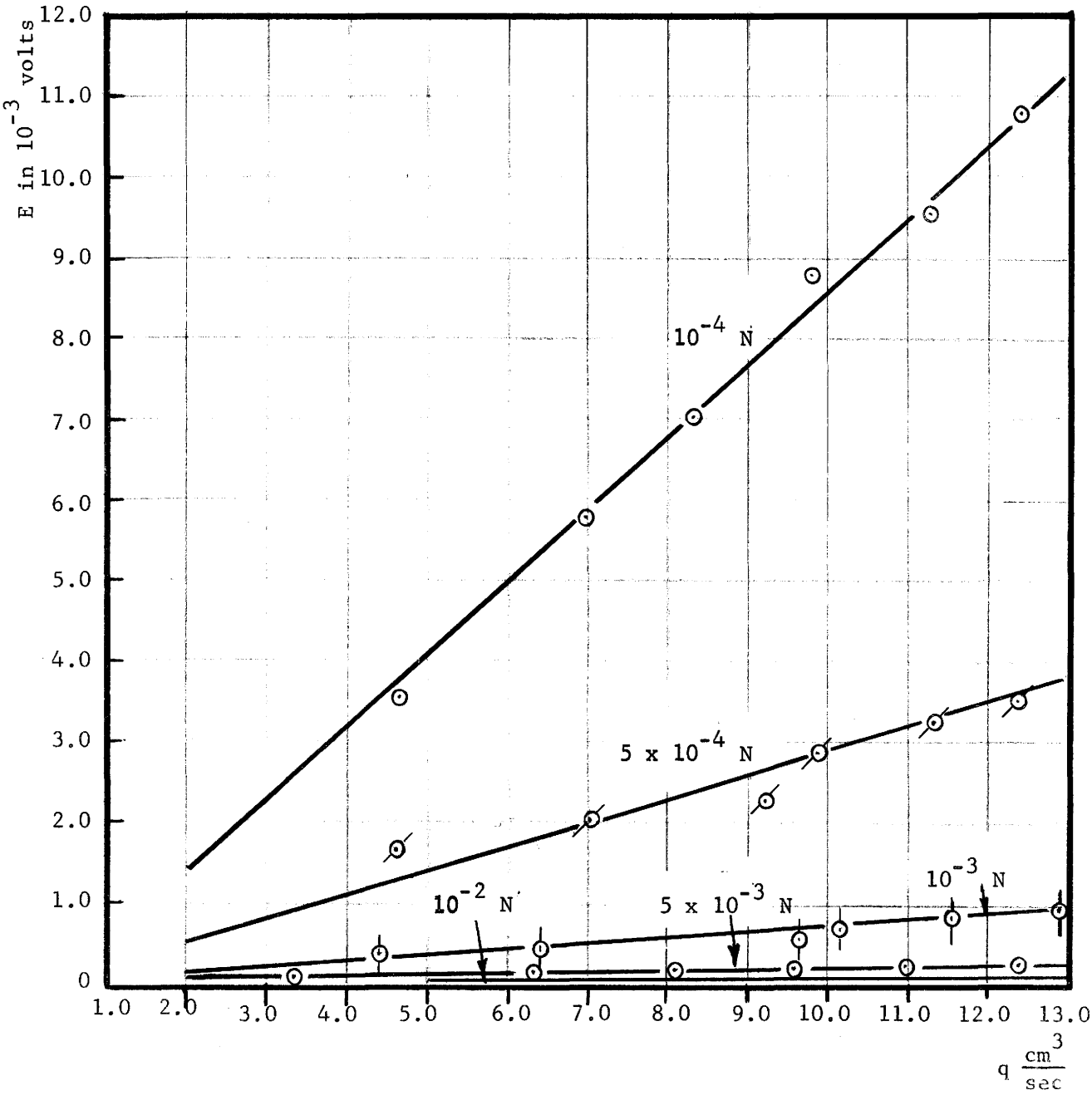

Figure 30. Discharge q versus streaming potential E for NaCl permeating through S_2 at different salt concentrations.

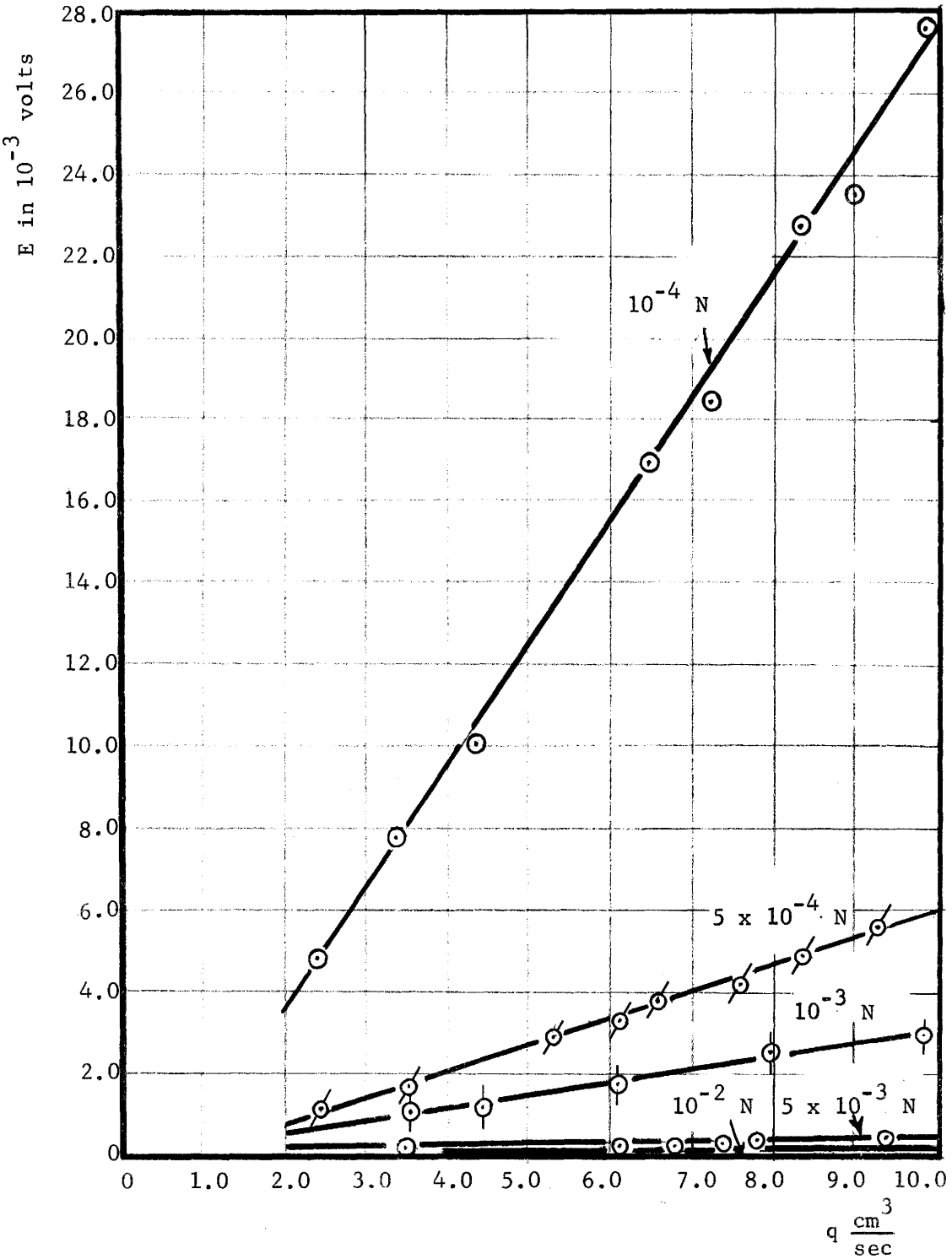

Figure 31. Discharge q versus streaming potential E for KCl permeating through S_1 at different salt concentrations.

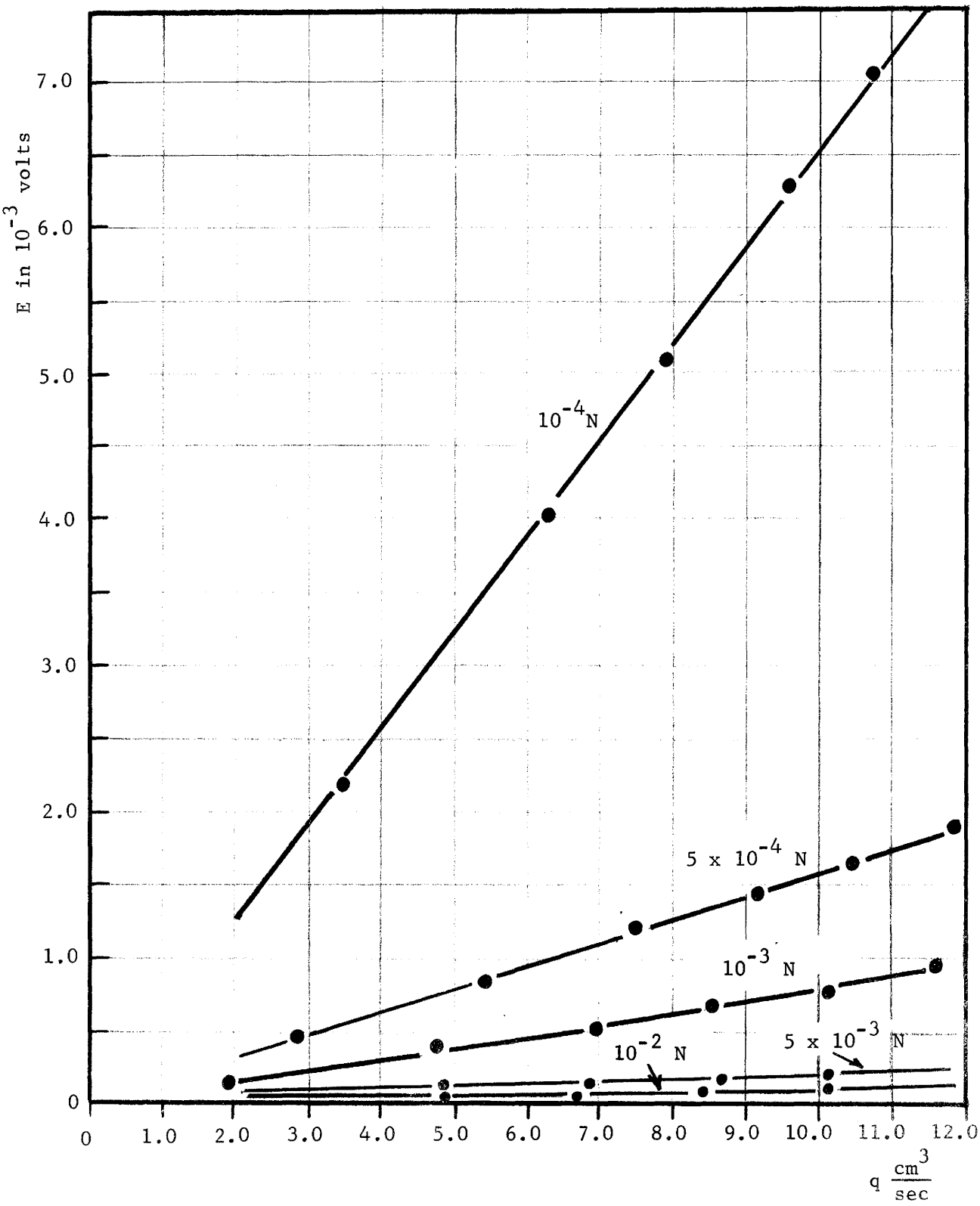

Figure 32. Discharge q versus streaming potential E for KCl permeating through S_2 at different salt concentrations.

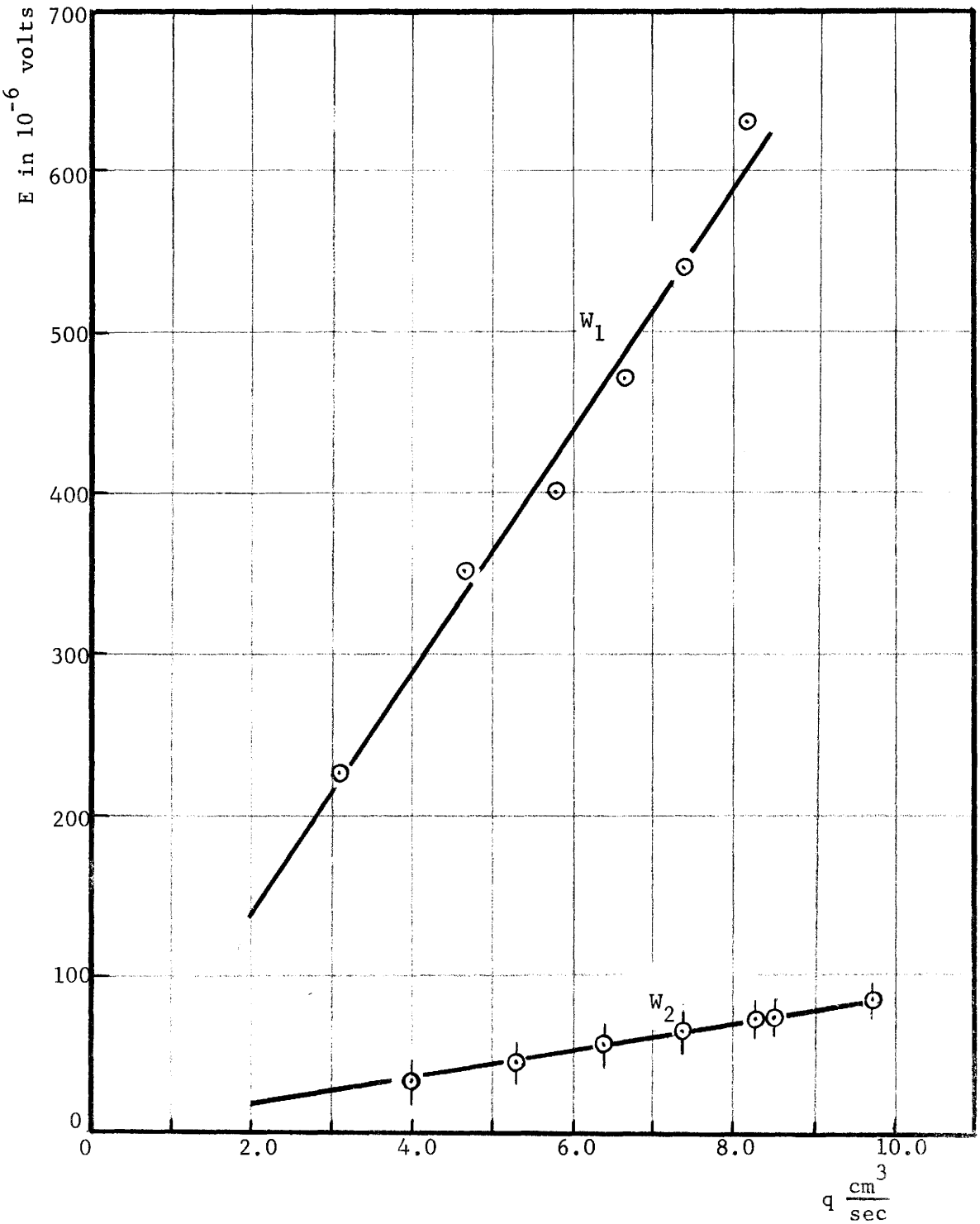

Figure 33. Discharge q versus streaming potential E for W_1 and W_2 permeating through S_1.

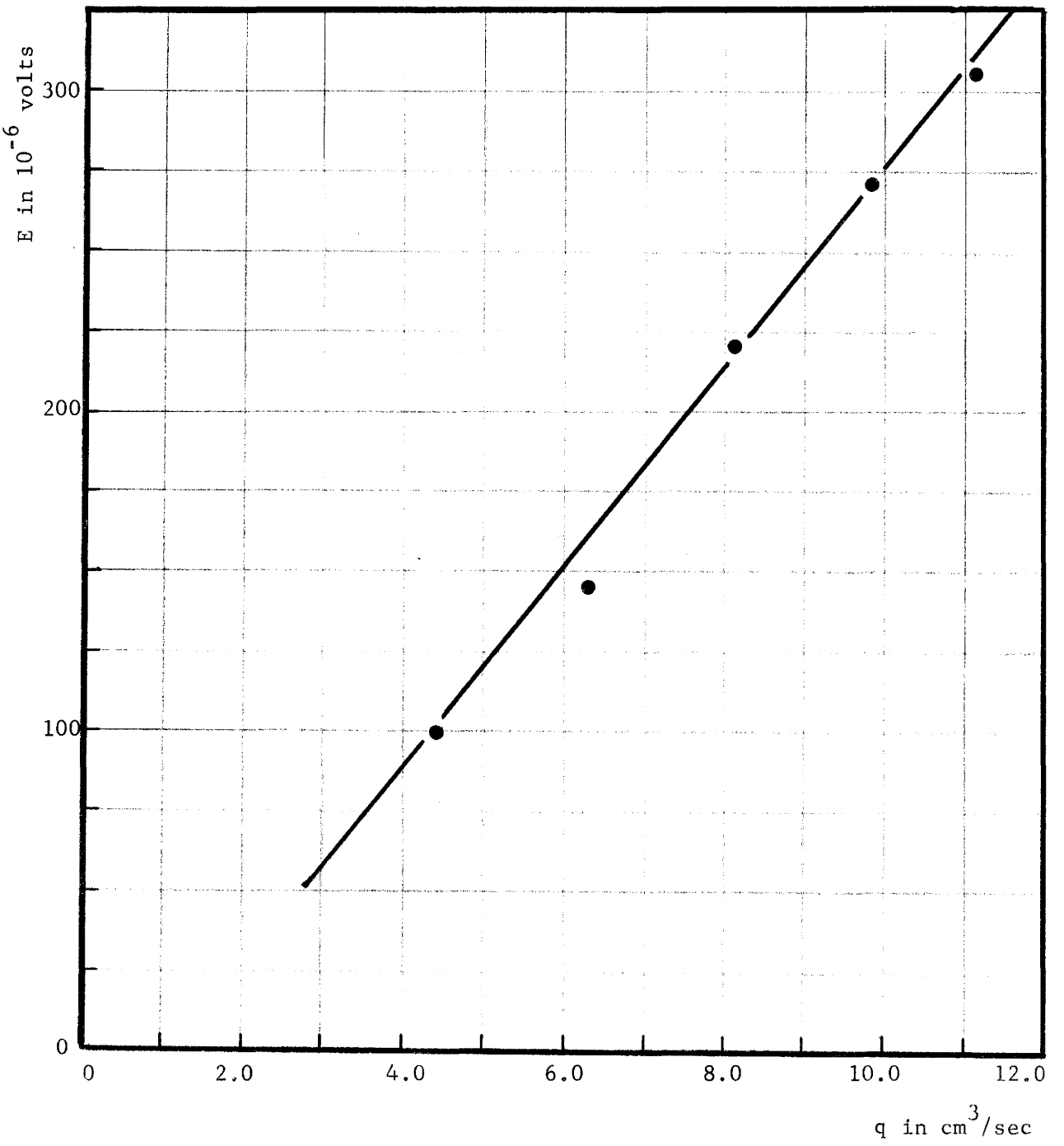

Figure 34. Discharge q versus streaming potential E for W_1 permeating through S_2.

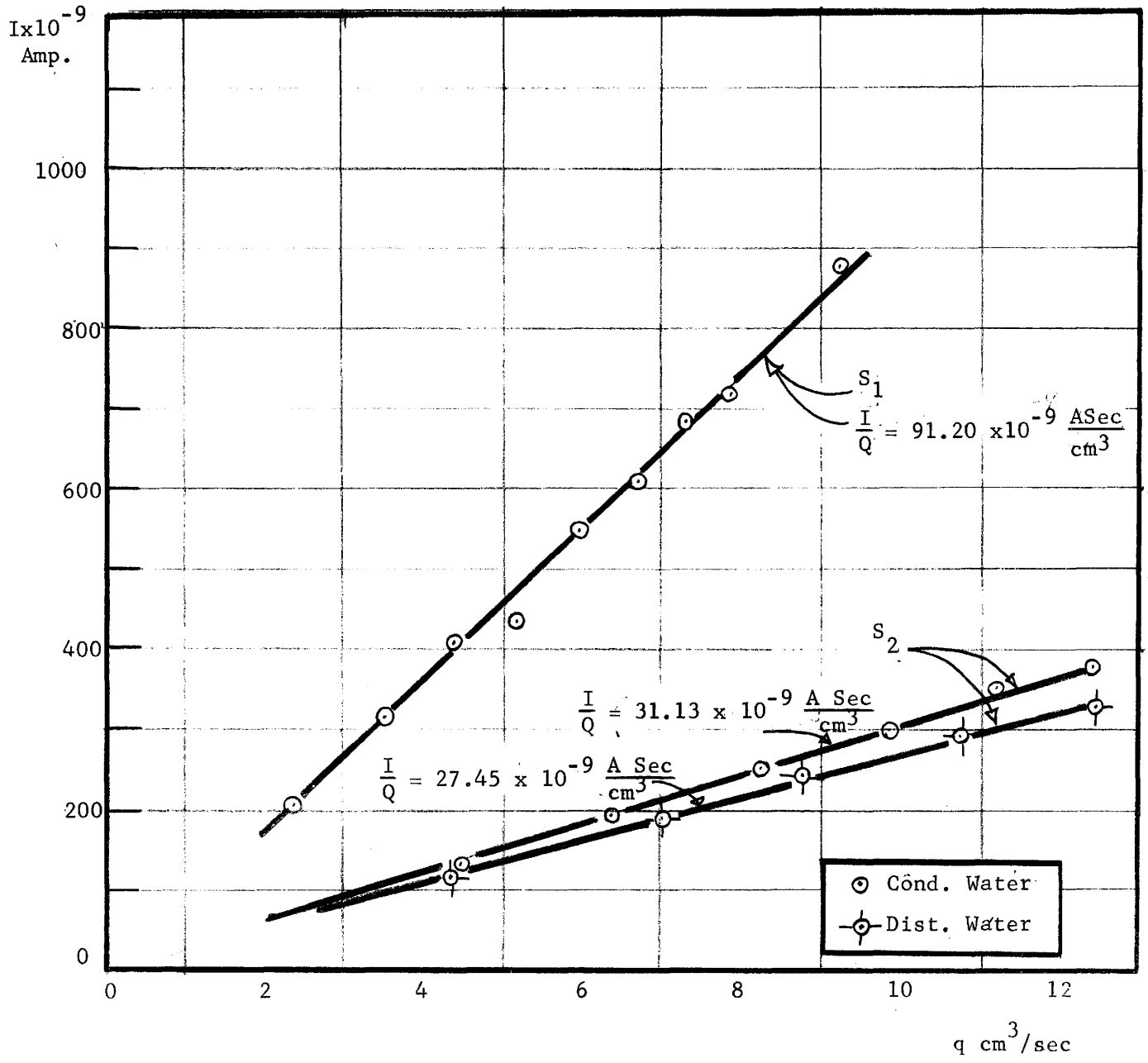

Figure 35. Discharge in cm^3/sec versus streaming current for conductance water and distilled water permeating through S_1 and S_2.

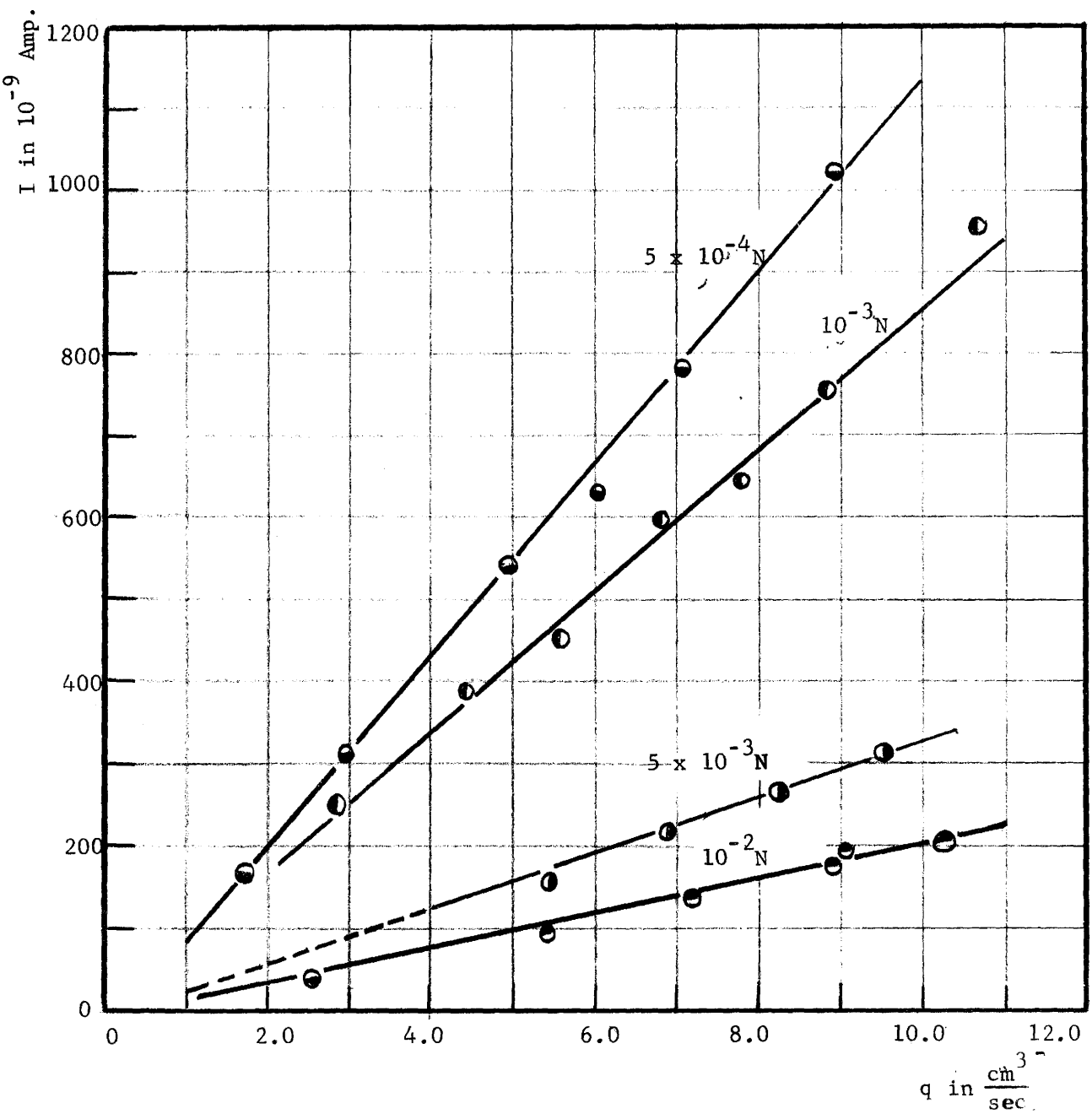

Figure 36. Discharge q versus streaming current I for NaCl solutions at different concentrations permeating through S_1.

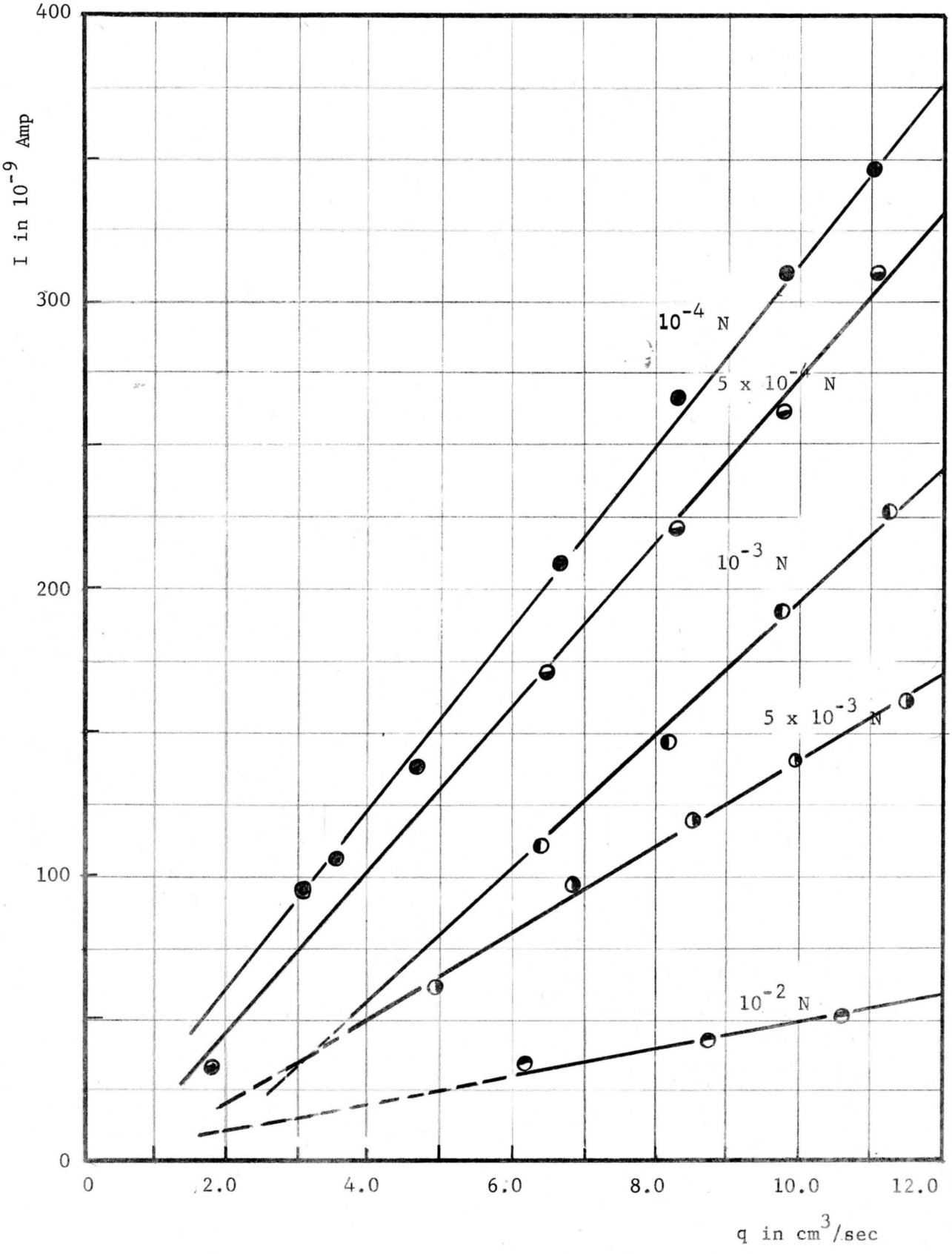

Figure 37. Discharge q versus streaming current I for NaCl solutions at different concentrations permeating through S_2.

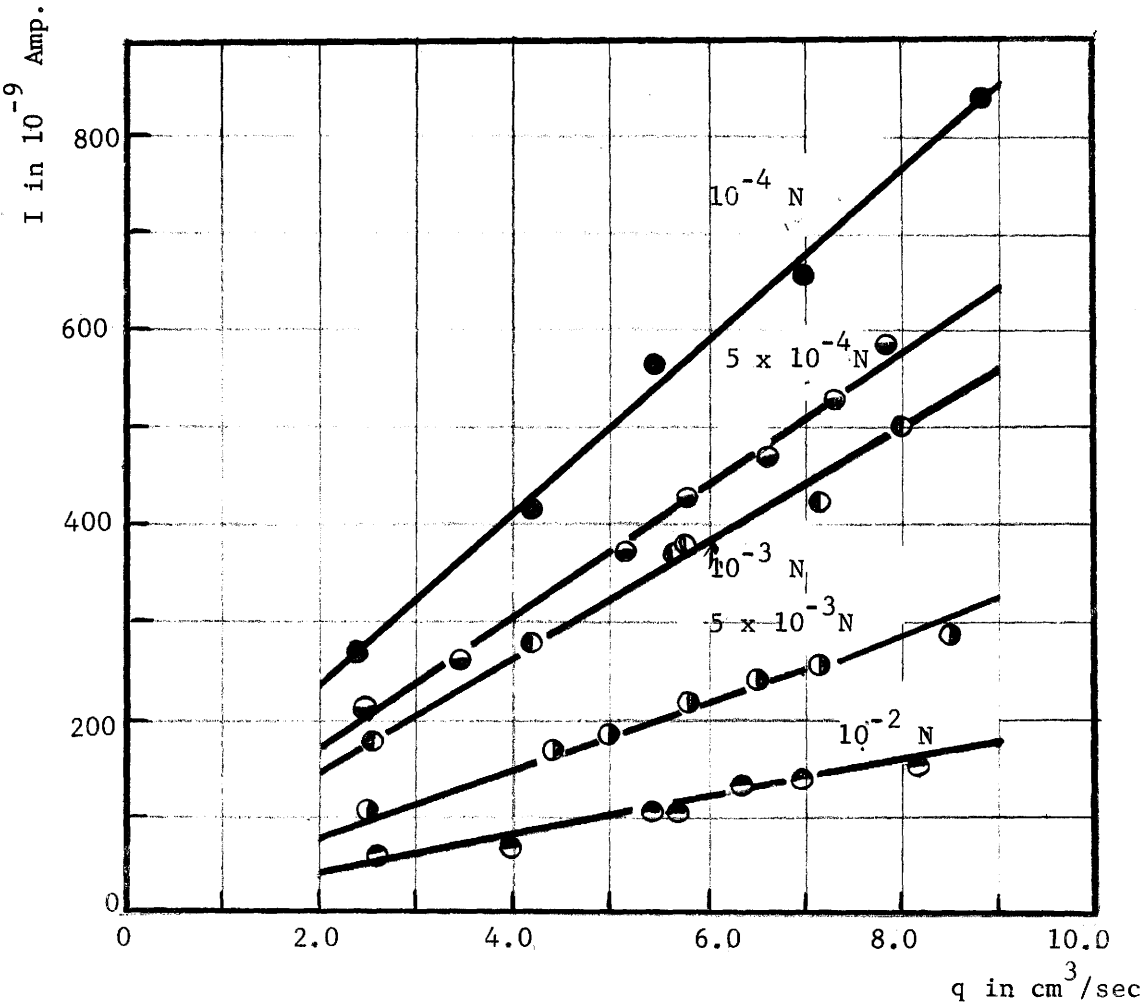

Figure 38. Discharge q versus streaming current I for KCl solution at different concentrations permeating through S_1.

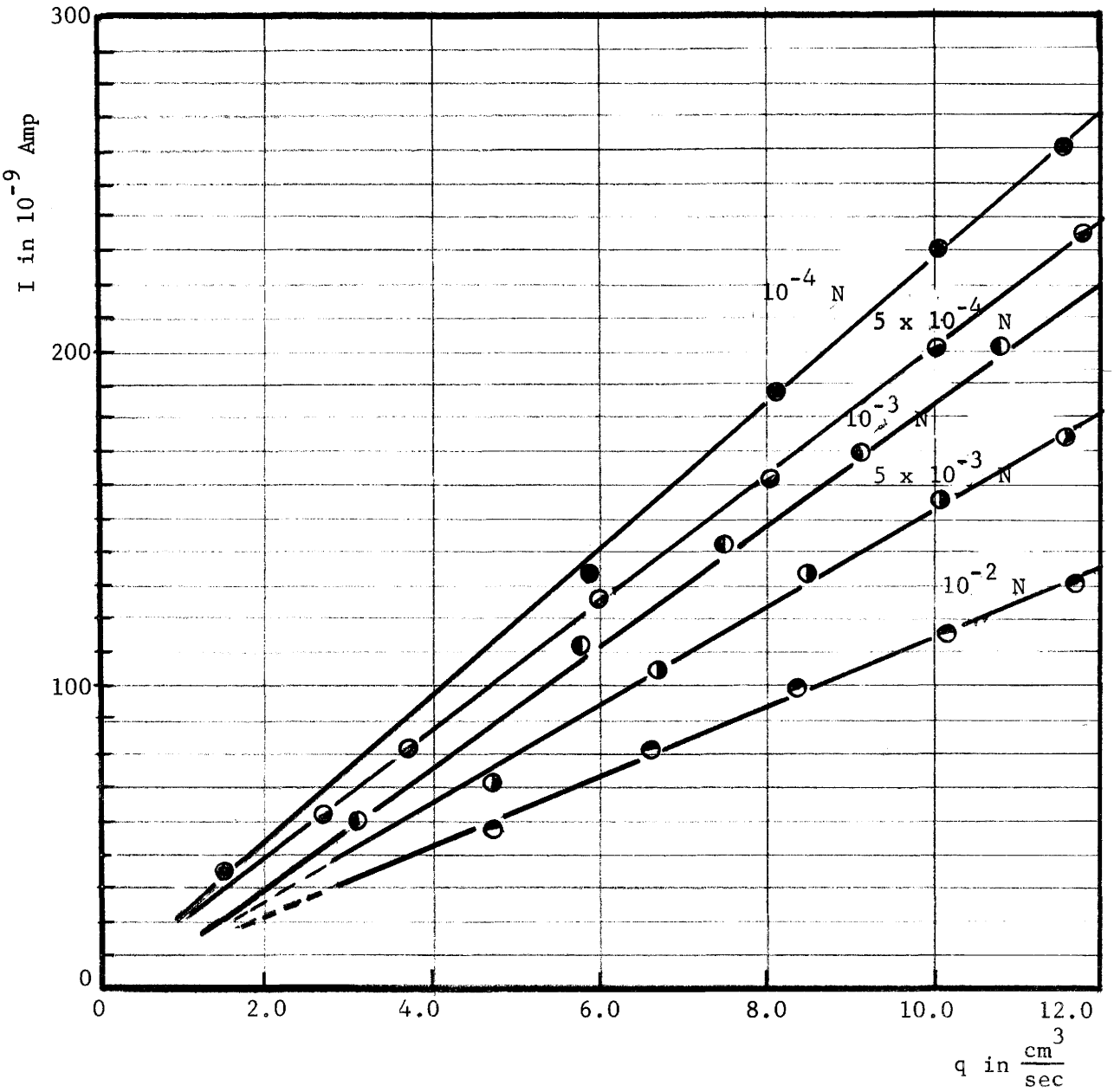

Figure 39. Discharge q versus streaming current I for KCl solution permeating at different concentrations through S_2.

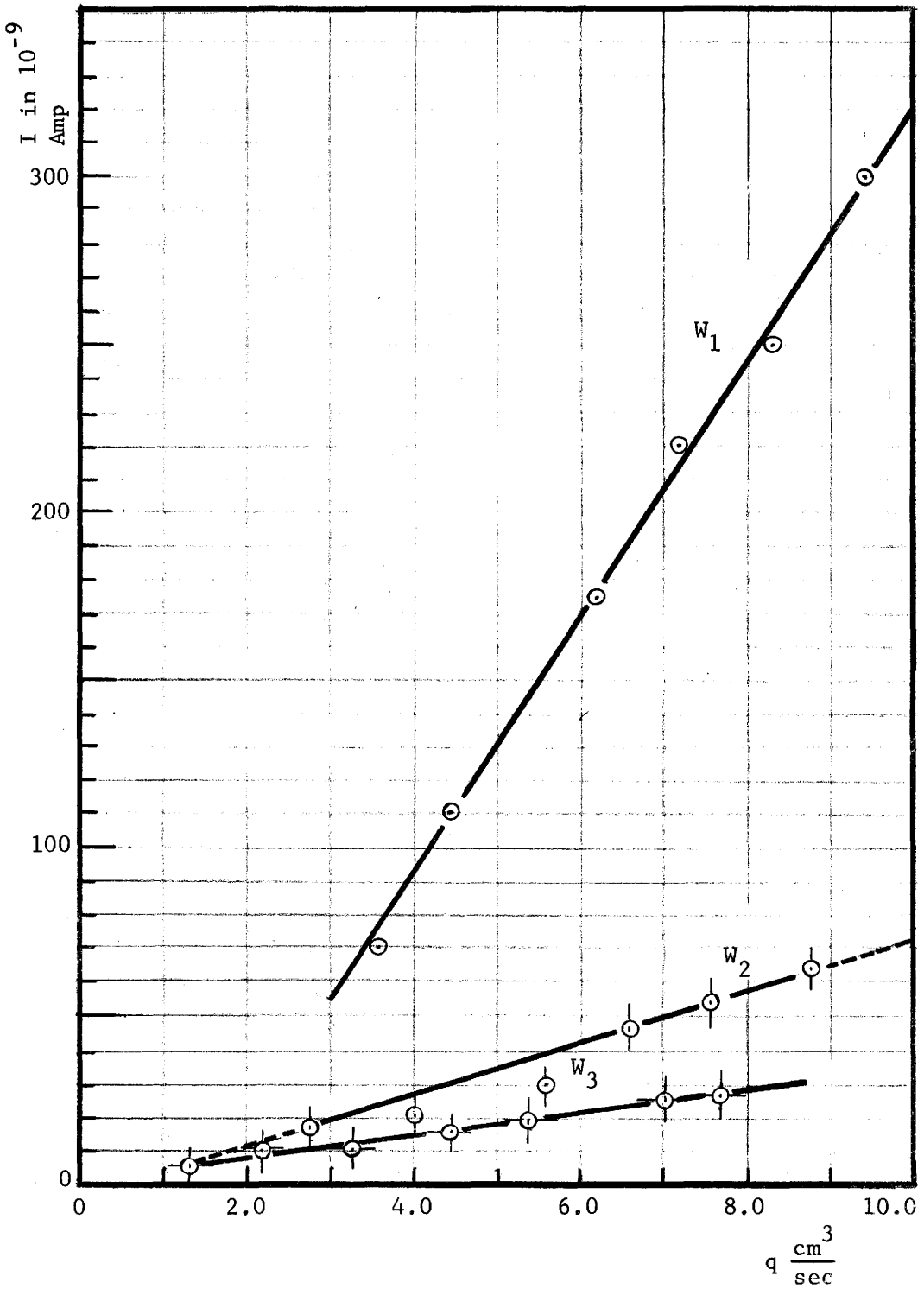

Figure 40. Discharge q versus streaming current I with W_1, W_2 and W_3 permeating through S_1.

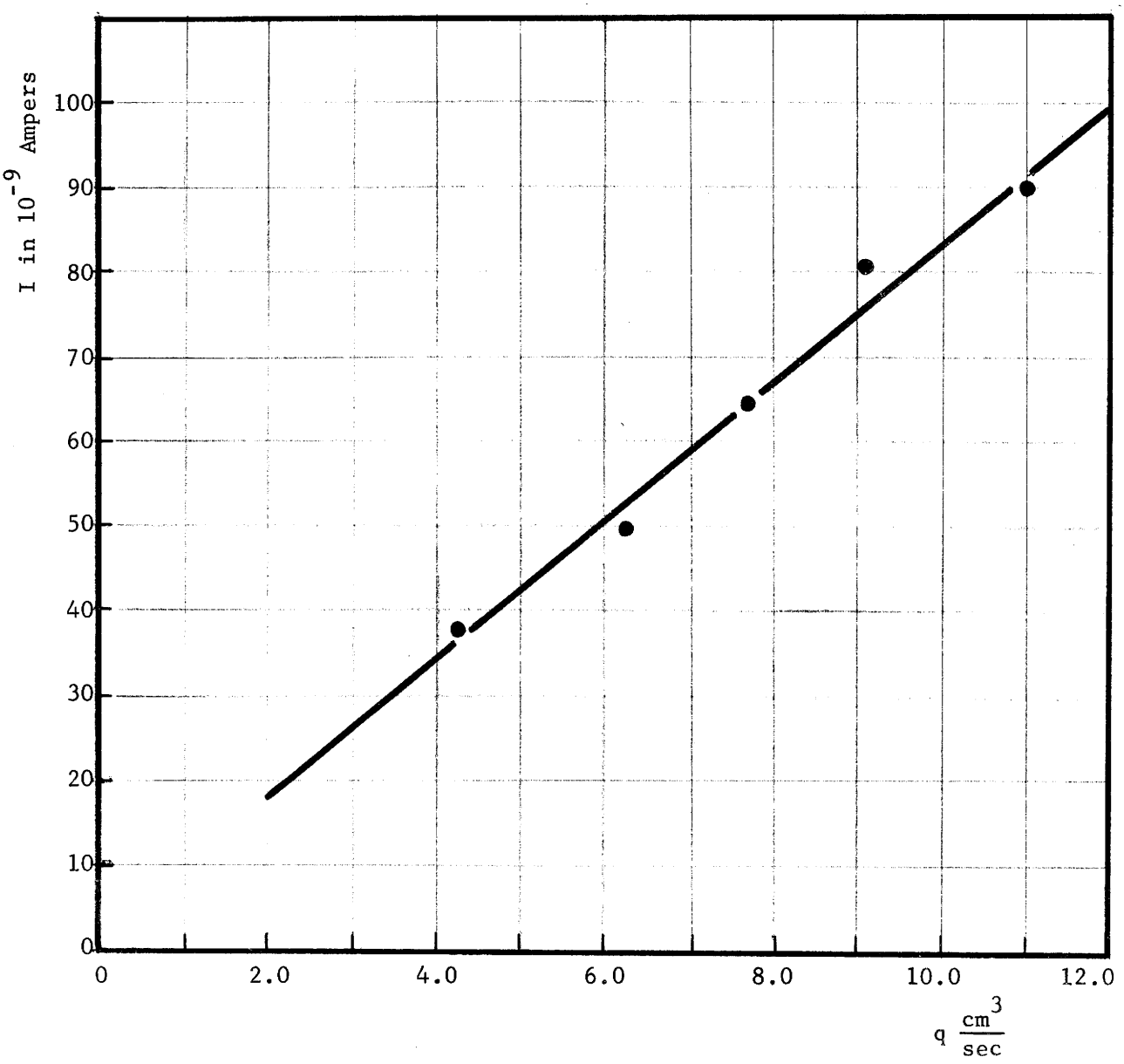

Figure 41. Discharge q versus streaming current I for W_1 permeating through S_2.

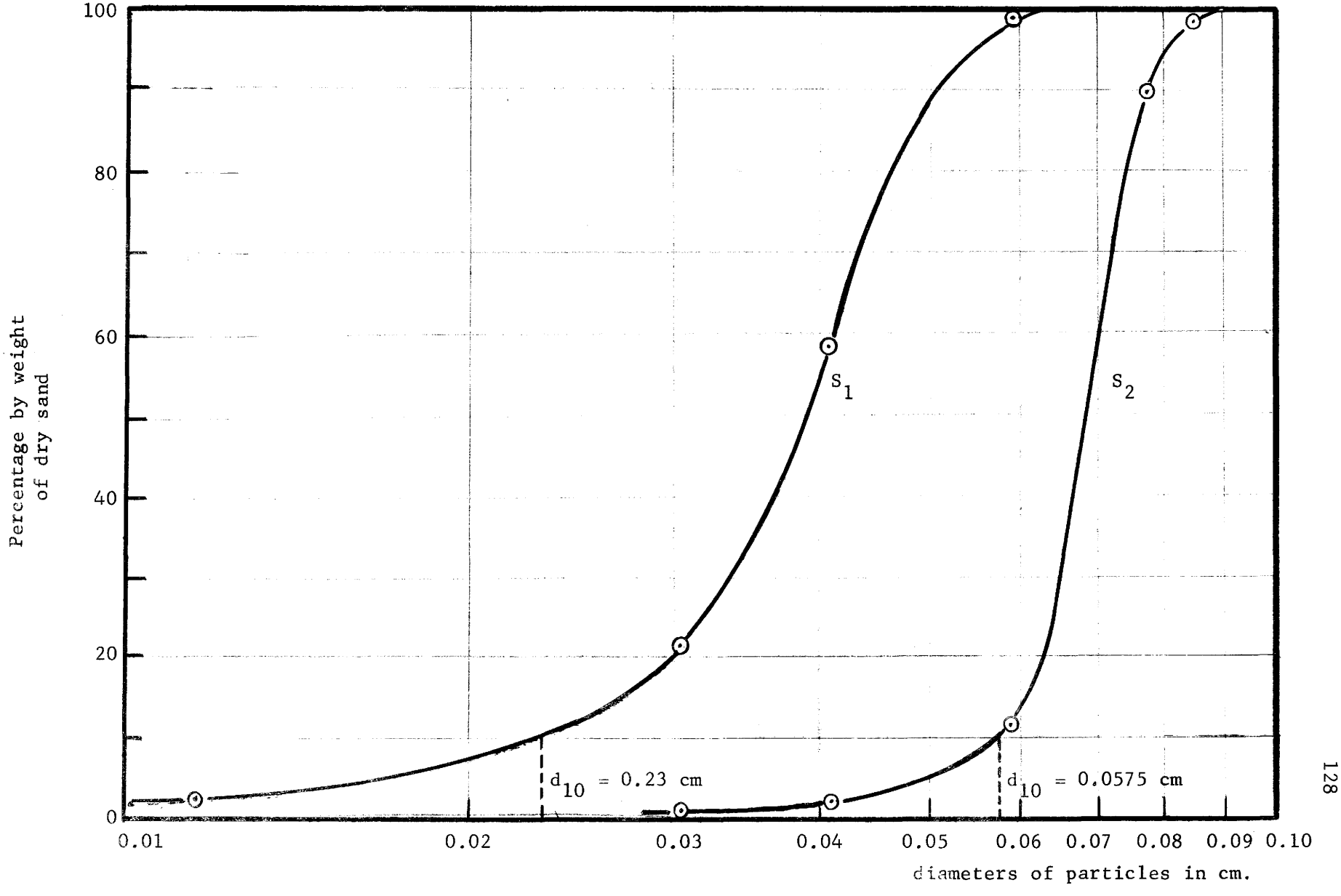

Figure 42. Particle size distribution for both sand samples.

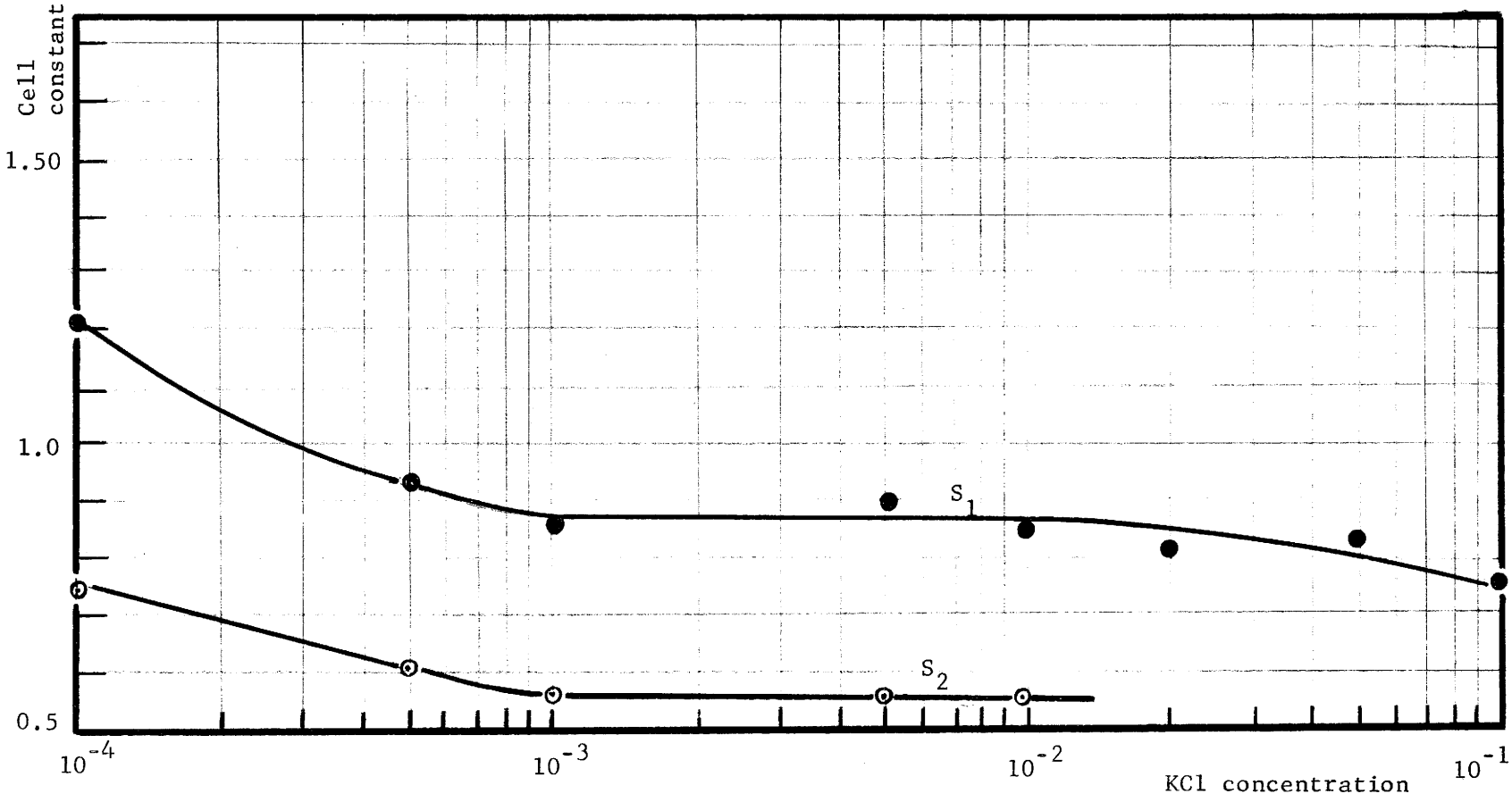

Figure 43. Cell constant for S_1 and S_2.